# Decomposition of Olfactory Memory by Dopamine Neural Cirucit in Drosophila

# DECOMPOSITION OF OLFACTORY MEMORY BY DOPAMINE NEURAL CIRUCIT IN DROSOPHILA

**A dissertation presented**

**by**

**Yang Jiang**

**to**

**The Department of Molecular and Cellular Biology**

**in partial fulfillment of the requirements**

**for the degree of Doctor of Philosophy**

**in the subject of Biochemistry**

**Harvard University, Cambridge, Massachusetts**

**May, 2017**

**Thesis Advisor: Sam Kunes** **Yang Jiang**

# DECOMPOSITION OF OLFACTORY MEMORY BY DOPAMINE NEURAL CIRUCIT IN *DROSOPHILA*

## Abstract

During the formation of an olfactory memory in *Drosophila*, the Mushroom Body (MB) receives olfactory cues (Conditioned Stimuli, CS) relayed from the antennal lobe and aversive or reward stimuli (Unconditioned Stimuli; US) from associated dopamine neurons (DANs). It has been shown that the pairing of a CS with dopamine release stimulated by a US is the key process for olfactory conditioning. The simplest mechanism might employ convergence at the MB of a CS and US through two separate and non-interacting circuit pathways. Here we show that the CS and US pathways interact in a novel and significant way to drive memory formation. First, we identified two types of *plastic* dopamine neurons (pDANs) that assign positive or negative valence to a CS during conditioning. Punishment pDANs are conditioned to respond uniquely to a CS (the CS+) that is associated with a punitive stimulus (US). Appetitive or reward pDANs exhibit coordinate plasticity to a distinct odor (CS-) that is not paired with a punitive US. By screening circuits for training dependent plasticity, we identified neurons that mediate DAN plasticity via a feedback loop from MB output to the pDAN input. A novel extrinsic neuron type we refer to as Recurrent Loop Neurons (RLNs) mediate this loop together with Mushroom body Output Neurons (MBONs). We show that reward pDANs participate in aversive conditioning by utilizing a tripartite feedback circuit

involving MBONs, DANs and RLNs to drive memory formation, especially to establish attraction to the CS- odor. We propose a model of bidirectional interaction between US and CS pathways has a specific role in learned binary decisions to memory.

# CONTENTS

# Acknowledgements

I would like to thank my advisor Sam Kunes for his support and advice throughout my graduate studies. Sam have always been a great resource on most of my research, ranging from contributing experiment ideas, solving technical problems, to criticizing data interpretations. I am also especially grateful for the freedom Sam has given while I was pursuing my research interests.

I would like to thank my thesis committee members Florian Engert, Nao Uchida and Ben de Bivort for their guidance and enthusiasm on my research. I am grateful for their encouragement and constructive suggestions.

I would like to thank the current members and former members of Kunes Laboratory for their help during my thesis research. In particular, former lab member Chuntao Dan taught me fly mounting technique for calcium imaging and building odor stimulation apparatus. Erin Song taught me various lab techniques, including buffer preparation and fly culture.

I would also like to thank Harvard research community. In particular, I thank Ed Soucy (Head Neuroengineer) for helping the design and manufacture of fly training apparatus. I thank my friend, Ye Ding (Harvard GSAS) for help with the design of imaging chamber and Harvard Center for Brain Imaging (HCBI) for providing microscopy resources.

I'm also grateful to *Drosophila* research community for generously providing technical support and reagents. In particular, I thank Yichun Shuai (Janelia Research Campus, HHMI) for help with designing training apparatus design and providing split-GAL4 lines.

Finally, I would like to thank my girlfriend He Yang, who is also a Kunes lab member for love, support, understanding and all kinds of help with my research.

## Chapter One

# Introduction

Animals adapt to rapidly changing environments through reinforcing appropriate and advantageous behavior while discouraging disadvantageous behavior. Neuromodulators are evolutionarily conserved molecules that serve as the reinforcement signals. Neuromodulators act on receptors of downstream neurons and trigger modifications of cellular and synaptic functions, leading to modifications of neural circuits and behavioral adaptations. In particular, pathways utilizing dopamine have been investigated extensively as providing key reinforcement signals. However, it is still unknown how dopamine neurons work on a neural circuit level, especially in *Drosophila*. This thesis studies, in the model system of *Drosophila* olfactory memory system, how dopamine neurons contribute to memory formation in a novel circuit level.

This Introductory chapter first reviews current understanding of dopamine's function in mammalian brain. Then I introduce *Drosophila* olfactory pathway and different types of *Drosophila* memory, especially olfactory memory and dopamine's roles in *Drosophila* olfactory memory. Last I introduce deeper analysis of the role which dopamine neural circuit plays in *Drosophila* olfactory memory and its potential connection to mammalian dopamine system.

## Part One: Dopamine and its role in learning and motivation

### 1.1 Molecular properties of dopamine and DA receptors

Dopamine (DA) is a predominant catecholamine neurotransmitter in the brain. It controls a wide range of brain functions, including locomotion activity, cognition, emotion, reinforcement, etc. Dopamine system has been the focus of research for decades since several pathological conditions, such as Parkinson disease and depression, are linked to dysfunction

of dopamine system. Moreover, dopamine is also closely related to learning and memory, a critical function of nervous system. Five homologues of dopamine receptors have been identified in mammals and those homologues can be divided into two groups based on structure and function similarities [1]. The $D_1$ and $D_5$ receptors share a high homology in transmembrane domain and are coupled to activation of adenylyl cyclase (AC). The $D_2$, $D_3$ and $D_4$ receptors are also conserved in transmembrane domain but inhibit cAMP pathways. Therefore, $D_1$ and $D_5$ subtypes are classified $D_1$-like and $D_2$, $D_3$ and $D_4$ subtypes as $D_2$-like. In *Drosophila*, $D_1$ –like, Dopamine Receptor in Mushroom body (DAMB) and $D_2$-like receptors D2R, [2] have also been identified, in addition to a non-canonical receptor (DopEcR) [3]. In a canonical model, dopamine neurons release dopamine onto neurons expressing dopamine receptors, which triggers downstream intraceullar signaling. More recent studies in mammalian brain reveal that dopamine neurons can also co-release other neurotransmitters, including GABA and glutamate [4]. Co-release of GABA from dopamine neurons was shown to inhibit striatal neurons [5]. Since the identification of dopamine receptors, studies have found a large set of DA receptor agonists and antagonists with variable affinity. Researchers have since been using those drugs to study the function of dopamine system in behavior.

### 1.2 DA neurons' roles in behavior

Researchers have been studying dopamine function since the 60s. In the earliest lesion studies, people found that selective damage to dopamine fibers causes deficits in feeding or forward locomotion [6]. With the development of selective DA receptor agonists and antagonists that can be used either to stimulate or to block dopamine pathways, researchers have been studying its effects on many behavior paradigms. Pavlovian conditioning and

operant learning are two major animal training paradigms to study learning and memory. Generally speaking, Pavlovian conditioning refers to passive stimulus-outcome associations whereas operant learning usually emphasizes association between an active instrumental act and its consequent outcome together with the motivation that precedes the instrumental act. A few models have been proposed to explain dopamine's roles in both Pavlovian conditioning and operant learning. Notably the differentiation between reinforcement of stimulus-outcome association and conditioned motivation preceding instrumental act, as proposed by Wise [6], appears to explain dopamine's function in learning process. In the hypothesis model of reinforcement, dopamine serves as the reinforcement of the association between stimulus and behavioral response. Lack of reinforcement, achieved by blocking dopamine activity, impairs memory. For example, rats fail to learn to lever-press for food or water if dopamine function is impaired [7]. Reinforcement model appears to explain learning in fruit flies as well. Studies have shown that silencing DA neurons causes memory deficits in olfactory [8] and taste memory [9]. In the hypothesis model of incentive motivation [6], dopamine endows an otherwise neutral stimulus with motivational importance through prior association with a reward. Incentive motivation emphasizes priming or drive-like effects of an encounter with conditioned stimulus before the animal receives the reward. For example, how fast an animal runs in an alley depends on the association between alley cues and a previous reward [6]. Intro Figure 1A illustrates the difference between incentive motivation and classical reinforcement in mouse conditioned place preference (CPP) experiments using drug as reinforcers [10]. In incentive driven behavior, conditioned stimuli (CS+) elicits a 'seek them out' incentive motivation. Animals may not necessarily like the CS+ but they tend to explore the area with CS+. In operant conditioned behavior, animals exhibit spontaneous behavior

that may be rewarded with drugs. In this case, animals are actively trying to obtain rewards by a spontaneous act instead of passively waiting for reward to come. In Pavlovian conditioned behavior, CS+ associated with drugs may elicit an innate response that can be the same as the response to US, such as feeding behavior. This innate response to US will also prevent animals from leaving CS+ area. In the end, all these three types of conditioning lead to the same behavioral outcome: mice prefer the CS+ zone to the CS- zone. It is likely that dopamine plays a role in all these types of conditioning mechanisms.

Another hypothesis was proposed by Hikosaka [11]. In order to explain DA neurons encoding both reward and non-rewarding events, they came up with a model to classify DA neurons into two types: DA neurons that encode motivational value and those that encode motivational salience (Intro Figure 1B). On one hand, value-encoding DA neurons are excited by reward and inhibited by aversive stimuli. Those neurons could encode prediction error and the valence of stimuli, thus providing reinforcement instructive signal for seeking and evaluation. On the other hand, salience-encoding DA neurons are excited by both reward and aversive stimuli but display weaker response to neutral stimuli [11, 12]. It could provide instructive signal for neural circuits to detect and predict events of high importance, no matter whether the events represent positive or negative valence. In addition to motivation and salience, a third alerting function was also proposed [11]. In this category, DA neurons respond to several types of sensory events that are not associated with rewarding or aversive experiences. This includes novelty, surprise, arousal and attention. Those alerting response reflects the extent to which the stimulus is surprising or captures attention; the alerting response would be reduced if attention is engaged elsewhere [11].

The criteria for DA neurons classification by Wise [6] emphasizes more on its involvement in behavior. DA neurons are classified as mediating reinforcement if they are involved in reward-stimulus association and they are classified as mediating motivation if they are required for exploration and operant learning. Hikosaka's classification criteria for DA neurons are based on how DA neurons respond to conditioned stimuli. It appears that value-encoding DA neurons correspond to those involved in reinforcement and salience-encoding DA neurons correspond to those involved in incentive motivation. However, these two aspects of DA neurons' function also seem to be intertwined to some extent. On one hand, it requires dopamine's reinforcement function for DA neurons to learn to encode event salience. Those DA neurons don't display naïve response to the salience of CS before conditioning and it is the dopamine reinforcement that causes DA neurons to encode salience after conditioning. On the other hand, salience-encoding DA neurons likely provide a motivational drive in operant learning and this could also facilitate the reinforcement process. Despite the progress in mammalian research, it remains unclear whether there is a saliency component in fruit flies' memory and there is even controversy over whether operant learning really exists in fruit fly behavior. Recently, it was reported that honey bees are able to perform a cap-pushing action which appears to be operant learning [13].

### 1.3 Reward circuitry in mammalian brain

The reward circuitry characterized in great detail in mouse brain is the VTA (ventral tegmental area) dopamine neurons that project to nucleus accumbens (NAc), part of ventral striatum. GABAergic medium spiny neurons (MSN) are the principle neurons of NAc, expressing $D_1$ or $D_2$ like DA receptors. As a heterogeneous midbrain structure, VTA also

comprises GABAergic interneurons (30%) and a relatively small fraction of glutamatergic neurons (5%), in addition to DA neurons (65%) [14]. DA neurons in VTA likely receive constant inhibition from its surrounding GABAergic inter-neurons. VTA dopamine neurons axons impinge on dendritic spines of MSNs and glutamatergic cortical afferents, forming a triad arrangement, which allows dopamine to modulate MSN postsynaptic processes in response to presynaptic cortical input [15]. In turn, GABA neurons in VTA receive inhibitory input from $D_1$ MSNs of NAc (Intro Figure 1C). It was reported that abnormal potentiation of this inhibitory pathway from NAc MSNs to VTA GABA neurons causes elevated activity of DA neurons due to dis-inhibition. This is closely related to cocaine-induced addiction [16]. There are two modes of DA neuron transmission in NAc. One is synaptic 'phasic' activation, which induces a rapid and spatially restricted dopamine release caused by DA neuron 'burst' firing. This type of firing is usually cause by primary reward or conditioned stimulus predicting primary reward. It is generally thought to serve as the instructive signal for conditioning [17]. The other type is extrasynaptic 'tonic' activation, which displays slow-timescale DA level changes. Tonic DA activity may affect broader populations of NAc neurons [17]. Dopamine acts on NAc MSNs through a complex array of mechanisms, which controls subsequent behavior through MSNs output. It has been shown that activation of $D_1$ or $D_2$ MSNs has opposite effects on behavior. Activation of $D_1$ MSNs optogenetically by ChR2 stimulation or knocking down Tyrosine receptor kinase B (TrkB) in $D_1$ MSNs potentiates cocaine induced reward effects and increases locomotor activity [18]. Knocking down TrkB in $D_2$ MSNs, on the other hand, attenuates reward effects of cocaine [18]. This is consistent with striatum direct and indirect pathway hypothesis. Activation of direct pathway MSNs promotes locomotion whereas activation of indirect pathway inhibits it [19].

In addition to NAc, VTA dopamine neurons also project axons to other brain regions, including prefrontal cortex, amygdala and hippocampus. It has been known for more than a decade that dopamine facilitates long-term potentiation in hippocampus and VTA was postulated to the neuronal source for dopamine [20, 21]. However, a recent study demonstrates that dopamine's novelty effect on hippocampus mostly comes from locus coeruleus when pharmacological blocking of VTA dopamine neurons doesn't affect novelty effect on memory [22]. Optogenetic activation of VTA dopamine neuron projections to mPFC was found to facilitate stimulus discrimination but carry no aversive or appetitive valence [23]. Although amygdala is critical for acquisition and storage of fear memory and dopamine is traditionally perceived as representing reward, it has been shown that dopamine activity induces long-term depression of pathway from lateral amygdala (LA) to intercalated cell mass (ITC) pathway [24]. It is still unclear which brain region provides dopamine input for amygdala.

As complex as its output pathways, VTA receives input from many brain areas as well, creating an inter-connected neural network (Intro Figure 1C). In addition to feedback from NAc, VTA receives projections from lateral habenula (LHb), lateral hypothalamus (LH), rostomedial tegmental area (RMTg) and laterodorsal tegmental area (LDTg). It has been shown that lateral habenula responds to aversive stimuli and optogenetic stimulation of LHb terminals in RMTg promotes inhibition of DA neurons in VTA, representing negative valence [25]. Another study shows that GABAergic pathway from lateral hypothalamus activates VTA dopamine neurons by inhibiting VTA GABAergic interneurons, facilitating dopamine release in NAc. This LH-VTA pathway is able to support positive reinforcement and conditioned place preference [26]. Similarly, in addition to VTA dopamine input, NAc also receives input from

multiple brain regions, such as mPFC. Together, this intertwined recurrent neural network constitutes a delicate reward circuitry that allows the animal to adapt to complicated and rapidly changing environments.

### 1.4 Mouse dopamine neurons encode prediction error

The initial hypothesis for prediction error comes from the seminal study by Schultz et al [27]. Mammalian midbrain dopamine neurons, such as VTA neurons, are able to calculate the difference between an actual and expected stimulus, and release dopamine accordingly to regulate synaptic transmission and thus shape behavior. In the original paper by Schultz, researchers found that dopamine neurons display phasic response to primary reward before conditioning. After conditioning, phasic response to primary reward shifts to reward predicting conditioned stimuli. Moreover, dopamine neurons exhibit suppression of DA activity if reward is withheld when it is supposed to be given shortly after reward predicting conditioned stimuli [27]. A decade later, Hikosaka et al shows that dopamine neurons encode prediction errors for both appetitive and aversive events [12]. Researchers went further to find out how DA neurons in VTA calculate prediction errors. First, it was found that after classical conditioning, VTA GABAergic interneurons display activity ramping up in response to reward predicting conditioned stimulus [28]. Later, it turns out that activity of VTA GABA interneurons indeed contributes to inhibition of DA neurons response to primary reward after odor has been conditioned [29]. A more thorough study by Tian et al shows that DA neurons in VTA receives a distributed and mixed input from many brain regions, including striatum and hypothalamus. Those neurons that project to VTA dopamine neurons respond to primary reward, calculate expectation or display mixed response [30]. It is unclear to what

extent those different brain regions contribute to the calculation of prediction errors in VTA dopamine neurons. Simple but sufficiently complicated organisms such as *Drosophila* thereby could provide us an opportunity to gain a deeper understanding of the fundamental principles of how dopamine neurons participate in memory formation and how they are regulated by other neurons. In this study, we focused on *Drosophila* mushroom body dopamine system.

## Part Two: Mushroom body is one of the memory centers in *Drosophila*

### 1.1 Structure and function of *Drosophila* olfactory sensory system

Insects rely on multiple primary sensory organs for olfaction. Adult *Drosophila* contains two olfactory organs, namely antenna and maxillary palp. Both organs contain sensory hairs, or sensilla housing the dendrites of olfactory receptor neurons (ORN). Antenna is the main olfactory sensory organ whereas maxillary palp lies close to labellum, the main taste organ of *Drosophila* head. There is evidence that olfactory stimuli via maxillary palp could facilitate taste related behavior [31]. Some of the antenna sensilla respond to general odorants while others respond solely to important pheromones. For example, a specific olfactory receptor Ord67d responds to male-specific pheromone 11-cis vaccenyl acetate (cVA), which is critical for courtship behavior [32]. Olfactory receptors repertoire comprises three olfactory receptor families: 60-340 members of insect Or (Odor receptor) family, a few members of Gr (Gustatory receptor) family and around 60 members of Ir (Inotropic receptor) family. Ors and Grs contain seven transmembrane domains whereas Irs contain three transmembrane domains and a pore-loop [33]. Contrary to its mammalian counterparts, odor receptors act as ionotropic receptors. Odorant binding produce a fast inward current and it doesn't require

function of a G protein. Each olfactory receptor has a wide-ranging affinity for different chemicals. Some receptors are excited by odorants while some are inhibited. Extensive analysis has been conducted on the responses of receptor repertoire to panels of odorants. As summarized by Carlson et al, there are three basic principles [33]. First, individual odorants activate subset of receptors, instead of a single receptor. Second, each receptor can be activated by subset of odorants. Some receptors have a wide tuning curve, responding to many odorants while others are narrowly tuned. Third, odorants of high concentration tend to activate a broader panel of receptors. The primary representation of odor identity is thus distributed across a large set of ORNs.

The second olfactory center, antennal lobe (AL), receives odor input from ORNs. ORNs expressing the same set of receptors usually innervate one or two glomeruli in AL while each glomerulus in AL receive innervation from roughly 50 ORNs [33]. The axons of ORNs synapse with the dendrites of the output neurons in AL, which are referred as projection neurons (PN). Analysis of PN odor response profile reveals that PNs are broadly tuned by odorants: each PN responds to a wide array of odorants and the response pattern is more complicated than ORNs. For example, a detailed analysis of glomerulus DM2 and its presynaptic input indicates that DM2 PNs respond to a larger set of odorants than its presynaptic ORNs [34]. Moreover, detailed analysis shows that PNs respond to odors more reliably and odor representation is better separated in AL than in ORNs [35]. Wilson et al also shows that lateral inhibition mediated by GABAergic inter-neurons is also important for signal processing in AL. This inhibition scales with the strength of ORN activation [36]. After processing in AL, odor response is further transformed to mushroom body, the third olfactory center.

Mushroom body (MB) consists of ~2000 intrinsic Kenyon cell (KCs) neurons. Those KCs extend dendrites into a neuropil region named as calyx and project axons into a highly organized structure named as mushroom body lobes. Receiving broadly tuned odor response from antennal lobe, MB transforms odor representation into a sparse activity code in odor-selective KC ensembles. KCs receive input from multiple glomeruli but are much more narrowly tuned than their presynaptic neurons. Odor stimuli evoke responses only from a small fraction of KCs [37]. Carefully designed mapping analysis shows that each Kenyon cell integrates input from a different and random combination of glomeruli and different classes of KC don't seem to integrate input from a specific group of glomeruli. Those glomeruli that synapse onto the same individual KC don't share a common odor tuning profile either [38]. This random organization of glomeruli connection to MB and global inhibition could explain the sparse activity code in KC odor response. The organization of *Drosophila* olfactory pathway is shown in Intro Figure 1D.

### 1.2 Various types of memory in *Drosophila*

Similar to mammals, insects are able to use memory to navigate and adapt to its surrounding environments. Fruit flies can be trained to memorize olfactory stimuli, visual patterns and place/locations cues through associative learning paradigms. In associative learning, fruit fly is trained to associate a conditioned stimulus (CS) with a rewarding or punishing unconditioned stimulus (US). Here I will introduce olfactory and visual memory in adult fruit flies.

In visual learning, flies are usually trained to memorize visual patterns, colors, illumination intensity, etc. Visual memory has been extensively examined by using flight simulator. In flight simulator, an individual fly is held in a stationary position, suspended by a hook glued to its thorax. The set-up is placed in the center of an arena with wall or screens that provide visual stimulation. The hook glued to fly's thorax is attached to a torque meter so that an individual fly's flight yaw force can be measured when the fly rotates in the arena. The visual surrounding on arena wall can serve as visual cues to guide animal's flight or it can be modulated in a closed loop based on tethered fly's flight direction. In classical conditioning, as an individual fly rotates and changes its flight direction, different visual patterns will be presented. In many studies, one visual pattern is presented together with heat pulse punishment while the other pattern is presented as a neutral stimulus. After conditioning, fly will learn to maintain its direction towards the neutral unpaired visual pattern so that memory score can be calculated based on the time spent on maintaining its direction towards the unpaired stimulus [39]. Later studies further show that *Drosophila* visual pattern memory is stored in fan-shaped body, part of *Drosophila* central complex [40]. In addition to flight stimulator, there are also visual memory tests for free moving flies. In this paradigm, a group of flies are placed on a transparent arena, with LED providing visual stimulation beneath the arena [41]. Usually light of two different colors are used as conditioned stimulus. One color is paired with reward or punishment while the other color is presented alone, not paired with anything. Afterwards flies are tested in a T-maze to measure memory score. A more elegant study further shows that flies are able to perform visual place learning. It was shown that flies are capable of learning and recognizing a comfort zone in an arena based on surrounding visual landmarks after being punished outside the comfort zone. It also found that ellipsoid

body, instead of mushroom body, is required for this type of visual place memory [42]. This paradigm is actually highly similar to Morris water maze experiment, in which mice search for a safe platform to escape from unpleasant water experience based on multiple visual cues [43].

It is generally believed that olfaction is the most important sensory modality for insects. Naturally, olfactory memory is most extensively studied in fruit flies. In olfactory learning paradigm with odorant used as conditioned stimuli (CS), many kinds of stimulation can be used as unconditioned stimuli (US) and US can be either punishment or reward. These include: aversive olfactory conditioning using electric shock or heat as punishment [44]; appetitive olfactory conditioning using sugar or water as reward [45, 46]; associative courtship conditioning with female courtship rejection as punishment [47]. In aversive or appetitive conditioning, two odorants are usually used as conditioned stimulus. First, one odorant is presented simultaneously with reward or punishment and this odorant is usually referred to as CS+. Then after a small interval (60s), the other odorant is presented without any US and this one is referred as CS-. Memory score is then measured by forced decision making in a T-maze after conditioning (Intro Figure 1E). In courtship conditioning, after rejection of courtship by mated females, male fruit flies exhibit an enhanced response to male pheromone 11-cis vaccenyl acetate (cVA), and thus suppress futile courtship with mated females afterwards. Fruit fly male pheromone is deposited on female body when courtship occurs and thus cVA serves as a marker to distinguish virgins from mated females. There is evidence that pairing cVA stimulation with courtship rejection activates a group of dopamine

neurons innervating mushroom body and dopamine release likely modulates neurotransmission from MB to MBONs [47].

### 1.3 Classical findings on olfactory memory in *Drosophila*

*Drosophila* aversive olfactory memory features a range of memory phases, including short-term memory (STM) [48], middle-term memory (MTM) [49], anesthesia-resistant memory (ARM) and long-term memory (LTM) [48]. Memory obtained by a single training trial is believed to last for hours and is composed of three phases of memory that doesn't require protein synthesis after conditioning: STM, MTM and ARM [50]. STM refers to memory maintained 3 to 30 minutes after conditioning and MTM emphasizes the memory that persists during 1 to 3 hours after conditioning. ARM refers to the memory component that is resistant to cold shock treatment. Putting flies on ice for 2min (cold shock) after conditioning reduces memory score and the remaining portion of memory is referred to as ARM. Spaced cycles of training create long-term memory that last for days and it requires de novo protein synthesis after conditioning [51]. Ever since the earliest days of research on *Drosophila* memory, researchers have been trying to identify genes required for aversive olfactory memory. A large set of genes was screened for memory defects and a few critical genes were identified. For example, *rutabaga* is one of the earliest genes identified. *Rutabaga* encodes an adenylyl cyclase and it regulates the canonical PKA pathway as a coincidence detector [52]. Interestingly, most of genes discovered in screening for memory defects have been found to be highly expressed in mushroom body [53], suggesting mushroom body is the memory center in *Drosophila*.

In order to understand how mushroom body mediates memory formation, a canonical tool called $Shi^{ts1}$ has been frequently used in research from the past two decades. $Shi^{ts1}$ is a temperature sensitive dynamin-like gene mutation that controls vesicular traffic [54]. At permissive temperature (21℃), the protein encoded by $Shi^{ts1}$ stays normal whereas at restrictive temperature (30℃), the protein becomes dysfunctional likely due to protein structure instability induced by high temperature. By driving $Shi^{ts1}$ in specific neurons using GAL4 lines, we can control synaptic output from the neuron in a time-dependent manner and examine its effects on memory. By using this tool, studies in the last decade have found that different MB lobes mediate memory of different phases. Mushroom body lobes, composed of KC axons that form a parallel neuropil alignment, can be roughly divided into five subgroups or 'lobes' (the $\alpha, \alpha', \beta, \beta'$ and $\gamma$ lobes). The $\gamma$ lobe is shown to be required for STM and MTM, whereas the $\alpha$ / $\beta$ lobes required for LTM [55, 56]. More recently, with the development of more sensitive and reliable calcium indicator, researchers have been using genetic encoded calcium indicator (GECI or GCaMP) to monitor neuron activity and identified training dependent plasticity in mushroom body related neurons. For example, there is evidence that mushroom body display differential response to CS+ and CS- after aversive olfactory conditioning [55]. Last, although it is believed *Drosophila* olfactory LTM is protein-synthesis dependent [51] and requires mushroom body function, one study claims that MB is indispensible for LTM and protein synthesis is only required in a group of neurons outside mushroom body [57]. This controversy needs to be settled in the future.

### 1.4 *Drosophila* dopamine system

Dopamine is involved in many aspects of *Drosophila* behavior, including locomotion, sleep, memory, etc. Blocking dopamine signaling by mutation or drugs causes behavior malfunction. One study blocks dopamine function by generating mutant flies that lack tyrosine hydroxylase, the enzyme for dopamine biosynthesis. Those mutant flies exhibit reduced walking speed, reduced daily walking distance, extended sleep time and impaired aversive olfactory memory but intact visual fixation ability [58]. In order to map out the distribution of dopamine neurons in adult fly brain, a study used anti-tyrosine hydroxylase (anti-TH) antibody to stain putative dopamine positive neurons and characterized eight clusters of DA neurons, totaling ~282 neurons [59]. Those neurons were named based on cell body location in fly brain. For instance, if a neuron's cell body is located in the posterior lateral region of fly protocerebrum, it will be named as PPL (protocerebral posterior lateral) neuron. There are four major clusters: PAM, PAL, PPM and PPL clusters. Neurons in different clusters may project axons into different brain regions and even neurons in the same cluster might have different axon projection patterns. In order to understand which specific group of dopamine neurons is required for certain behavior, researchers usually use $Shi^{ts1}$ and specific GAL4 lines to block synaptic output from a specific group of dopamine neurons and to analyze its effects on behavior. There is evidence that PPL1 DA neurons are required for aversive olfactory memory [60], sleep/wakefulness regulation [61] and aversive taste memory [9]. A certain group of PPL1 DA neurons innervate MB and activation of those neurons induces aversive olfactory memory. Some other neurons regulate sleep via innervation of fan-shaped body, a structure involved in sleep control. PAM dopamine neurons have been shown to be critical for appetitive or reward conditioning, including olfactory memory induced by sugar [8] or water [46] and courtship conditioning [47]. All PAM dopamine neurons innervate mushroom body

lobes (Intro Figure 1F) and thus it is likely that memory induced by PAM dopamine neuron activation is stored in mushroom body lobes. There is also evidence that PPM3 neurons are involved in choosing ethanol-containing food in oviposition behavior. Flies prefer oviposition on food with high ethanol concentration. Silencing PPM3 neurons impair flies' preference to ethanol [62]. As we can see from the discussion above, most studies in fruit flies focus on which brain regions DA neurons project their axons to and how those DA neurons regulate those brain regions. It is unclear what's the input to those DA neurons and how the DA neurons are regulated.

## Part Three: Mushroom body dopamine neurons receive feedback from olfactory pathway

### 1.1 Each mushroom body lobe is divided into multiple functional compartments

The Mushroom body (MB) is the hub of olfactory memory in *Drosophila* [8, 48, 63, 64]. As the third component of *Drosophila* olfactory pathway, MB receives input from antennal lobes (AL) projection neurons. Consisting of ~2000 intrinsic Kenyon cell (KCs) neurons, the MB transforms AL odor inputs into a sparse activity code in odor-selective KC ensembles [37, 38]. KC dendritic odor input is propagated to KC axons that form a parallel alignment in neuropil that can be roughly divided into five subgroups or 'lobes' (the $\alpha, \alpha', \beta, \beta'$ and $\gamma$ lobes). In recent years, studies have found each MB lobe has orthogonal divisions (zones) that are formed of functional compartments along the lengths of the KC axons. These zones are tiled with the synaptic inputs and outputs of numerous MB extrinsic neurons (MBENs) that modulate and execute odor memory [65, 66]. The executive MBENs include at least 21 classes of MB output neurons (MBONs); modulatory neurons include dopamine neurons (DANs). For

instance, there are five classes of MBONs innervating $\gamma$ lobe and those MBONs are named from $\gamma 1$ to $\gamma 5$ MBONs based on their positions in the lobe from the most lateral region to midline (Intro Figure 1G). MBONs receive dopamine input from DANs and MBON response to odors can be modified by dopamine release stimulated by unconditioned stimulus (US). For example, $\alpha 2$ MBON, have been shown to respond differentially to CS+ and CS-, encoding the valence associated with learned odors [67]. Based on morphological analyses, the dendrites of specific MBONs overlap with the axons of select groups of DANs in each lobe compartment (Intro Figure 1G) [66]. An attractive explanation for the tiled zonal division of MBENs is that specific zones are required for memories of different valence (aversive/appetitive) and phases (STM, MTM, LTM) [67-69]. For example, the $\gamma 4, \gamma 5$ and $\beta' 2$ DANs are activated by reward stimuli, such as sugar and water whereas $\gamma 1$ DANs are activated by punitive stimuli, such as electric shocks [45, 70]. Furthermore, a recent study revealed that DANs only act on the MBONs that project dendrites in the same compartment, which eliminates potential interference across different compartments [71], although Cohn et al claims the opposite: DANs are able to regulate KC activity across lobe compartments [72]. This controversy needs to be resolved in future research.

Dopamine has been shown to be critical for olfactory memory in *Drosophila*. Memory can be generated by pairing of dopamine release with sensory stimulation in different modalities, including vision, olfaction, taste and courtship [45, 73, 74]. In aversive olfactory conditioning, an odorant is paired with simultaneous delivery of punitive electric shocks, which triggers the activity of a specific group of dopamine neurons [48, 73]. Pairing dopamine release with odor stimulation modifies neurotransmission from mushroom body lobes to mushroom body

output neurons. For example, Hige et al shows that pairing induces inhibition of MBON response to odors [71]. Because of the synaptic modification, flies learn to avoid the odor associated with electric shocks. Roughly speaking, *Drosophila* dopamine neurons can be divided into two types based on their valence [75]. DANs are referred to as aversive or punishing if they are required for aversive memory or if they can drive aversive learning via artificial activation. They are referred as appetitive or rewarding if their activity is involved in learning that leads to approach or attraction. For instance, PPL1 $\gamma 1$ DANs are critical for aversive memory and artificial activation of it by dTrpA1 paired with odor stimulation induces aversive memory [60]. Conversely, PAM $\gamma 4$ and $\beta' 2$ DANs are critical for appetitive memory and pairing its activation with odor stimulation creates appetitive memory [45]. The valence of DANs innervating mushroom body is summarized in Intro Figure 1F. Here, we focused on $\gamma$ and $\beta'$ lobes to systematically investigate how DANs and MBONs interact to drive memory formation.

### 1.2 Dopamine neurons display conditioned response to odors

In the mammalian nervous system, dopamine VTA neurons perform a calculation of prediction error [27, 28], updating the valence of extrinsic stimuli based on learned experience. Whether fruit fly dopamine neurons are able to learn odor valence remains unclear (see [76]), although DANs have been shown to respond to odor stimulation in fruit flies [59]. Here, we used calcium imaging, optogenetics and behavioral approaches to systematically study how DANs' respond to odors (CS) during and after associative conditioning and its underlying mechanism. We found that during aversive training, punishment DANs, such as the $\gamma 3$, learn to respond more strongly to an odor coincident with

an electric shock (the CS+), whereas reward DANs, such as $\gamma 4$, $\beta'2$ and $\beta'1$ DANs, learn to respond more strongly to an odor (the CS-) that follows the presentation of the shock and CS+ odor. We refer to these neurons as *plastic* DANs (pDANs). In addition, a group of reward DANs displays enhanced activity immediately when odor presentation ends; this odor-OFF response is enhanced by recent experience of an odor paired with shock.

### 1.3 Dopamine neurons receive feedback from MBONs and RLNs

As discussed in previous paragraphs, dopamine neurons in VTA receive input from multiple brain regions and the input to VTA DA neurons' leads to its ability to encode prediction errors. In order to understand the pathway that relays the response of conditioned stimuli to DANs, we screened uncharacterized neurons based on branches locations to identify those that display training dependent plasticity. We identify a new class of neurons, Recurrent Loop Neurons (RLNs) and enlarge the known group of MBONs that participate in aversive memory and feedback onto DANs. We show that there are indeed both anatomical and functional connections between DANs, MBONs and RLNs, by using GRASP and optogenetic activation. We also show that a circuit of MBONs, RLNs and DANs contribute to odor-evoked differential responses of DANs in a manner that relays the valence of CS. In order to confirm that DANs' response to odors, especially CS-, indeed plays a role in memory formation, we modified classical aversive olfactory conditioning paradigms and show that flies indeed come to memorize the valence of CS- and prefer CS- to a third new odor. Moreover, attraction to CS- contributes to fly aversive olfactory memory at different memory phases. Taken together, we demonstrate that there is a feedback pathway routing mushroom body to dopamine neurons, conveying olfactory information of valence. Considering that mouse VTA DA neurons receive

input from many brain areas, it is intriguing to investigate whether the dopamine neural network from these two evolutionarily diverged species share some fundamental similarities in future research.

**Intro Figure 1 Introduction to mouse dopamine system and *Drosophila* olfactory system.** (A) Different learning processes lead to conditioned place preference (CPP) in mice; adapted from [10]. Panel (a) illustrates incentive motivation driven behavior; panel (b) illustrates operant conditioned behavior; panel (c) illustrates Pavlovian conditioned behavior. (B) Diagram of value-encoding and salience-encoding dopamine neurons; adapted from [11]. (C) Diagram of the connectivity between VTA dopamine neuron and GABA neuron and their upstream input neurons; adapted from [77]. (D) Diagram of *Drosophila* olfactory pathway; adapted from [78]. (E) Illustration of aversive olfactory training experiment; adapted from [79]. Flies are trained by paring odor A with electric shock punishment and pairing odor B with nothing. Then flies are forced to choose between two odors in a T-maze. (F) Diagram of dopamine neurons of opposite valence in mushroom body lobes; adapted from [41]. PAM dopamine neurons are positive reward DA neurons and they respond to sugar stimulation. PPL1 dopamine neurons are negative punishment DA neurons and they respond to electric shock stimulation. Reward and punishment DA neurons innervate separate regions of mushroom body lobes. (G) Functional compartmentalization of mushroom body lobes; adapted from [69].

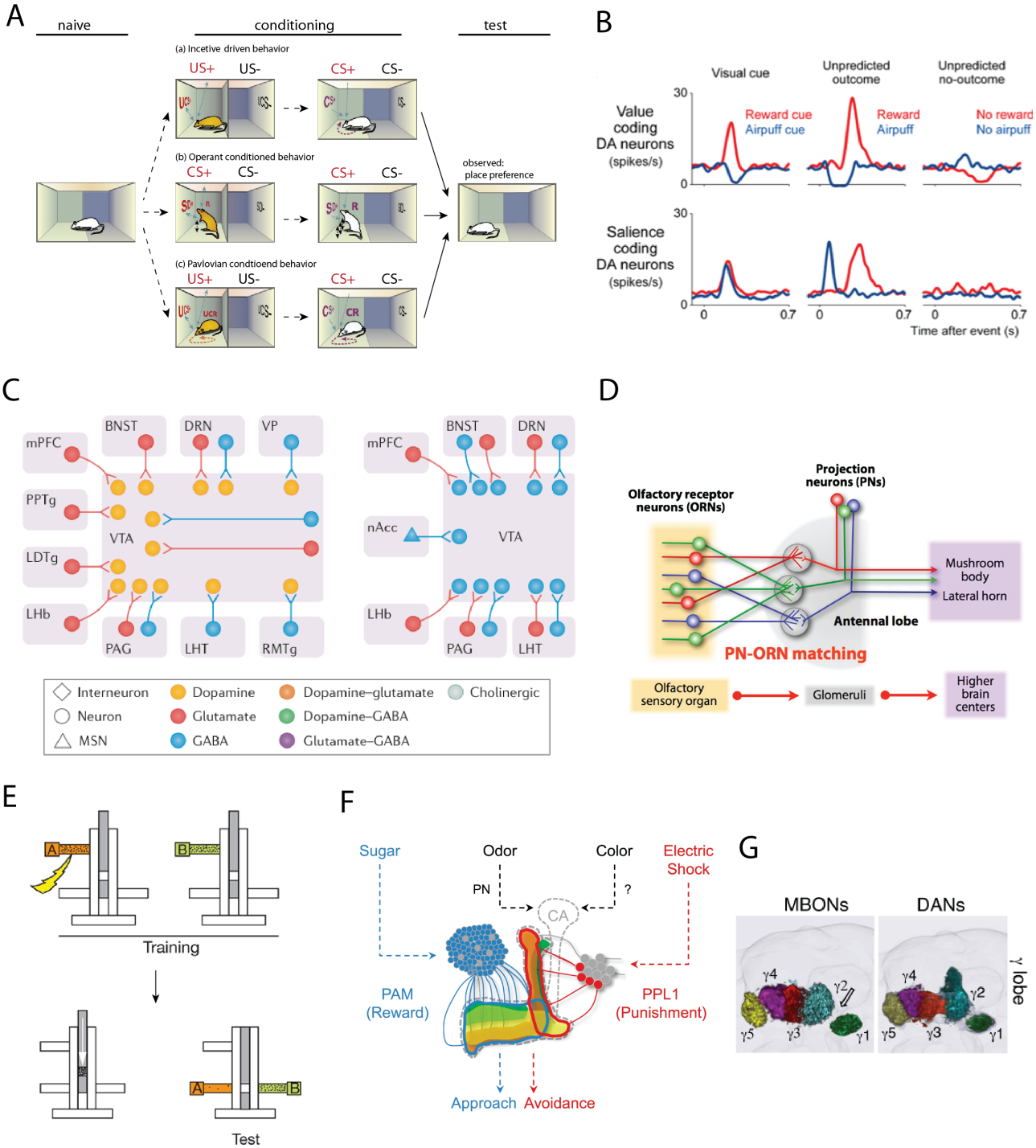
A
naive
conditioning
test
(a) Incetive driven behavior
US+
US-
CS+
CS-
(b) Operant conditioned behavior
(c) Pavlovian condtioend behavior
observed:
place preference
B
Visual cue
Unpredicted
outcome
Unpredicted
no-outcome
Value
coding
DA neurons
(spikes/s)
Reward cue
Airpuff cue
Reward
Airpuff
No reward
No airpuff
Salience
coding
DA neurons
(spikes/s)
Time after event (s)
C
mPFC
BNST
DRN
VP
PPTg
VTA
LDTg
LHb
PAG
LHT
RMTg
nAcc
Interneuron
Neuron
MSN
Dopamine
Glutamate
GABA
Dopamine–glutamate
Dopamine–GABA
Glutamate–GABA
Cholinergic
D
Olfactory receptor
neurons (ORNs)
Projection
neurons (PNs)
Mushroom
body
Lateral horn
Antennal lobe
PN-ORN matching
Olfactory
sensory organ
Glomeruli
Higher
brain
centers
E
A
B
Training
Test
F
Sugar
Odor
Color
Electric
Shock
PN
?
CA
PAM
(Reward)
PPL1
(Punishment)
Approach
Avoidance
G
MBONs
DANs
γ lobe
γ1
γ2
γ3
γ4
γ5

## Chapter Two

# Mushroom body dopamine neurons, output neurons and RLNs form a tripartite network

## Introduction

It is well known that dopamine neurons in mammals encode prediction errors. In appetitive or reward conditioning using odor as conditioned stimuli, dopamine neurons initially respond to primary rewards but not to odor stimulation. After many trials of conditioning, dopamine neurons terminate or reduce its response to primary rewards but start to respond to reward predicting conditioned stimuli. Moreover, dopamine neurons even show suppression of activity in response to omission of rewards, representing surprise or unexpected errors. Naturally, people ask whether dopamine neurons also encode prediction errors in insects, such as fruit flies. However, it is still unclear whether fruit fly dopamine neurons (DANs) are capable of doing so. Therefore, we designed a training-under-the-microscope setup to investigate dopamine neurons activity during aversive olfactory conditioning. In this setup, neurons of interest were monitored by GCaMP6, when odor stimulation was being paired with 1 $\mu$A electric shocks delivered to individual fruit fly's legs as punishment. By using the setup, we performed an unbiased screen to identify neurons that undergo changes in response to CS+/CS- during and after aversive olfactory conditioning. First we found that punishment DANs display stronger response to CS+ than CS-. Conversely, reward DANs display stronger response to CS- than CS+. It suggests that because of dopamine neuron firing in response to CS-, CS- is also encoded as part of aversive olfactory memory. Second, we identified a group of previously unknown neurons, which we refer to as recurrent loop neurons (RLNs). Those RLNs also encode the valence of conditioned stimuli: one group of RLNs shows stronger response to CS+ while the other group shows stronger response to CS-. Third, we demonstrate that RLNs as well as MBONs activate dopamine neurons in a way that relays the conditioned valence of reward or punishment. RLNs or MBONs of negative valence

activate punishment DANs. The same is true with positive-valence RLNs/MBONs and reward DANs. Last, we examined DANs' activity during conditioning with RLNs' or MBONs' output blocked by *Shi*$^{ts1}$. We found that with RLN1 output blocked, reward DANs' response to CS- was suppressed. With avoidance MBONs' output blocked, inhibition of reward DANs' response to CS+ was relieved. It indicates that RLN or MBONs activity is critical for normal function of DANs during conditioning.

# Results

## 1. A screen of horizontal lobe extrinsic neurons for plasticity

To screen MB horizontal lobe extrinsic neurons for plasticity, we devised a robust method for live imaging of $Ca^{2+}$ dynamics during aversive olfactory conditioning (Figure S1). In this method, a fly's legs were tethered to copper wires in a non-toxic conductive way. The animals were subjected to electric current similar to what is usually used for free moving animals in a large-scale training apparatus when they were being exposed to an airstream containing an odorant (CS+ odorant). After a short exposure to pure air, a second odor (CS-) was presented in the absence of shock. With this approach, pairing an odor with electric shock punishment resulted in robust plasticity in neurons, such as MB extrinsic neurons, that could potentially participate in memory storage and execution. In most of our experiments, multiple cycles of conditioning were used to examine the change of neuronal responses as memory could be strengthened by repetition, which could make it easier to detect subtle changes. Using this method, we screened for neurons that changed their activity during conditioning reported by calcium indicators, instead of conventional behavioral assays. Lines of interest were selected by visual inspection. After identifying all relevant neurons, we then applied optogenetics and

morphological or GRASP analysis, in an effort to examine their connectivity and to assemble them into a neural circuit. These circuit components were then examined by genetic silencing to investigate whether silencing those neurons causes defects in behavior and whether those behavior defects correspond with neurons' functions in the circuit.

**2. Mushroom body dopamine neurons display training dependent plasticity**

Among neurons that could be readily identified based on prior work, we first focused on DANs that project axons into the MB horizontal lobes. Most of these DANs respond strongly to either electric shock or to odor (Figure 1 and S2). For example, the $\gamma 3$ DAN, which plays a role in aversive conditioning, responds strongly to electric shocks (ES) (Figure 1C). Interestingly, the DANs $\gamma 4$ and $\gamma 5$, which are required for appetitive memory [8, 45, 46], also appear to respond to ES during a canonical one minute odor-paired training regime (Figure 1D), as well as in single short ES trials (Figure S2A). Careful analysis shows that these DANs are actually slightly inhibited by punitive electric shocks and rebound in $Ca^{2+}$ mediated fluorescence after the shock pulse ends (blue and green arrowheads in Figure S2A). Cross-correlation analysis reveals that activation of the $\gamma 4$ DAN commences about 1s after $\gamma 3$ DAN response ends; the $\gamma 5$ DAN displays a similar inverse correlation with a lag of $\sim$2s (Figure S2B). The long-term dynamics of shock-evoked responses varied across the DANs; the $\gamma 4$ DAN's response rebounds briefly and then returns to baseline, whereas the $\gamma 5$ DAN exhibits a sustained, relatively strong and slowly increasing response to shock (Figure S2A). It is possible that the rebound activity of the reward-associated DANs encodes a small 'relief response' that signals the end of a punitive stimulus.

We define neurons as plastic if they exhibit training dependent changes in odor-evoked responses to CS+ or CS- odors during conditioning or afterward, in the test cycle. The horizontal lobe $\gamma 3, \gamma 4, \gamma 5, \beta' 1$ and $\beta' 2$ DANs displayed response plasticity (Figure 1C, 1D, 1E and S4a). For the $\gamma 3$ DAN, plasticity was obscured during conditioning by strong ES activation but revealed by the subsequent 'odor only' test cycle: the $\gamma 3$ response to CS+ became increased relative to CS- eventually (Figure 1C). DANs with reward functions, such as $\gamma 4$ and $\beta' 2$ DANs, on the other hand, responded more strongly to CS- than to CS+ after five spaced cycles of conditioning (Figure 1D and 1F). For instance, the $\gamma 4$ DAN response to paired CS+ and ES was initially much stronger than to CS-, a response that was not observed with presentation of odor or shock alone (see below).

This response was rapidly modified after the first training cycle. The $\gamma 4$ response to CS- odor increased dramatically whereas the CS+ response decreased, as the cycles progressed. At the test cycle, the CS- evoked response was significantly stronger than the CS+ response. In contrast, the reward $\beta' 2$ DANs mostly decreased their response to CS+ paired with ES as training continued, such that the CS- response was differentially greater by the test cycle (Figure 1E and 1F). The reward DANs $\beta' 1$ and $\alpha 1$ likewise displayed a differential increase in the response to CS- over the course of training (Figure S4a). In contrast to the other DANs, the reward $\gamma 5$ DAN displayed an enhanced response to both the CS+ and CS- odors by the test cycle. Thus, overall, punishment DANs implicated in learned aversive responses increased its relative response to CS+, while reward DANs implicated in learned appetitive responses increased their relative response to CS-. A second feature of DAN plasticity occurred at the cessation of odor presentation. The $\gamma 4$ and $\beta' 2$ DANs displayed a strong odor-off response that was modified by training (Figure 3B and 3C). In particular, the $\gamma 4$ DAN's odor-OFF

response to CS+ increased relative to CS- (Figure 3B and 3E), and might represent relief from the odor paired with punishment. The odor-OFF response might thus encode the valence associated with the transition from a conditioned odor to pure air.

The odor-evoked responses and response plasticity of mock-trained animals (odor presentation without ES) were significantly lower than those observed in trained animals (Figure 1G). There was some evidence of plasticity due to the repeated odor presentation. For example, the first presentation of CS+ to the $\gamma 4$ DAN resulted in a small response that diminished in subsequent cycles. Interestingly, in combination with ES, this response to odor in the first training cycle was much (2-fold) larger and longer lasting (compare Figure 1F and G). This initial excitation was completely abolished by the third cycle in both the control and trained animals. A similar phenomenon was observed for the $\gamma 5$ DAN, but with an amplitude that increased over training cycles (Figure S4a). One might suppose that the $\gamma 4$ and $\gamma 5$ neurons are combinatorially gated by odor and ES, a gating that is subject to plasticity. Our data suggests that DANs that contribute to aversive and reward learning display corresponding valence changes in responses to CS+ and CS- odors. Hereafter, we refer to DANs that displayed training dependent plasticity as *plastic* DANs (pDANs). In summary, these results demonstrate that MB horizontal lobe DANs display training dependent odor-ON and odor-Off response plasticity in a manner consistent with their behavioral valence, creating a self-reinforcing loop. The existence of the self-reinforcing loop raises the question of whether reward or punishment DANs both play a direct role in decision-making or memory recall by directly signaling with downstream neurons, in addition to releasing reinforcement signal during conditioning.

**Figure 1. Aversive olfactory conditioning induces enhanced response to CS+ in punishment DANs and enhanced response to CS- in reward DANs.**

(A-B) Example images of CS+ and CS- evoked GCaMP6s fluorescence recorded from PAM-DANs axons in a living fly on two different imaging focal planes. Genotype: R58E02>GAL4; UAS>GCaMP6s. (A): $\gamma 3, \gamma 4$ and $\gamma 5$ DANs were imaged on the same focal plane. (B): $\alpha 1, \beta 2$ and $\beta' 2$ DANs were on the same focal plane. (C-E) Aversive olfactory training induces self-reinforcing changes of odor-evoked activity of DANs. (C-E): in each row, calcium activity of $\gamma 3$ (n=11), $\gamma 4$ (n=11) and $\beta' 2$ (n=9) DANs were imaged during 5-cycle conditioning. The first 3 columns display DANs calcium traces in cycle 1,3,5 (training cycles) and the last column displays DANs calcium trace in test cycle. Dashed line denotes odor onset. Red trace denotes DANs activity during CS+ presentation (CS+ plus shock in training cycles) and green trace denotes DANs activity during CS- presentation. Data are mean [solid line] $\pm$ MSE [shaded area] curves. (F-G) Plot of DANs GCaMP6s fluorescence over training cycles. Calcium activity was calculated by averaging the fluorescence over the first 8 seconds after odor onset. Red curved lines denote DAN activity during CS+ presentation and green curved line during CS- presentation. Data are mean $\pm$ MSE. One asterisk denotes $p<0.05$ and two asterisks denotes $p<0.01$. (Paired t-test) (F): DANs activity in aversive olfactory training. (G): DANs activity in mock-train controls.

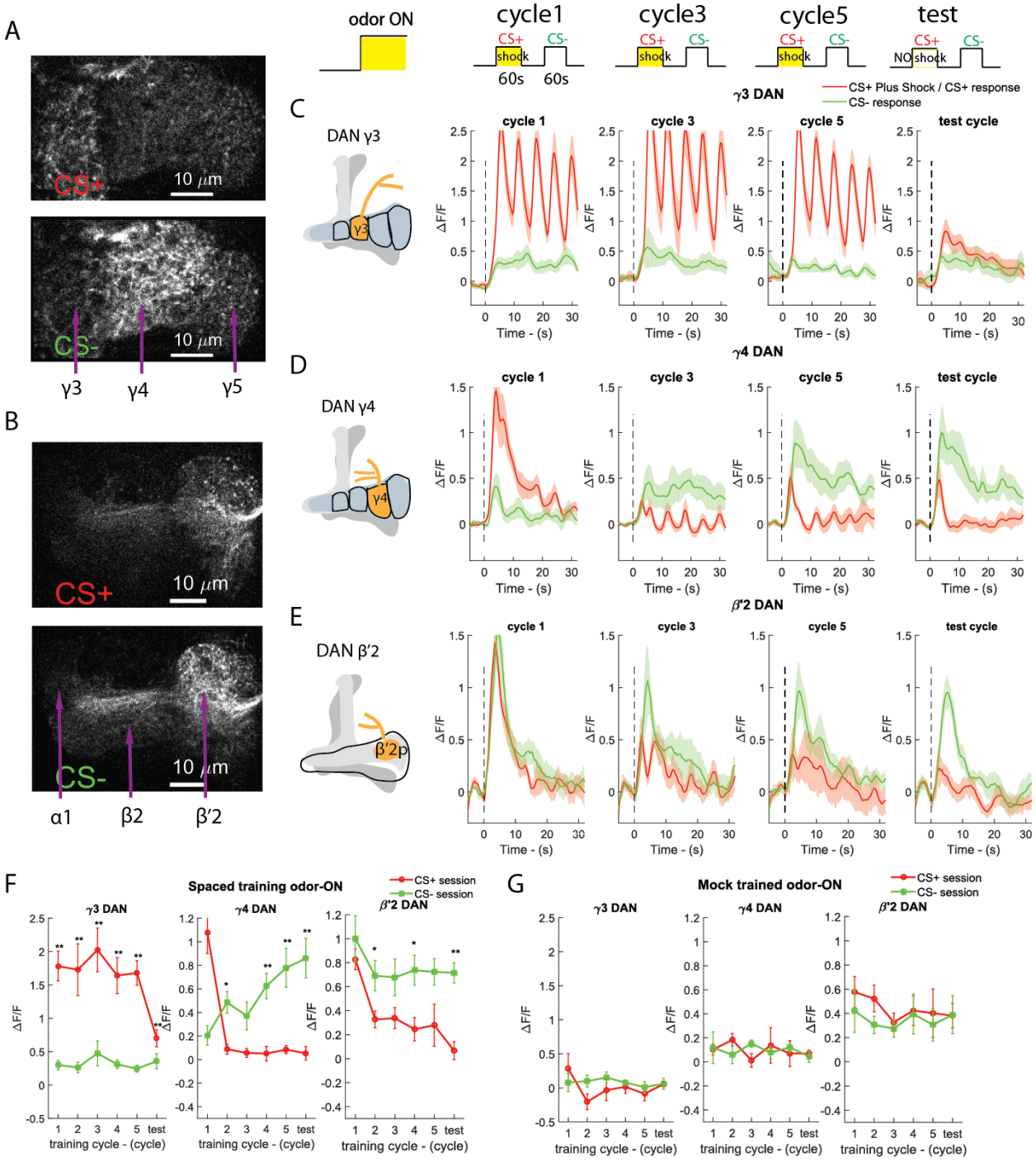
A
CS+
10 μm
CS-
10 μm
γ3
γ4
γ5
B
CS+
10 μm
CS-
10 μm
α1
β2
β'2
odor ON
cycle1
cycle3
cycle5
test
CS+
CS-
shock
NO shock
60s
60s
C
DAN γ3
γ3
γ3 DAN
CS+ Plus Shock / CS+ response
CS- response
cycle 1
cycle 3
cycle 5
test cycle
ΔF/F
Time - (s)
D
DAN γ4
γ4
γ4 DAN
E
DAN β'2
β'2p
β'2 DAN
F
Spaced training odor-ON
CS+ session
CS- session
γ3 DAN
γ4 DAN
β'2 DAN
training cycle - (cycle)
G
Mock trained odor-ON
CS+ session
CS- session
γ3 DAN
γ4 DAN
β'2 DAN
training cycle - (cycle)

**3. Recurrent loop neurons (RLNs)**

Since we observed that most DANs are activated by odorants (Figure 1) and many display plasticity, we sought similar plastic circuit components that might act upstream and transmit odor inputs to the DANs. We considered neurons with projections into regions that include the DAN's dendritic fields, such as the Crepine (CRE) and Superiomedial Protocerebrum (SMP) neuropil (Figure 2A). Five lines were identified that conferred GCaMP6s expression in neurons in these regions, and which displayed training-dependent plasticity in their odor-evoked $Ca^{2+}$ response. From these lines, we identified two neurons, which we refer to as Recurrent Loop Neurons (RLN1, R86D02 and RLN2, R33E06) that evidently act upstream of pDANs to transmit conditioned odor inputs. Both RLN1 and RLN2 are glutamatergic (Figure 2B, 2C, S5A and S5B). With their cell bodies distributed in irregular regions across the brain as shown in diagrams in Figure 2D and 2G, their presynaptic axonal terminals are both located in SMP (Figure 2F and 2I). It is worth to mention that RLN1's branches are mostly located in lateral regions of SMP (Figure 2E) whereas RLN2's branches are close to midline (Figure 2H). There are multiple neurons in line R86D02 and separate labeling of these neurons by MCFO [80] is described in Figure S5.

Like the $\gamma$4 DANs, neuron RLN1 displayed an odor-evoked calcium response to CS- that was modified over the course of the conditioning protocol (Figure 2J). At the outset of training (cycle 1), the response to CS+ and CS- was equivalent. As training progressed, the response to CS+ decreased dramatically as the response to CS- increased. By the test cycle, the relative responses to CS+ and CS- differed by approximately 2-fold (Figure 2J and 2L). The odor activation of RLN1 notably begins strongly and diminishes over the course of the 30-second odor presentation. Interestingly the pattern of RLN1 odor response and modification over the

course of the conditioning protocol roughly matches the behavior of the $\gamma 4$ and $\beta' 2$ DANs (compare Figure 2J and Figure 1D-E). Notably, RLN1 fires as strongly at the cessation of odor stimulation as it does at the onset of odor (Figure 3A). This odor-OFF response also mirrors the activity of reward $\gamma 4$ and $\beta' 2$p DANs (Figure 3). Moreover, the off-response displays plasticity of opposite polarity to the neuron's odor-ON response. RLN1 neurons exhibit stronger odor-OFF response to ending of CS+ paired ES. It is worth to notice that RLN1's strong odor-OFF response to ending of CS+ paired ES is similar to reward DANs as well (Figure 3). The overall similarity between RLN1 and reward DANs activity suggests that RLN1 could be one of the main excitatory inputs for reward DANs, contributing to both plastic odor-ON and odor-OFF response.

In contrast, the neuron RLN2 displayed behavior reminiscent of the $\gamma 3$ DAN. Like the $\gamma 3$ DAN, the RLN2 neuron responded to the combined presentation of ES and CS+, a response that slightly increased in amplitude over the training cycles (Figure 2K). Moreover, the response to CS- slightly decreased over the course of the training cycles. By the odor test presentation, RLN2 was activated by CS+ and inhibited by CS- (Figure 2K and 2L). This behavior is roughly similar to that of the $\gamma 3$ DAN, though different in some significant respects. The amplitude of the RLN2 response to CS+ and ES is considerably less than that for the $\gamma 3$ DAN. Electric shock excites $\gamma 3$ DAN to a high peak of activity whereas the excitation of RLN2 is more persistent with weak peaks of activity caused by ES. Besides, the difference in response to CS- relative to CS+ at the test cycle was considerably greater for RLN2 than for the $\gamma 3$ DAN. These data reveal that RLN1 and RLN2 respond to odor and ES stimulation and display plasticity reminiscent of DANs that respond with opposing valences to conditioning. Since RLN1 and RLN2 project axons into SMP close to the dendrites of DANs, it appears that they participate in

a feedback loop that connects odor input and aversive conditioning to the modified activity of reward and punishment DANs, respectively. Therefore, we went on to investigate the connectivity between RLNs and DANs.

In summary, RLN1 encodes the positive and attraction valence of CS- since RLN1 response to CS- becomes stronger after conditioning. Therefore, we define RLN1 as an attraction neuron. Likewise RLN2 encodes the negative and repulsion valence of CS+ since its response to CS+ becomes stronger. We define RLN2 as a repulsion neuron. We'll see the importance of the definition in the paragraphs below.

**Figure 2. Aversive olfactory conditioning induces changes in odor-evoked responses in recurrent loop neurons (RLNs).**

(A) Schematic of Superior medial protocerebrum (SMP) and Crepine (CRE) regions close to mushroom body lobes. (B-C) Immunoreactivity of RLNs axon terminals. Single optical focal planes; axon terminals are shown in green and antibody staining in magenta. Axon terminals of both RLN1 (R86D02) and RLN2 (R33E06) were labeled with anti *Drosophila* vesicular glutamate transporter (anti-dVGluT) antibody (arrows), indicating they are both glutamatergic. (D, G) Schematic of RLN1 and RLN2 neurons in proximity to MB lobes. (E, H) Distribution of myristoylate::GFP (green) in RLN neurons driven by R86D02 (RLN1) and R33E06 (RLN2). Neuropils were labeled with an antibody to bruchpilot (nc82). Mushroom body (MB) lobes were outlined in dashed lines. From left to right are shown RLNs branches from shallow to deeper areas in SMP and CRE regions, surrounding but not inside MB lobes. (F,I) Distribution of synaptotagmin::GFP (green) in RLN neurons driven by R86D02 (RLN1) and R33E06 (RLN2). MB lobes were outlined in dashed lines. Axon terminals of both RLNs are located in SMP outside MB lobes. (J-K) Aversive olfactory training induces changes of odor-evoked activity of RLNs. Left: Example images of CS+ and CS- evoked GCaMP6s fluorescence recorded from RLN1 and RLN2 axons in a living fly; right: calcium traces of RLN1 (R86D02, n=10) and RLN2 (R33E06, n=9) in cycle 1,2,3,5 and test cycle in aversive olfactory training. Red trace denotes response to CS+ presentation (CS+ plus shock in training cycles) and green trace to CS- presentation. Data are mean [solid line] $\pm$ MSE [shaded area] curves. Dashed line denotes odor onset. (L-M) Plot of RLNs GCaMP6s fluorescence over training cycles. Calcium activity was calculated by averaging the fluorescence over the first 8 seconds after odor onset. Red curved lines denote activity during CS+ presentation and green curved line during CS- presentation. Data are mean $\pm$ MSE. One asterisk denotes $p<0.05$ and two asterisks denotes

$p<0.01$. (Paired t-test) (L): RLNs activity in aversive olfactory training. (M): RLNs activity in mock-train controls.

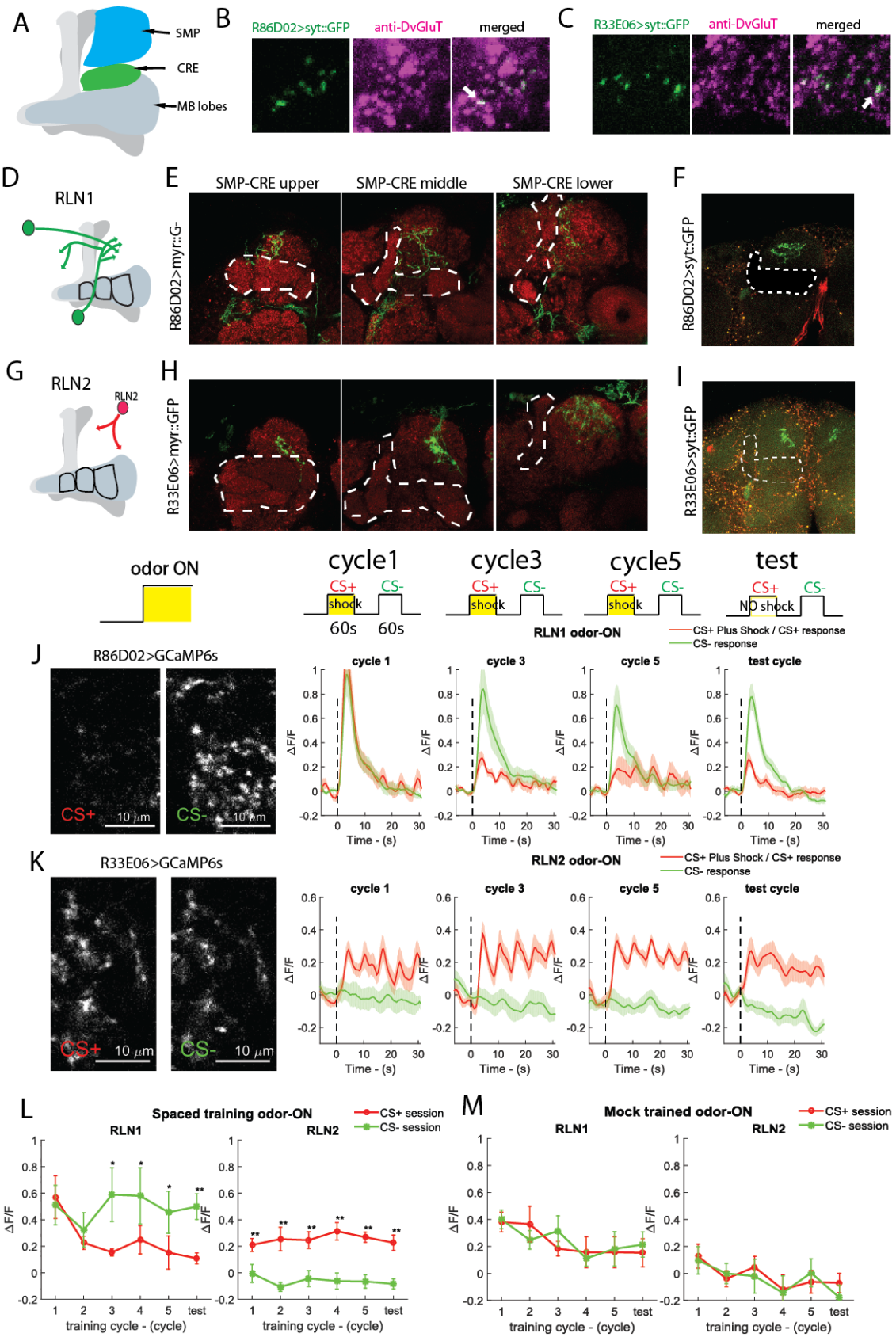
A
SMP
CRE
MB lobes
B
R86D02>syt::GFP
anti-DvGluT
merged
C
R33E06>syt::GFP
anti-DvGluT
merged
D
RLN1
E
SMP-CRE upper
SMP-CRE middle
SMP-CRE lower
R86D02>myr::GFP
F
R86D02>syt::GFP
G
RLN2
RLN2
H
R33E06>myr::GFP
I
R33E06>syt::GFP
odor ON
cycle1
cycle3
cycle5
test
CS+
CS-
shock
NO shock
60s
60s
J
R86D02>GCaMP6s
CS+
CS-
10 μm
RLN1 odor-ON
CS+ Plus Shock / CS+ response
CS- response
cycle 1
cycle 3
cycle 5
test cycle
ΔF/F
Time - (s)
K
R33E06>GCaMP6s
RLN2 odor-ON
L
Spaced training odor-ON
CS+ session
CS- session
RLN1
RLN2
training cycle - (cycle)
M
Mock trained odor-ON

**Figure 3. RLN1 and reward DANs display strong odor-OFF response**

(A-C) Attraction neuron RLN1 and reward DANs respond to cessation of odor stimulation during aversive olfactory conditioning. In each row, calcium activity of RLN1 (n=10), $\gamma 4$ (n=11) and $\beta' 2$ (n=9) DANs were imaged during 5-cycle conditioning. Calcium traces in cycle 1,3,5 (training cycles) are displayed in the first three columns and the calcium trace in test cycle displayed in test cycle. Red trace denotes activity during CS+ presentation (CS+ plus shock in training cycles) and green trace denotes activity during CS- presentation. Data are mean [solid line] $\pm$ MSE [shaded area] curves. Dashed line in each panel denotes odor cessation point after 60s long odor presentation; time point 0 represents odor cessation time point (60s after odor onset). (D-F) Plot of GCaMP6s fluorescence in response to odor cessation over training cycles. Calcium activity was calculated by averaging the fluorescence over the first 8 seconds after odor cessation. Red curved lines denote activity during CS+ presentation (CS+ plus shock in training cycles) and green curved line during CS- presentation. Data are mean $\pm$ MSE. One asterisk denotes $p<0.05$ and two asterisks denotes $p<0.01$. (Paired t-test) For each row, column on the left shows data in aversive olfactory training and column on the right shows mock-train controls.

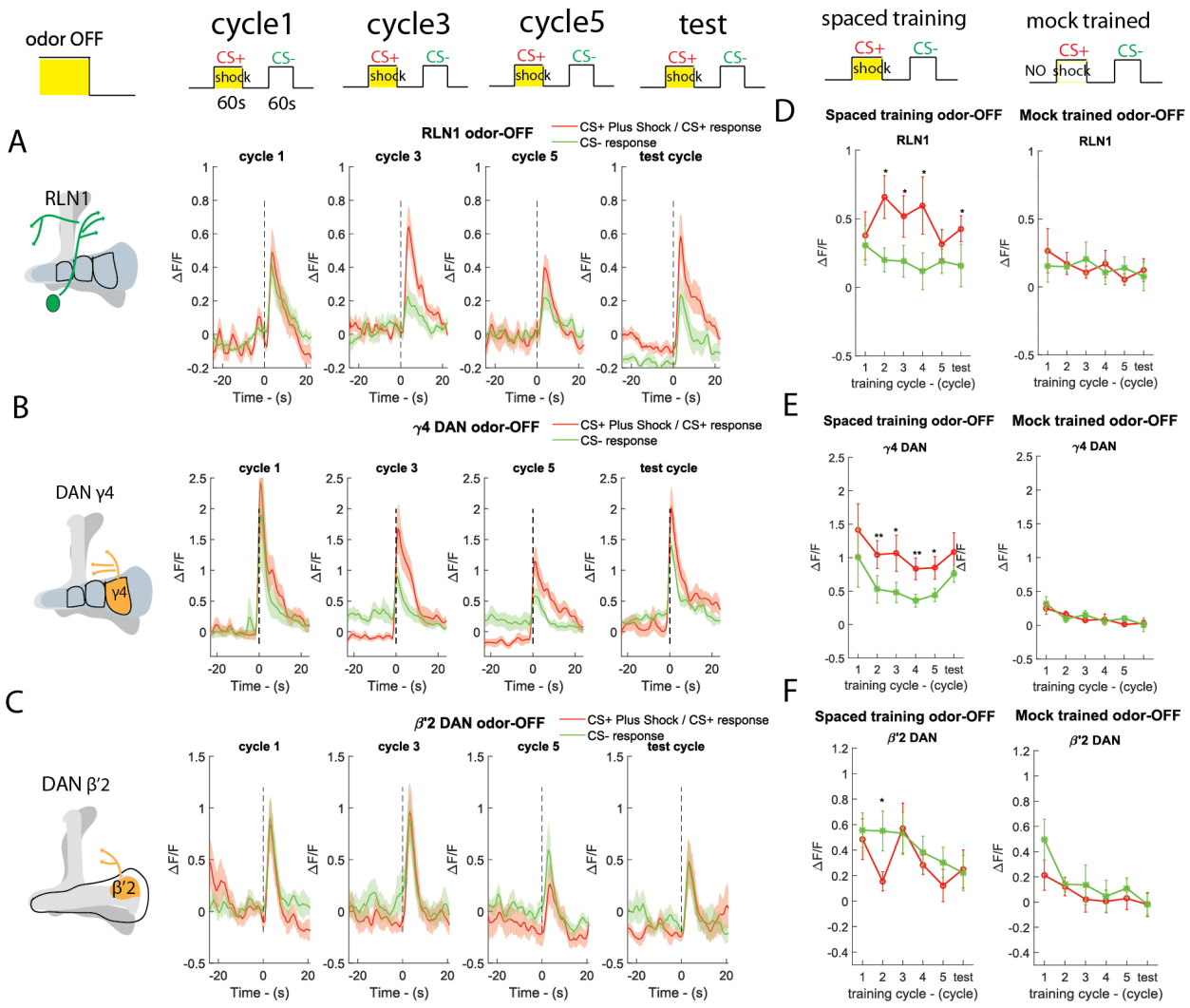
odor OFF
cycle1
cycle3
cycle5
test
CS+
CS-
shock
60s
60s
spaced training
mock trained
NO shock
A
RLN1
RLN1 odor-OFF
CS+ Plus Shock / CS+ response
CS- response
cycle 1
cycle 3
cycle 5
test cycle
ΔF/F
Time - (s)
B
DAN γ4
γ4 DAN odor-OFF
C
DAN β'2
β'2 DAN odor-OFF
D
Spaced training odor-OFF
Mock trained odor-OFF
RLN1
training cycle - (cycle)
E
γ4 DAN
F
β'2 DAN

**4. RLNs relay valence of conditioned stimuli to Mushroom body Dopamine Neurons**

Given the convergent localizations of MBON, pDAN and RLN axons and dendrites, we sought to determine to what extent these reflected close membranous associations that are typical of synapses. We used GFP Reconstitution Across Synaptic Partners (GRASP) approach [81], in which two complementary GFP fragments becomes a functional fully fluorescent protein when presented in close proximity at synapses between pre- and post-synaptic partners. The possible interactions between RLNs and DANs was explored by expressing Split-GFP11 in RLN1 (with R86D06-lexA) or RLN2 (with R33E06-lexA) and complementary splitGFP1-10 in a set of horizontal lobe MBONs ($\gamma 3, \gamma 4$ or $\beta' 2$) using split-GAL4 lines [65] to achieve high selectivity in MBON expression. In Figure 5, nc82 staining is presented in red, reconstituted GFP in green, and spGFP1-10 staining in blue. Since spGFP1-10 is expressed in MBONs, neuronal fibers of MBONs are shown in blue. Z-projection was performed on green and blue channels so that all GFP punctae in one image stack are clumped into a single slice to allow for a rough estimate of the amount and strength of punctae. As we can see in Figure 4, while there is only a low level of connection between RLN1 and $\gamma 3$ (Figure 4A), RLN2 makes strong connections with $\gamma 3$ DANs (Figure 4D). On the other hand, RLN2 makes more extensive connections with $\beta' 2$ DAN (Figure 4C) whereas RLN1 only makes a few contacts with it (Figure 4F). Since attraction neuron RLN1 encodes the valence of CS- and repulsion neuron RLN2 encodes the valence of CS+, it suggests that punishment DANs likely receive input from avoidance neuron and reward DANs likely receive input from attraction neurons. In this scenario, reward DANs should display stronger response to CS- because of connection to attraction neuron RLN1 and the same goes with punishment DANs and repulsion neuron RLN2. Notably, careful examination shows that connections made by RLN1 and RLN2 are

located in separate regions. RLN1's connections tend to be in lateral regions of SMP whereas RLN2's connections tend to be close to brain midline, reflecting RLNs' branch locations in SMP.

In order to verify the existence of feedback loop, we sought to map out the functional connectivity between DANs and RLNs. In order to activate specific group of neurons, we used optogenetics approach by expressing CsChrimson in RLNs. CsChrimson was expressed selectively in RLNs by split GAL4 drivers for activation by 633nm red light when GCaMP6s was expressed in horizontal-lobe DANs by R58E02-lexA for recording. We recorded activity in $\gamma 3$, $\gamma 4$, $\gamma 5$ and $\beta' 2$ DANs. GAL4 lines R86D02 and R33E06 were used to stimulate RLN1 and RLN2 respectively. As shown in Figure 4, attraction neuron RLN1 strongly activated reward $\gamma 4$ and $\beta' 2$ DAN (Figure 4B and C) but only slightly activated punishment DAN $\gamma 3$ (Figure 4A). On the opposite, repulsion neuron RLN2 inhibited punishment $\gamma 4$ and $\beta' 2$ DANs (Figure 4F) and activated punishment DAN $\gamma 3$ (Figure 4D). It indicates that reward DANs receives not only excitatory input from attraction neurons but also inhibitory input from repulsion neurons and the opposite goes with punishment DANs.

**5. A Tripartite Feedback Circuit of MBONs, RLNs and pDANs**

A prominent class of neurons exhibiting plasticity in our screen was the previously identified MBONs. These included the $\gamma 1$ MBON and $\gamma 5 \beta' 2$ MBON, which previously were shown to display conditioned plasticity [71, 82]. In addition, we found the horizontal-lobe MBONs $\gamma 2 \alpha' 1$, $\gamma 3$ and $\gamma 4$->$\gamma 1 \gamma 2$ displayed conditioned plasticity (Figure 5). Given that MBONs are the principal output of odor representations in the MB, we explored their relationship to RLN and DAN odor responses and conditioned plasticity.

**Figure 4. Dopamine neurons (DANs) receive feedback input from RLNs.**

In each panel, on the left is anatomical connectivity examined by GFP Reconstitution Across Synaptic Partners (GRASP). MB lobes were outlined in dashed lines; nc82 is in red, DANs in blue and GFP in green (arrows). All GFP punctae in an entire image stack was projected onto one plane. On the right is functional connectivity examined by artificial activation of RLNs. CsChrimson was expressed in RLNs by GAL4 lines and GCaMP6s was expressed in DANs by R58E02>lexA. DANs activity was recorded while $\sim 10 \mu w/mm^2$. Red dashed line denotes ~80ms light stimulations and 3 light pulses were delivered with an interval of 2sec for a total of 5.5 seconds. (A-C): Connectivity between RLN1 and $\gamma 3$ (mb441b), $\gamma 4$ (mb316b) and $\beta' 2$ (mb056b) DANs. (D-F): Connectivity between RLN2 and DANs.

RLN1 connection with γ3 DAN, γ4 DAN and β'2 DANs

RLN2 conection with γ3 DAN, γ4 DAN and β'2 DANs

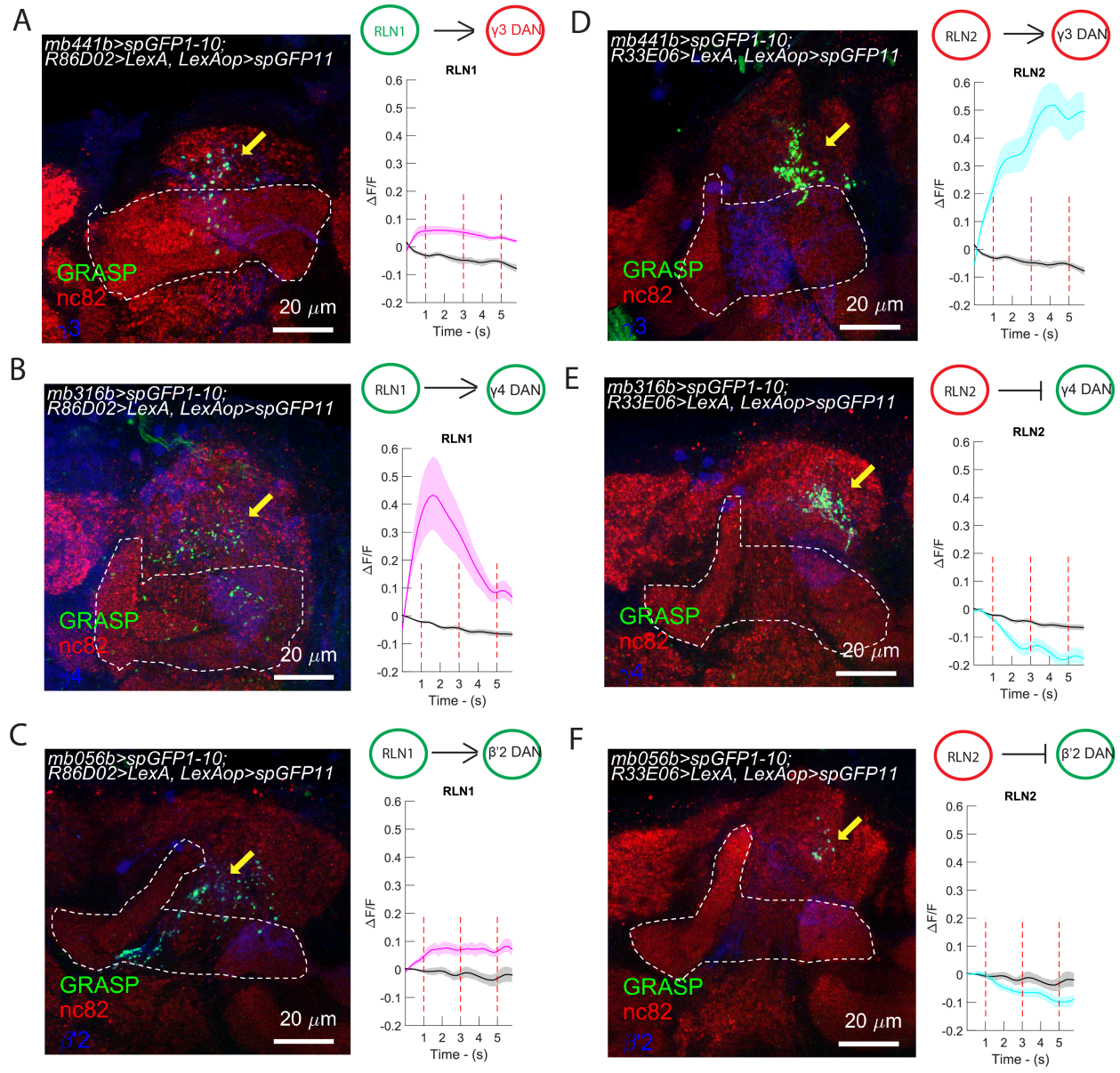

MBONs displayed various conditioning-related dynamic changes in $Ca^{2+}$ reporter fluorescence in response to odor exposure. Most significantly, these included responses of opposing valences to the CS+ and CS- odors during and after conditioning. For nearly all MBONs, the response to odorants decreased to a certain extent over the course of repetitive training cycles (Figure 5E, F, G and H), which might reflect mere habituation to repeated odor presentations. However, the $\gamma 2\alpha' 1$ and $\gamma 3$ MBONs retained a much greater response to the CS- odor as compared to CS+ odor (Figure 5A and 5B). In contrast, for $\gamma 4$->$\gamma 1\gamma 2$ and $\gamma 5\beta' 2$ MBONs, the response to CS+ remained stronger than to the CS- odor during conditioning and the test cycle (Figure 5C and 5D). As a general rule, dopamine release inhibits conditioned odor response. Moreover, training-induced change in the response to CS+ and CS- takes place as early as the first training cycle for nearly all MBONs investigated. For instance, the differential response of MBON- $\gamma 2\alpha' 1$ becomes significant just 12 minutes at the second cycle of conditioning (Figure 5A). Based on these data, we define MBONs as mediating attraction or repulsion in a manner analogous to RLNs; on the basis of conditioned odor valence (see Discussion).

We further used GRASP to investigate connections between MBONs and RLNs. Similar to the setup discussed earlier, lexA line were used to drive expression of split-GFP11 in RLNs and split-GAL4 lines to drive expression of split-GFP1-10 in MBONs. From Figure 5I and 5J, we can see that RLN1 make strong connections with $\beta' 2$ (mb011b) and $\gamma 2\alpha' 1$ (mb077b) MBONs, and RLN2 make strong connections with $\beta' 2$ MBONs. Connections between RLNs and $\gamma 3$ and $\gamma 4$ MBONs were also tested but little GFP signal was observed. Both RLN1 and RLN2 receive input from MBONs [66]. Furthermore, RLN1's connection with $\beta' 2$ and $\gamma 2\alpha' 1$ MBONs could potentially explain its stronger response to CS-. $\beta' 2$ and $\gamma 2\alpha' 1$ MBONs are glutamatergic and

cholinergic respectively. Glutamate can be inhibitory neurotransmitter and acetylchoine is excitatory. With $\beta'2$ MBON displaying weaker response to CS- (Figure 5D) and $\gamma2\alpha'1$ MBONs displaying stronger response to CS+ (Figure 5A), RLN1 will display stronger response to CS-. Although RLN2 also makes connections with $\beta'2$ MBONs, glutamate could be excitatory on RLN2, depending on its glutamate receptor.

We also mapped functional connections between MBONs and DANs. Split-GAL4 lines mb011b, mb-$\gamma4$ and mb077b were used to drive CsChrimson in order to stimulate $\gamma5\beta'2$ MBONs, $\gamma4$ MBONs and $\gamma2\alpha'1$ MBONs respectively. As shown in Figure 6, attraction neuron $\gamma2\alpha'1$ MBONs activate both reward $\gamma4$ DANs and $\beta'2$ DANs (Figure 6E), whereas repulsion neurons $\gamma4$ and $\gamma5\beta'2$ MBONs inhibit $\gamma4$ DANs and $\beta'2$ DANs (Figure 6B and D). Similar to pathways from RLNs to DANs, those reward DANs receives excitatory input from attraction MBONs and inhibitory input from avoidance MBONs. Punishment $\gamma3$ DANs are also activated by $\gamma5\beta'2$ MBONs (Figure 6C) and $\gamma4$ MBONs (Figure 6A). Although $\gamma2\alpha'1$ MBONs are attraction neurons, they slightly activate $\gamma3$ DANs as well (Figure 6E). Possible direct connection between DANs and MBONs were also explored by GRASP in Figure 6. Compared to few punctae between $\gamma4$ MBONs and $\gamma3$ DANs and $\beta'2$ DANs (Figure 6A and B), there are more stronger punctae between $\gamma5\beta'2$ MBONs and $\gamma3$ DANs and $\beta'2$ DANs (Figure 6C and D), suggesting direct connection. In summary, we propose a tripartite feedback circuit model with cross-over connectivity as shown in Figure 6F. Reward DANs receive excitatory input from attraction MBONs or RLNs while punishment DANs receive excitatory input from repulsion MBONs or RLNs. At the same time, reward DANs also receive inhibitory input from repulsion MBONs or RLNs and the same could be true with punishment DANs. This circuit mediates experience-dependent modification of odor-evoked response of DANs. Dopamine

release in response to conditioned odors, as a result, further modifies odor-evoked response of MBONs.

**6. Silencing RLNs affects pDAN plasticity**

In order to investigate whether RLNs and MBONs indeed contribute to DANs' conditioned odor response, we used *shi*$^{ts}$ to inhibit the synaptic output of RLNs while imaging the activity of DANs during 5-cycle aversive olfactory conditioning. In comparison to controls, inactivating RLN1 substantially inhibits $\gamma$4 DANs' odor-ON response evoked by CS- especially during cycle 2 to cycle 4 (Figure 7B, D and F), while leaving $\gamma$4 DANs' odor-ON response to CS+ intact. With RLN1 output blocked, $\gamma$4 DANs' response to CS+ was inhibited starting at cycle 2 (Figure 7E). Notably, inactivating RLN1 doesn't affect $\gamma$4 DANs' response to either CS+ or CS- during cycle 1. This could be due to other neurons contributing to $\gamma$4 DANs' activities during the initial phase of conditioning. Blocking output from RLN2 has no effect on $\gamma$4 DANs' conditioned response to odors whereas blocking RLN2 impairs $\gamma$3 DANs response to CS+ during test cycle (Figure 7E). It suggests that RLN2 contributes considerably to $\gamma$3 DANs conditioned response to punitive CS+. However, blocking RLN2 output doesn't impair $\gamma$3 DANs response to electric shocks, suggesting that it doesn't play a major role in ES triggered response of $\gamma$3 DANs. It is likely that somatosensory system for electric shock sensation is the major pathway for $\gamma$3 DANs' response to ES. Although both RLN1 and reward DANs display stronger odor-OFF response to CS+, blocking RLN1 doesn't impair $\gamma$4 DANs' odor-OFF response to CS+ (Figure 7G).

**Figure 5. Mushroom body output neurons (MBONs) are part of dopamine recurrent loop circuits.**

(A-D) Aversive olfactory conditioning induces changes in odor-evoked responses in MBONs. Schematic of each MBON is on the left. From top to bottom, in each row, calcium activity of $\gamma 2\alpha' 1$ (n=11), $\gamma 3$ (n=7), $\gamma 4$ (n=12) and $\beta' 2$ (n=8) MBONs were imaged during 5-cycle conditioning. Calcium traces in cycle 1,3,5 (training cycles) are displayed in the first three columns and the calcium trace in test cycle displayed in the last column. Red trace denotes activity during CS+ presentation (CS+ plus shock in training cycles) and green trace denotes activity during CS- presentation. Data are mean [solid line] $\pm$ MSE [shaded area] curves. Dashed line denotes odor onset. (E-H) On the left are plots of DANs GCaMP6s fluorescence over training cycles. On the right are example pseudo-color images of CS+ and CS- evoked GCaMP6s fluorescence in each MBON type on a single optical plane. Calcium activity in plots was calculated by averaging the fluorescence over the first 8 seconds after odor onset. Data are mean $\pm$ MSE. One asterisk denotes $p<0.05$ and two asterisks denotes $p<0.01$. (Paired t-test) (I-J) Anatomical connectivity betwwen MBONs and RLNs examined by GRASP. MB lobes were outlined in dashed lines; nc82 is in red, DANs in blue and GFP in green (arrows). All GFP punctae in an entire image stack was projected onto one plane. (I): Connectivity between RLN1 and $\beta' 2$(mb011b) and $\gamma 2\alpha' 1$(mb077b) MBONs. (J): Connectivity between RLN2 and MBONs. (K) MBONs respond to odor cessation during aversive olfactory training.

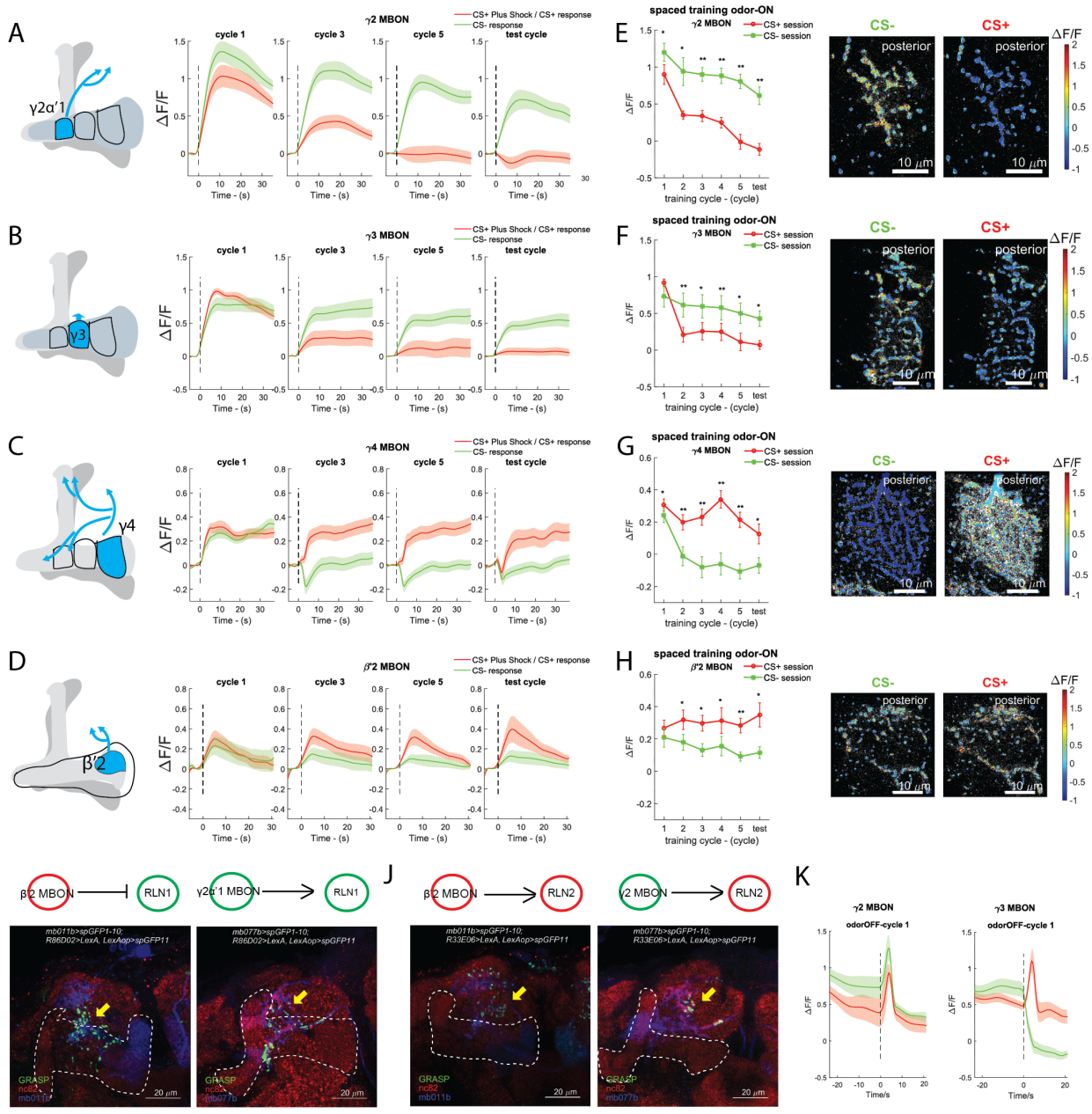
A
γ2α′1
γ2 MBON
CS+ Plus Shock / CS+ response
CS- response
cycle 1
cycle 3
cycle 5
test cycle
ΔF/F
Time - (s)
B
γ3
γ3 MBON
C
γ4
γ4 MBON
D
β′2
β′2 MBON
E
spaced training odor-ON
CS+ session
CS- session
training cycle - (cycle)
F
G
H
CS-
CS+
posterior
10 μm
I
β2 MBON
RLN1
γ2α′1 MBON
J
RLN2
γ2 MBON
mb011b>spGFP1-10; R86D02>LexA, LexAop>spGFP11
mb077b>spGFP1-10; R86D02>LexA, LexAop>spGFP11
mb077b>spGFP1-10; R33E06>LexA, LexAop>spGFP11
GRASP
nc82
20 μm
K
odorOFF-cycle 1
Time/s

**Figure 6. Dopamine neurons (DANs) receive feedback input from RLNs.**

In each panel, on the left is anatomical connectivity examined by GFP Reconstitution Across Synaptic Partners (GRASP). MB lobes were outlined in dashed lines; nc82 is in red, DANs in blue and GFP in green (arrows). All GFP punctae in an entire image stack was projected onto one plane. On the right is functional connectivity examined by artificial activation of RLNs. dTrpA1 was expressed in RLNs by GAL4 lines and GCaMP6s was expressed in DANs by R58E02>lexA. CsChrimson was expressed in RLNs by GAL4 lines and GCaMP6s was expressed in DANs by R58E02>lexA. DANs activity was recorded while ~10$\mu$w/mm$^2$. Red dashed line denotes ~80ms light stimulations and 3 light pulses were delivered with an interval of 2sec for a total of 5.5 seconds. (A-B): Connectivity between $\gamma$4 MBONs and $\gamma$3 (mb441b) and $\beta'$2(mb056b) DANs. (C-D): Connectivity between $\beta'$2 MBONs and DANs. (E): Connectivity between $\gamma$2 MBONs and DANs. (F): Working model of tripartite feedback network.

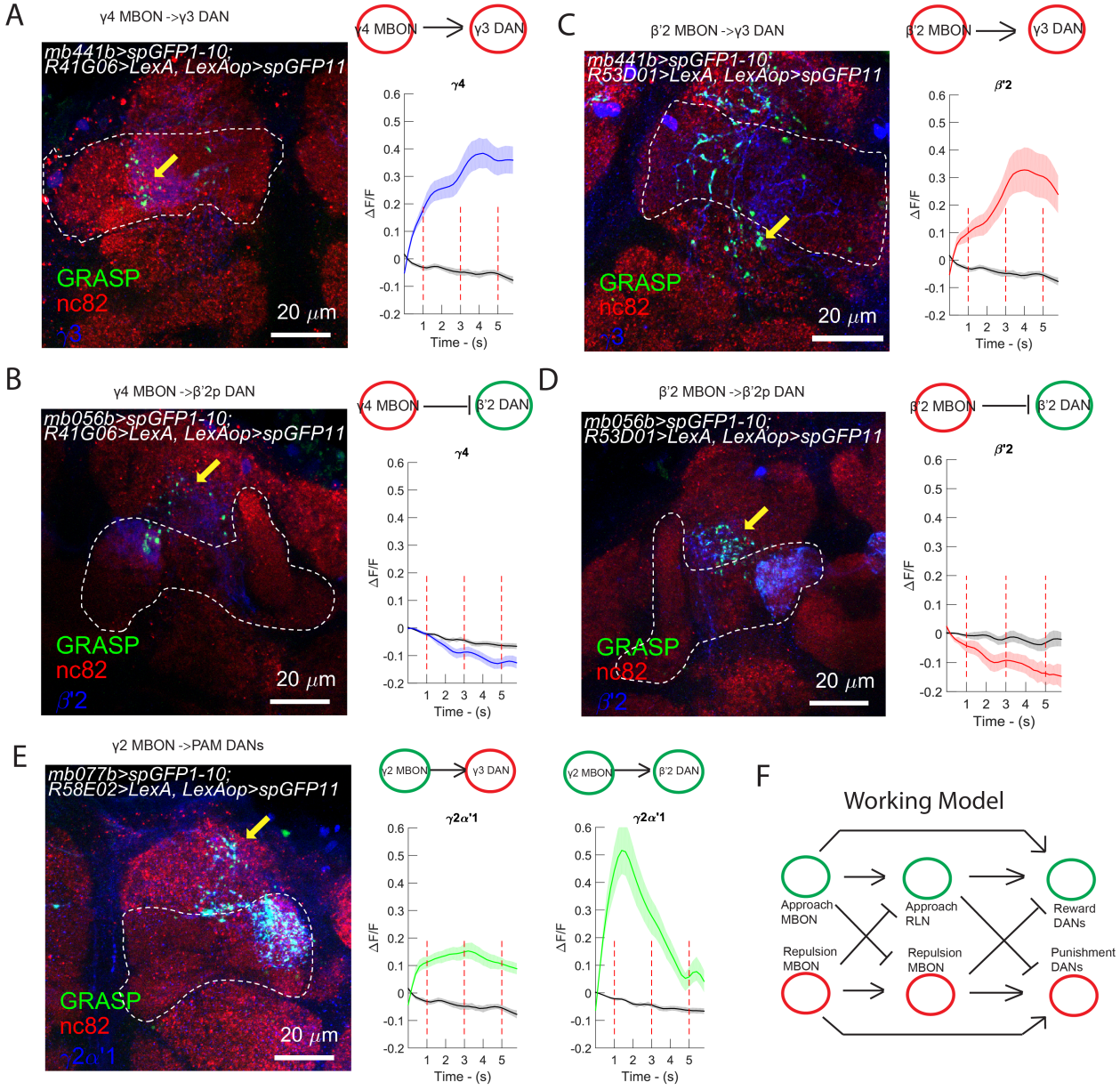
A
γ4 MBON ->γ3 DAN
mb441b>spGFP1-10;
R41G06>LexA, LexAop>spGFP11
GRASP
nc82
γ3
20 μm
γ4 MBON
γ3 DAN
γ4
ΔF/F
Time - (s)
C
β'2 MBON ->γ3 DAN
mb441b>spGFP1-10;
R53D01>LexA, LexAop>spGFP11
GRASP
nc82
γ3
20 μm
β'2 MBON
γ3 DAN
β'2
ΔF/F
Time - (s)
B
γ4 MBON ->β'2p DAN
mb056b>spGFP1-10;
R41G06>LexA, LexAop>spGFP11
GRASP
nc82
β'2
20 μm
γ4 MBON
β'2 DAN
γ4
ΔF/F
Time - (s)
D
β'2 MBON ->β'2p DAN
mb056b>spGFP1-10;
R53D01>LexA, LexAop>spGFP11
GRASP
nc82
β'2
20 μm
β'2 MBON
β'2 DAN
β'2
ΔF/F
Time - (s)
E
γ2 MBON ->PAM DANs
mb077b>spGFP1-10;
R58E02>LexA, LexAop>spGFP11
GRASP
nc82
γ2α'1
20 μm
γ2 MBON
γ3 DAN
γ2 MBON
β'2 DAN
γ2α'1
ΔF/F
Time - (s)
F
Working Model
Approach MBON
Repulsion MBON
Approach RLN
Repulsion MBON
Reward DANs
Punishment DANs

**Figure 7. Blocking output of RLNs impairs conditioned DAN response to odors.**

(A-D) Activity of $\gamma 3$ and $\gamma 4$ DANs during 5-cycle aversive conditioning with RLN1 (n=19) or RLN2 (n=11) output blocked. In each panel, the first 3 columns display DANs calcium traces in cycle 1,3,5 (training cycles) and the last column displays DANs calcium trace in test cycle. Dashed line denotes odor onset. Red trace denotes DANs activity during CS+ presentation (CS+ plus shock in training cycles) and green trace denotes DANs activity during CS- presentation. Data are mean [solid line] $\pm$ MSE [shaded area] curves. (A-B): Activity of $\gamma 3$ and $\gamma 4$ DANs with RLN1 blocked. (C-D): Activity of $\gamma 3$ and $\gamma 4$ DANs with RLN2 blocked. (E-G) Plot of DANs GCaMP6s fluorescence over training cycles. Calcium activity was calculated by averaging the fluorescence over the first 8 seconds after odor onset. Green curved lines denote DAN activity with RLN1 blocked; green curved line denotes RLN2; black curved line denotes control. Data are mean $\pm$ MSE. One asterisk denotes $p<0.05$ and two asterisks denotes $p<0.01$. (E): DANs' odor-ON response to CS+. (F): DANs' odor-ON response to CS-. (G): DANs' odor-OFF response to CS+.

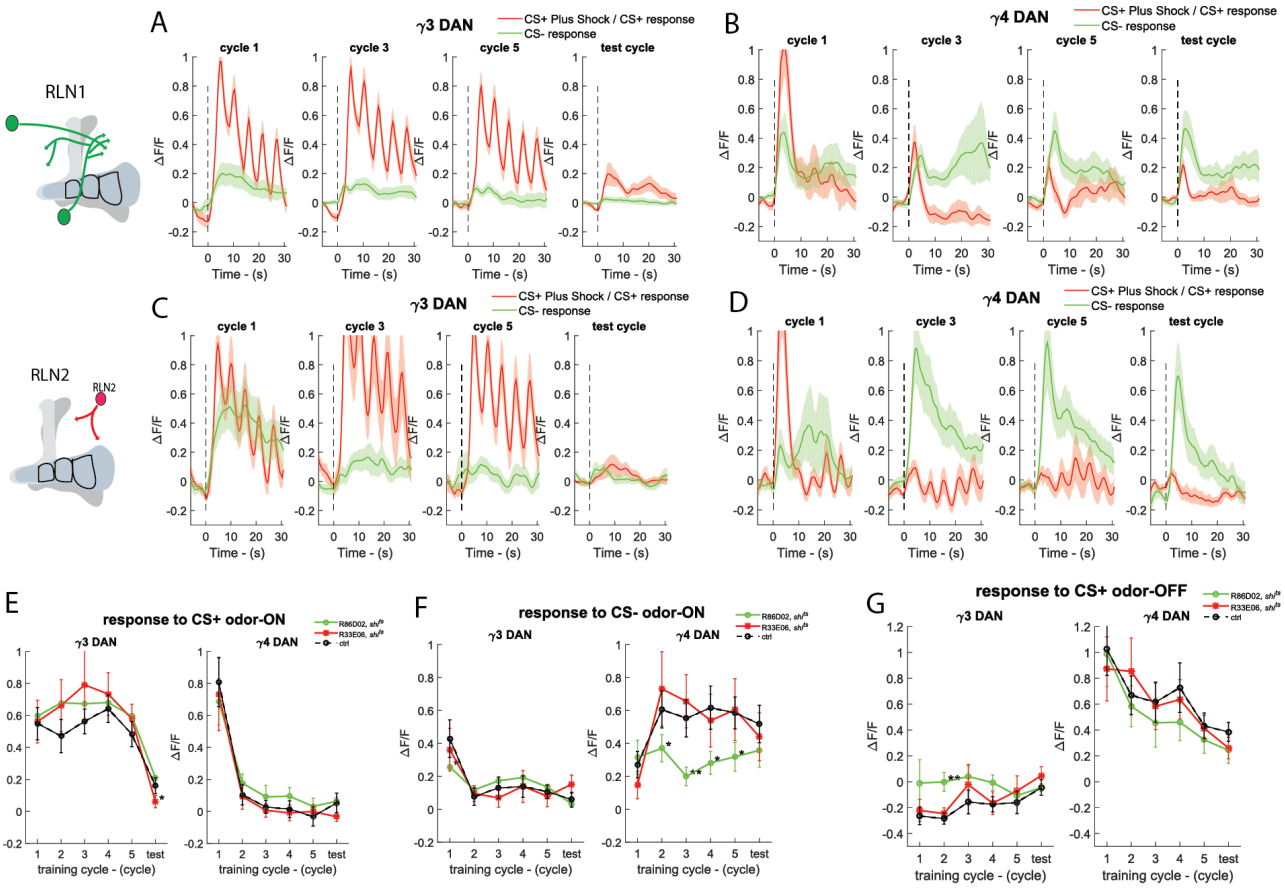
A
γ3 DAN
CS+ Plus Shock / CS+ response
CS- response
cycle 1
cycle 3
cycle 5
test cycle
ΔF/F
Time - (s)
B
γ4 DAN
C
D
RLN1
RLN2
E
response to CS+ odor-ON
F
response to CS- odor-ON
G
response to CS+ odor-OFF
training cycle - (cycle)
test

## Discussion

By training-under-microscope approach, we investigated how DANs participate in aversive olfactory memory. DANs innervating *Drosophila* mushroom body lobes can be divided into two groups of opposite valence. Positive reward DANs respond to primary reward stimulation, such as sugar, whereas negative punishment DANs respond to punitive stimuli, such as electric shocks. As expected, we found that aversive DANs respond to electric shock punishment. More importantly, we also found that aversive DANs display conditioned response to conditioned stimuli after multiple cycles of conditioning. Aversive DANs show stronger response to CS+ than CS-, which means that negative conditioned valence of CS+ is encoded by aversive DANs. Unexpectedly, we found that reward DANs also directly participate in aversive olfactory conditioning. Reward DANs fire strongly to CS- stimulation, likely due to presence of electric shocks. Moreover, reward DANs also display conditioned response to CS. Contrary to punishment DANs, reward DANs show stronger response to CS-, instead of CS+. It means that positive conditioned valence of CS- is encoded by reward DANs. Our data reveal that the negative and positive valence of CS+ and CS- are represented by punishment and reward DANs respectively.

In order to understand what neurons DANs receive input from and how the input contributes to DANs encoding the valence of CS+/CS-, we conducted a small-scale screening to identify upstream neurons that might regulate DANs by using training-under-microscope method. The conventional way of screening for novel neurons is through inspection of behavior defects caused by $Shi^{ts1}$ silencing neurons of interest. However, this approach is restricted by lack of clean GAL4 lines with specific neuron expression. It is difficult to determine which neurons are responsible for the behavior defect if multiple groups of neurons are present in the GAL4

line. Calcium imaging may help us circumvent the problem since imaging enables us to focus on a small and specific group of neurons of interest. Through this method, we identified two groups of neurons of opposite valence, which we refer to as recurrent loop neurons (RLNs). One group of neurons of positive valence encodes the positive valence of CS- whereas other group of neurons of negative valence encodes the negative valence of CS+. We also found that RLNs of positive valence activate reward DANs and RLNs of negative valence activate punishment DANs. It is the first time that neurons were identified downstream of mushroom body output neurons. Moreover, those neuron downstream of MBONs feedback onto DANs, suggesting that there could be an unexpected complicated unstructured processing center further downstream in olfactory pathway that could be critical for memory formation.

## Chapter Three

# *Drosophila* aversive olfactory memory is binary of attraction and repulsion memory

## Introduction

In canonical aversive olfactory conditioning paradigm, two odorants are used as CS+ and CS-. CS+ stimulation is paired with electric shock punishment whereas CS- is not paired with any unconditioned stimuli (US). Afterwards, flies are forced to choose between CS+ and CS- in a T-maze for memory score measurement. The initial design of using CS+ and CS- originates from the concern that flies may have variable innate preference for CS+ and CS-. To eliminate innate preference bias, researchers perform two reciprocal training with two odorants. In the first experiment, odor 1 is used as CS+ and odor 2 is used as CS-. In the reciprocal experiment, odor 2 is used as CS+ and odor 1 is used CS+. It enables us to obtain a memory score without innate odor preference bias. Despite concern about innate preference, it was never asked whether CS- also contributes to memory formation and even whether CS- is actually encoded as part of aversive olfactory memory. However, our calcium imaging data reveal that reward DANs respond to CS- but not to CS+, suggesting that CS- could be encoded as part of memory due to paring with dopamine activation. Therefore, we went on to investigate the roles CS- plays in aversive olfactory memory. In order to measure the half score contributed by CS- or CS+ alone instead of the combined score, we can no longer let flies choose between CS+ and CS-. Instead, we should force flies to choose between CS and a third odor. Out of concern of innate preference as well, a parallel mock-train experiment was conducted to measure a reference or baseline score. By subtracting reference score from half score, we calculated unbiased score with innate preference eliminated. By this approach, we were able to determine the contribution of CS- to memory and we demonstrated that memory is indeed composed of repulsion memory of CS+ and attraction memory of CS-. Aversive olfactory

memory features multiple phases and memory decays with time. We also showed that attraction memory of CS- stays relatively stable over time.

Moreover, studies from the past decades are based on the assumption that only CS+ is conditioned as aversive. Now that we've demonstrated that memory is binary consisting of attraction and repulsion, we investigated whether MBONs and RLNs encode attraction and repulsion memory in different ways. It turns out RLNs are responsible for the memory type of corresponding valence whereas MBONs are responsible for memory of both valence likely due to the cross-over in feedback connectivity with DANs. In all, we demonstrated that aversive olfactory memory could be decomposed into attraction and repulsion memory.

## Results

### 1. Aversive olfactory memory is binary consisting of attraction and repulsion

As shown in Figure 1, reward DANs respond strongly to CS- during aversive training than odor controls. Moreover, attraction MBONs only show reduced responses to CS+ but maintain response to CS- while avoidance MBONs display reduced response to CS- (Figure 5). People used to hold the opinion that, in aversive training, only CS+ is conditioned as repulsive whereas CS- is perceived as neutral or irrelevant. Our data suggests CS- could directly be conditioned as attractive, induced by released dopamine of reward DANs. To figure out the role of CS- in memory, we modified classical aversive olfactory training paradigms. In contrary to the standard memory test between CS+ and CS- (Figure 8A), I let flies choose either between CS- and blank pure air, or between CS- and an un-experienced odor, Benzaldehyde (Ben). Due to innate aversion to odors and variation in odor preference across different batches and genotypes, mock-trained flies of the same batch with exposure only to

odors but no electric shocks, were used as reference (Figure 8B). As shown in Figure 8F, after 5 cycles of spaced aversive olfactory training, flies chose CS- more than blank air compared to reference flies. The PI score is significantly larger than zero, which indicates that flies indeed learn to prefer CS- after conditioning. To test the odor specificity of attraction to CS-, flies were also tested between CS- and Ben, a newly experienced odorant. It turns out that flies also learn to walk into CS- after 5 cycles of spaced training (Figure 8D and E). Preference to CS- doesn't originate from memory over-generalization since training with CS+ alone doesn't generate the preference. (Figure 8G)

Next we wonder to what extent repulsion to CS+ and attraction to CS- contribute to full memory score. Similarly, we measured repulsion to CS+ by allowing flies to choose between CS+ and a third odor, Ben. We first decomposed 1-cycle short-term memory (STM). As shown in Figure 8H, it turns out standard 1-cycle STM score (~0.75) is made of repulsion score of ~0.6 and attraction score of ~0.15. Next, we focused on memory measured at gradually increasing time points after 5-cycle spaced training, the paradigm we used for calcium imaging. As shown in Figure 8I, at 30min after spaced training, full memory score reaches a saturating level of ~0.9 while repulsion score is ~0.8 and attraction score is ~0.35. At 3hrs after spaced training, full memory score drops to ~0.65 while repulsion score drops to ~0.4 and attraction score remains around 0.35 (Figure 8J). It appears that attraction memory is more stable than repulsion memory. Interestingly, at 24hrs after spaced training, with full memory score of ~0.35, repulsion score is ~0.2 and attraction score is ~0.2 (Figure 8K), indicating that attraction to CS- could even contribute to protein-synthesis dependent LTM.

Interestingly, massed-trained flies fail to learn to prefer CS- after aversive conditioning. (Figure S6) Detailed analysis shows that the choice between Ben and CS- depends on initial

naïve preference. (Figure S6A and C) If flies dislike CS- more than Ben in mock-trained controls, aversion to CS- will be suppressed after massed training, leading to preference to CS- (Figure S6B). If flies prefer CS- to Ben in the beginning, attraction to CS- will be suppressed, leading to aversion to CS- (Figure S6A). After massed training, flies seem to become indifferent between Ben and CS-. In order to understand the difference between massed and spaced training in terms of attraction to CS-, we also characterized the responses of DANs during massed training. (Figure S6E). It turns out that during massed training, response to CS- of reward $\gamma 4$ DANs, is weaker than spaced training, especially during the last 2 cycles (Figure S6E). In addition, after massed training, aversive $\gamma 3$ DAN's response to CS- is stronger than spaced training. These two factors could contribute to reduced attraction to CS- and increased aversion to CS-, eventually leading to flies' indifference between Ben and CS- after massed training.

**2. Disruption of the Feedback Circuit causes defects in attraction or repulsion memory**

In order to understand how MBONs contribute to attraction and repulsion memory, we first performed a series of aversive olfactory conditioning assays with potassium channel *Kir2.1* instead of *shi*$^{ts1}$ out of the concern of incomplete inactivation by *shi*$^{ts1}$. We focused on $\gamma 1$, $\gamma 2\alpha' 1$, $\gamma 4$ and $\beta' 2$ MBONs. We first examined those MBONs' contribution to attraction and repulsion memory for 1-cycle STM. As shown in Figure 9A and B, silencing $\gamma 1$ and $\gamma 2\alpha' 1$ MBONs causes defects in repulsion memory but not in attraction memory since $\gamma 1$ and $\gamma 2$ DANs are punishment DANs. Silencing $\gamma 4$ MBONs causes defects in attraction memory but not in repulsion memory since $\gamma 4$ DANs are rewarding. Interestingly, $\beta' 2$ MBONs are required for both repulsion and attraction memory.

Next, we investigated MBONs' functions in 3hrs memory after 5-cycle spaced training. Similar to 1-cycle STM, silencing $\gamma 1$ only impairs repulsion memory (Figure 9C and D). Nevertheless, silencing $\gamma 2\alpha' 1$ and $\gamma 4$ MBONs impairs both attraction and repulsion memory (Figure 9C and D). $\gamma 4$ MBONs' requirement for repulsion memory is likely the consequence of inhibition of reward $\gamma 4$ DANs during CS+ presentation. Indeed, pairing reward DANs inhibition with odors creates repulsion memory (data not shown). Although $\gamma 2$ and $\alpha' 1$ DANs mediate punishment, $\gamma 2\alpha' 1$ MBONs' requirement could result from the fact that $\gamma 2\alpha' 1$ MBONs activate reward DANs (Figure 6E). It appears that in certain MBONs, attraction and repulsion memories are written inseparably.

We continued to investigate DANs and RLNs' roles in memory. Since pDANs are self-reinforcing, we ask whether pDANs are required for decision-making after training. *Shi*$^{ts1}$ was first used to block PAM-DANs output by R58E02 during test. As shown in Figure 8E and F, silencing PAM DANs during test impairs both attraction and repulsion memory. It indicates that pDANs not only release dopamine as reinforcement signal during conditioning but also facilitates memory recall during decision-making, likely due to its self-reinforcing property. Likewise, we silence RLN1 and RLN2 by *shi*$^{ts1}$. It turns out RLN1 is only required for attraction memory recall but not repulsion memory (Figure 9E and F). Conversely, RLN2 is only required for repulsion memory recall but not attraction memory. It appears that unlike MBONs, RLN1 and RLN2 are in charge of attraction and repulsion memories respectively. Last but not the least, we ask whether RLNs are required during training since they already display training dependent plasticity at the 2rd training cycle. As shown in Figure 9G and H, flies with RLN1 silenced during training display defects in attraction memory but not repulsion memory. Silencing RLN2 during training only impairs repulsion memory. However, silencing

PAM-DANs during training impairs both attraction and repulsion memory, indicating PAM-DANs are required for both attraction and repulsion memory. This is consistent with the defects caused by silencing $\gamma 4$ and $\beta' 2$ MBONs.

**3. Electric shocks directly potentiates odor-evoked response of reward DANs**

In previous studies, it has been shown that flies can associate 'relief' from punitive stimuli, such as ES, with odors. This was referred to as relief learning or backward conditioning [83]. However, as discussed earlier in Figure S2, although reward DANs rebound immediately after electric shock stops, the strength of the rebound might be too weak to condition odors, especially if we compare it with the response to odors (compare Figure S2 and Figure 1). Indeed, even in backward conditioning, it is the potentiated odor-evoked response of reward DANs that provides the rewarding reinforcement signal. First, we conducted backward conditioning while imaging reward DANs including $\gamma 3$, $\gamma 4$ and $\gamma 5$ DANs. Odor was given 3 seconds after ES delivery stopped. As shown in Figure 10, in backward conditioning, odor-evoked response of $\gamma 4$ to the first odor immediately after ES is significantly higher than mock-trained controls (Figure 10C). Response to the first odor is even higher than the response to CS- in spaced training (compare Figure 10C and Figure 1F). Behaviorally, in 5-cycle single-odor relief learning, flies are also attracted to the associated odor if they are let choose between CS- and Ben after conditioning (Figure 10). Therefore, in backward or relief conditioning, the mere ending of shock pulse itself doesn't provide the pain relief. Rather, sensation of ES potentiates recurrent loop mediated odor-evoked response that provides the reinforcement signal for pain-relief learning. This also explains why $\gamma 4$ DANs' response to CS+ during the first training cycle is abnormally higher. It is likely that the sensation of electric

shock directly modifies the brain state of fruit fly's dopamine pathways such that any conditioned stimulus given after the shocks would trigger a stronger response of reward DANs.

## Discussion

In most studies, CS- tends to be treated as a reference or neutral stimulus. Here by using *Drosophila* olfactory memory, we show that CS- actively participates in memory formation. Sensation of electric shocks during conditioning potentiates reward DANs' response to both CS+/CS-. Due to CS+ pairing with electric shock punishment, reward DNAs response to CS+ is suppressed while its response to CS- is maintained. As a result, CS- is paired with reward DANs' activation which induces attraction memory to CS-. Furthermore, we demonstrate that a significant portion of aversive memory can be attributed to CS- attraction memory and this attraction memory component stays more stable than CS+ repulsion memory. By silencing select group of neurons, we dissect the roles DANs, RLNs and MBONs play in both attraction and repulsion memory. RLNs are required for either attraction or repulsion memory whereas MBONs are required for both attraction and repulsion memory likely due to cross-over in dopamine neuron feedback connectivity.

**Figure 8 Aversive olfactory memory is bipartite consisting of repulsion and attraction**

(A) Schematic of classical aversive olfactory training. CS+ and CS- can be either OCT or MCH. (B) Schematic of modified aversive olfactory training. Standard training and mock-training were performed on flies from the same batch. Flies are then tested between CS- and a third stimulus, such as Benzaldehyde or pure air. Performance index is calculated by subtracting mock-trained PI score from trained PI score. (C) Decay rate of 5-cycle spaced memory differs for attraction and repulsion memory. (D-G) Aversive olfactory training induces attraction to CS-. In each panel, on the top is diagram of 5x spaced training and test. On the bottom is performance index (PI) for trained and mock-trained flies. Three asterisks denotes $p<0.001$. (Paired t-test) (D): Training induces attraction to OCT as CS- with Ben as reference. (n=15) (E): Training induces attraction to MCH as CS- with Ben as reference. (n=12) (F): Training induces attraction to CS- with pure air as reference. PI scores were averaged over MCH and OCT. (G): Pairing flies with CS+ in the absence of CS- doesn't induce attraction to CS-. (H-K) Phases of attraction, repulsion and full memories. Data are mean $\pm$ MSE; n>8 for every memory type and phase. (H): Memories at 10min after 1-cycle training. (I-K): Memories at 30min, 3hrs, 24hrs after 5-cycle training.

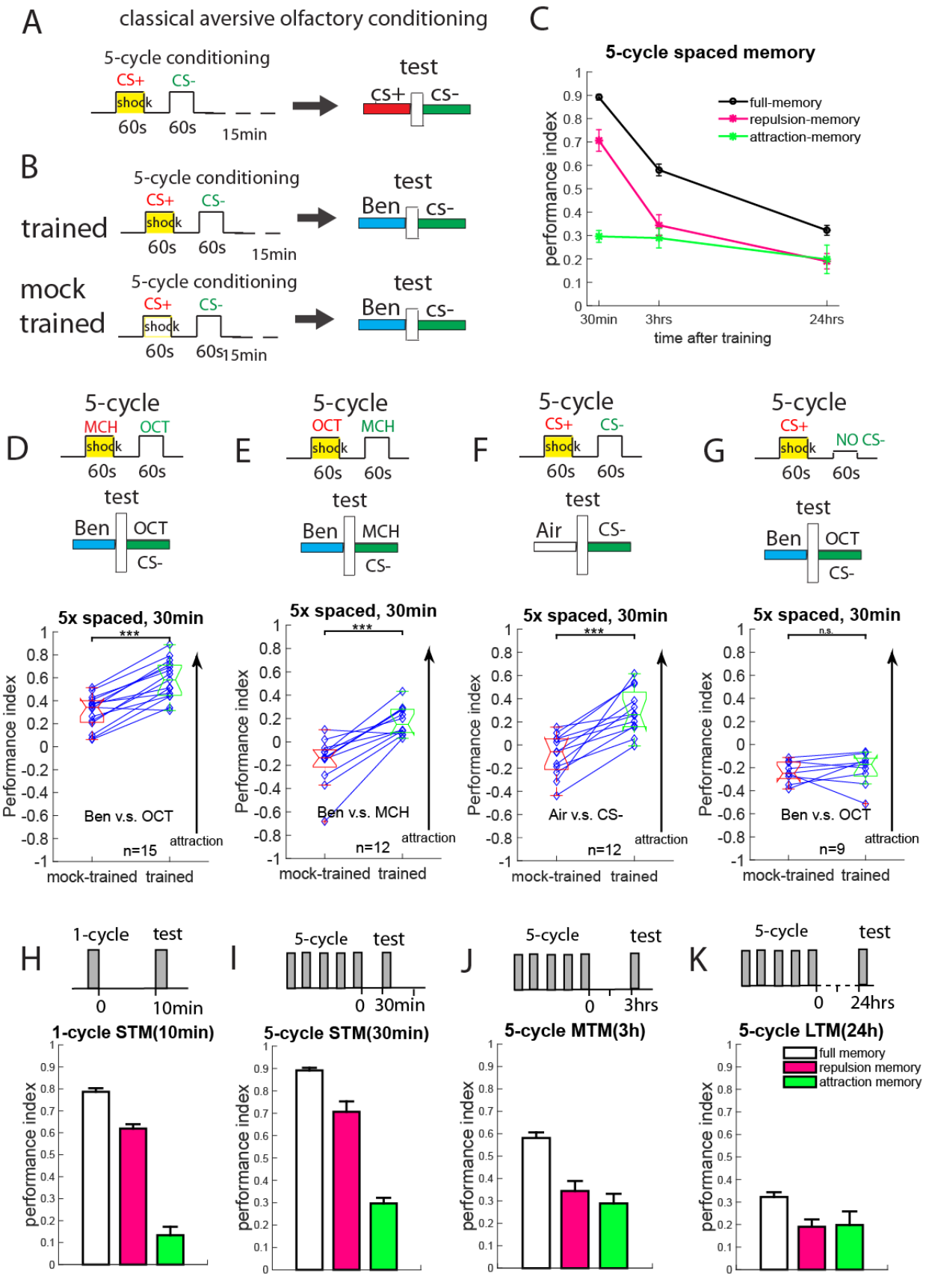
A
classical aversive olfactory conditioning
5-cycle conditioning
CS+
CS-
shock
60s
60s
15min
test
cs+
cs-
B
trained
mock trained
Ben
C
5-cycle spaced memory
full-memory
repulsion-memory
attraction-memory
performance index
30min
3hrs
24hrs
time after training
D
E
F
G
5-cycle
MCH
OCT
NO CS-
Air
Ben v.s. OCT
Ben v.s. MCH
Air v.s. CS-
5x spaced, 30min
***
n.s.
n=15
n=12
n=9
attraction
mock-trained
trained
H
I
J
K
1-cycle
0
10min
0 30min
0 3hrs
0 24hrs
1-cycle STM(10min)
5-cycle STM(30min)
5-cycle MTM(3h)
5-cycle LTM(24h)
full memory
repulsion memory
attraction memory

**Figure 9 Blocking output from MBONs or RLNs impairs repulsion or attraction memory**
(A-B, C-D) Silencing MBONs by Kir2.1 causes defects in repulsion or attraction memory. $\gamma 1$, $\gamma 2\alpha' 1$, $\gamma 4$ and $\beta' 2$ MBONs were silenced by driving Kir2.1 by split-GAL4 lines: mb112c, mb077b, $\gamma 4$ and mb011b. (A): Silencing $\gamma 1$, $\gamma 2\alpha' 1$ or $\beta' 2$ MBONs impairs 10min repulsion memory but silencing $\gamma 4$ MBONs doesn't cause any defect. (Kruskal-Wallis, n>8 for each genotype, p(mb112c)<0.001; p(mb077b)<0.01; p($\gamma 4$)>0.2; p(mb011b)<0.01) (B): Silencing $\gamma 4$ or $\beta' 2$ MBONs impairs 10min attraction memory but silencing $\gamma 1$ or $\gamma 2\alpha' 1$ MBONs doesn't cause any defect. (Kruskal-Wallis, n>8 for each genotype, p(mb112c)>0.2; p(mb077b)>0.2; p($\gamma 4$)<0.05; p(mb011b)<0.01) (C): Silencing $\gamma 1$, $\gamma 2\alpha' 1$ $\gamma 4$ or $\beta' 2$ MBONs, all the MBONs examined, impairs 3hrs repulsion memory after 5-cycle spaced training. (Kruskal-Wallis, n>8 for each genotype, p(mb112c)<0.01; p(mb077b)<0.01; p($\gamma 4$)<0.05; p(mb011b)<0.01) (D): Silencing $\gamma 2\alpha' 1$, $\gamma 4$ or $\beta' 2$ MBONs, except $\gamma 1$ MBONs, impairs 3hrs attraction memory after 5-cycle spaced training. (Kruskal-Wallis, n>8 for each genotype, p(mb112c)>0.2; p(mb077b)<0.01; p($\gamma 4$)<0.05; p(mb011b)<0.01) (E-F, G-H) Blocking output from RLNs or DANs by shi$^{ts}$ causes defect in repulsion or attraction memory. (E): Blocking output from R58E02 (PAM-DANs) or R33G12 (RLN2) neurons after 5-cycle spaced training impairs 30min repulsion memory. Blocking output from R86D02 (RLN1) neurons doesn't cause the defect. (Kruskal-Wallis, n>10 for each genotype, p(R58E02)<0.01; p(R86D02)>0.2; p(R33G12)<0.05) (F): Blocking output from R58E02 (PAM-DANs) or R86D02 (RLN1) neurons after 5-cycle spaced training impairs 30min attraction memory. Blocking output from R33G12 (RLN2) neurons doesn't cause the defect. (Kruskal-Wallis, n>10 for each genotype, p(R58E02)<0.05; p(R86D02)<0.05; p(R33G12)>0.2) (G): Blocking output from R58E02 (PAM-DANs) or R33G12 (RLN2) neurons during 5-cycle spaced training impairs 3hrs repulsion memory. Blocking output from R86D02 (RLN1) neurons doesn't cause the defect. 3hrs memory was chosen to allow for full neuron function recovery after shi$^{ts}$ inactivation for 1.5 hrs. (Kruskal-Wallis, n>10 for each genotype, p(R58E02)<0.01; p(R86D02)>0.2; p(R33G12) <0.01) (H): Blocking output from R58E02 (PAM-DANs) or R86D02 (RLN1) neurons during 5-cycle spaced training impairs 3hrs attraction memory. Blocking output from R33G12 (RLN2) neurons doesn't cause the defect. (Kruskal-Wallis, n>10 for each genotype, p(R58E02)<0.01; p(R86D02)<0.01; p(R33G12)>0.2)

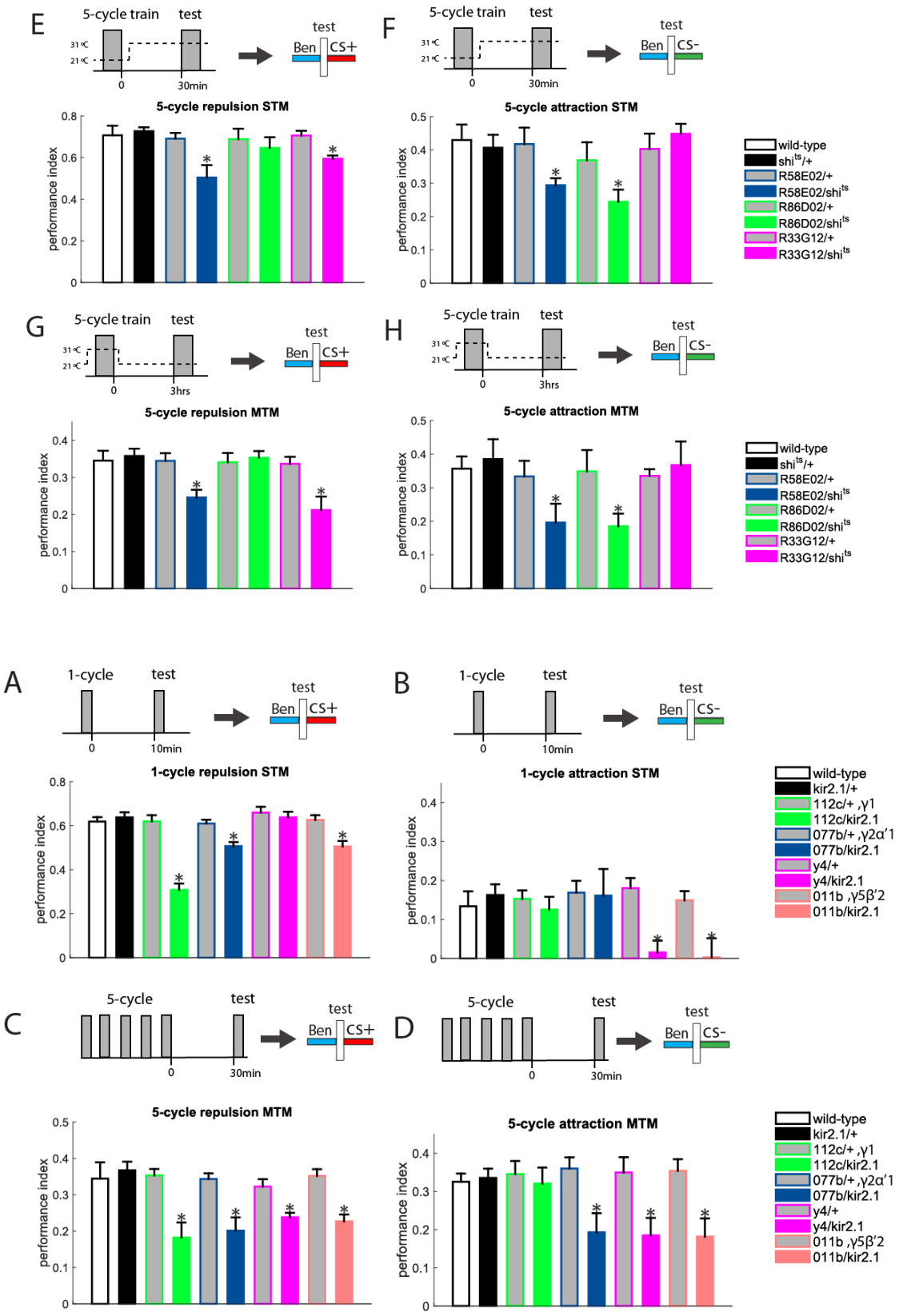
E
5-cycle train
test
31℃
21℃
0
30min
test
Ben
CS+
5-cycle repulsion STM
performance index
F
5-cycle attraction STM
CS-
G
3hrs
5-cycle repulsion MTM
H
5-cycle attraction MTM
A
1-cycle
10min
1-cycle repulsion STM
B
1-cycle attraction STM
C
5-cycle
D
wild-type
shi^ts/+
R58E02/+
R58E02/shi^ts
R86D02/+
R86D02/shi^ts
R33G12/+
R33G12/shi^ts
kir2.1/+
112c/+ ,γ1
112c/kir2.1
077b/+ ,γ2α′1
077b/kir2.1
γ4/+
γ4/kir2.1
011b ,γ5β′2
011b/kir2.1

## Chapter Four

# DANs don't encode negative prediction errors in *Drosophila*

## Introduction

It is well documented that mammalian reward dopamine neurons encode prediction errors. The prominent feature of dopamine error is suppression of dopamine neuron activity in response to omission of primary reward supposed to be given after reward predicting conditioned stimuli. Now that we found dopamine neurons encode the valence of CS+/CS-, we ask whether dopamine neurons fruit fly encode negative prediction errors in aversive olfactory conditioning. It turns out that DANs investigated fail to respond to omission of electric shocks presented after CS+.

## Results

### 1. DANs don't encode negative prediction error in *Drosophila*

Prediction error model has been popular since late 90s thanks to studies on monkeys and mice. One of the key characteristics of prediction error is that neurons are able to respond to omission of US-associated CS. For example, dopamine neurons in VTA fires strongly to omission of reward predicting cues. Since we identified a lot of plastic DANs, we ask whether those neurons respond to omission of electric shocks. However, in experiments performed on mice/monkeys, CS is usually after cessation of US whereas in classical olfactory conditioning on flies, electric shocks are usually simultaneously delivered when odor is being presented. Therefore, in order to figure out the existence of prediction errors in fruit flies, we modified classical olfactory training paradigm (Figure 11). In this paradigm, we presented 15 seconds of CS+ and CS- in each cycle. 5 electric shock pulses were given 10sec after CS+ was presented to serve as punishment. We refer to this paradigm as delayed-shock paradigm.

In this new paradigm, we first demonstrated that behaviorally, animals successfully associate punishment with CS+. Then I further performed calcium imaging to investigate whether DANs are also able to associate CS+ with punishment. Interestingly, $\gamma 3$, $\gamma 4$ and $\gamma 5$ DANs in mushroom body horizontal lobes are also able to learn the valence of CS+ and CS- in this new paradigm. Similar to that under classical aversive olfactory conditioning paradigm, after multiple training cycles, $\gamma 3$ DNAs respond more strongly to CS+ than CS- and $\gamma 4$ DNAs respond more strongly to CS- than CS+ (Figure 11B-C). Moreover, after multiple training cycles, stronger $\gamma 3$ DNAs response to CS+ persists even after after cessation of CS+ stimulation, indicating punitive electric shocks following CS+. Despite DANs' ability to learn odor valence even in delayed-shock paradigm, we failed to find any DNAs that are able to respond to omission of electric shocks, even after 10 training cycles (Figure 11D). It suggests that fruit flies may not be able to encode negative prediction errors. Nevertheless, there is still possibility that mushroom body DANs could respond to omission of sugar-predicting conditioned stimuli, encoding positive prediction errors.

## Discussion

Failure to detect encoding of negative prediction errors in *Drosophila* dopamine neurons doesn't necessarily mean it doesn't exit in *Drosophila*. There are two ways to explain the failure. First, punishment was used as unconditioned stimuli in our experiments while most of studies on prediction errors utilize reward as unconditioned stimuli. It is unclear whether mushroom body reward DAN encodes positive prediction errors. Second, in our paradigm, punishment was delivered with a delay of 10 seconds after odor stimulation. In most studies on mammals, reward is delivered 2-3 seconds after 1 second odor stimulation. 10-second

delay could be too long for fruit flies to respond to omission of unconditioned stimuli and it is unclear whether 1 second odor stimulation is strong and long enough for fruit fly to memorize the odor. Future studies need to be based on careful consideration of these potential problems.

**Figure 10 Reward DANs activity is potentiated in backward conditioning**

(A) Schematic of backward conditioning. 10 pulses of electric shocks were given first and then the first odor was given 3sec afterwards. The second odor was given 60sec after the 1st odor. The first and second odor can be either OCT or MCH. Test cycle was given after 5 cycles of backward conditioning (B1-B2) Activities of $\gamma 3$, $\gamma 4$ and $\gamma 5$ DANs in backward conditioning. Green trace denotes DANs activity during the first odor presentation and green trace denotes DANs activity during the second odor. Data are mean [solid line] $\pm$ MSE [shaded area] curves. Dashed line denotes odor onset. (B1): Activities of DANs in the first cycle. (B2): Activities of DANs in the final test cycle. (C) Plot of DANs GCaMP6s fluorescence over training cycles. Calcium activity was calculated by averaging the fluorescence over the first 8 seconds after odor onset. Green curved lines denote DAN activity during the first odor presentation in backward conditioning; red curved line denotes the second presentation; blue curved line denotes the first odor in mock train controls. Data are mean $\pm$ MSE. One asterisk denotes $p<0.05$ and two asterisks denotes $p<0.01$. (Two sample T-test)

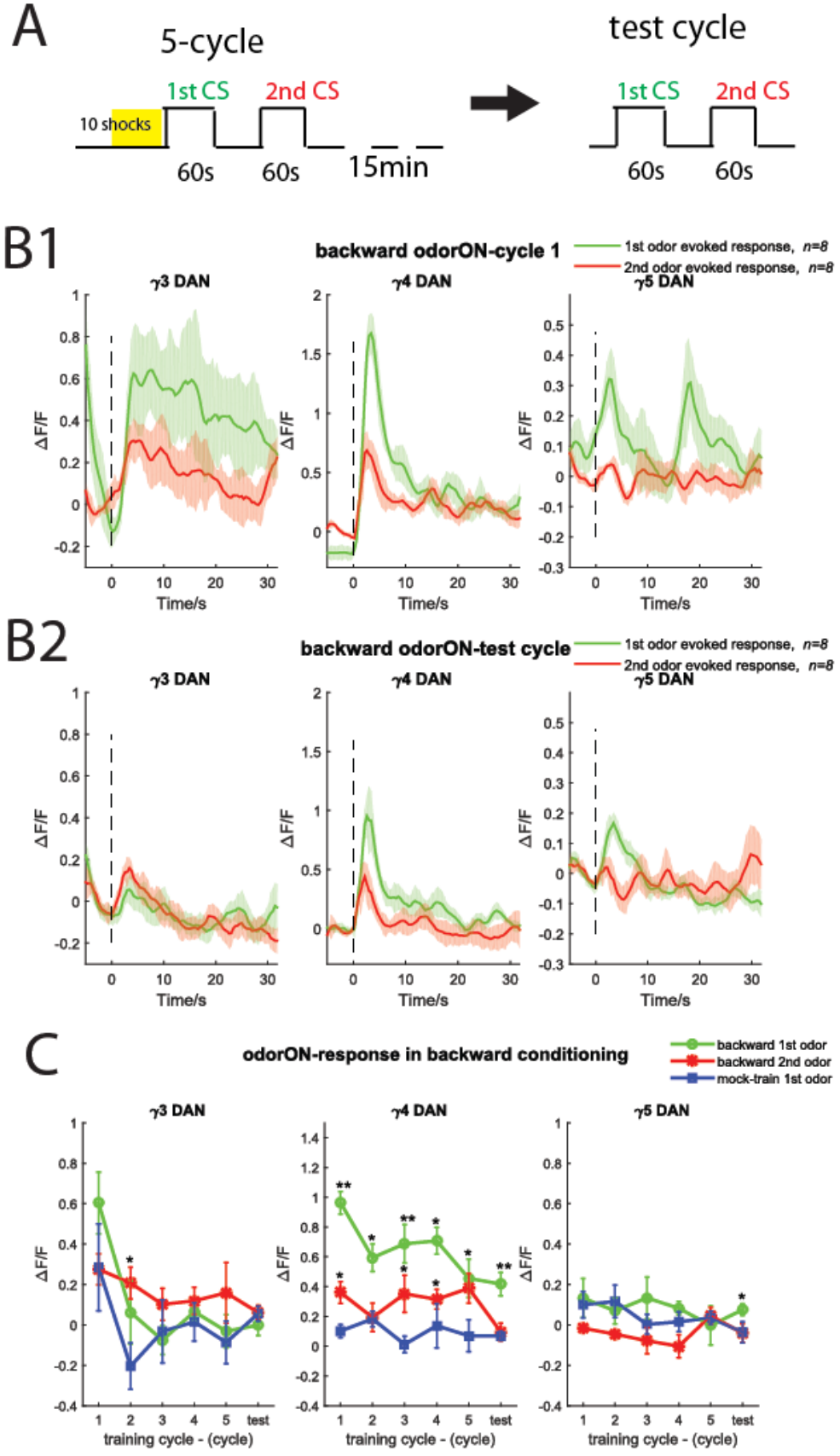
A
5-cycle
1st CS
2nd CS
10 shocks
60s
60s
15min
test cycle
1st CS
2nd CS
60s
60s
B1
backward odorON-cycle 1
1st odor evoked response, n=8
2nd odor evoked response, n=8
γ3 DAN
γ4 DAN
γ5 DAN
ΔF/F
Time/s
B2
backward odorON-test cycle
1st odor evoked response, n=8
2nd odor evoked response, n=8
γ3 DAN
γ4 DAN
γ5 DAN
ΔF/F
Time/s
C
odorON-response in backward conditioning
backward 1st odor
backward 2nd odor
mock-train 1st odor
γ3 DAN
γ4 DAN
γ5 DAN
ΔF/F
training cycle - (cycle)
1
2
3
4
5
test

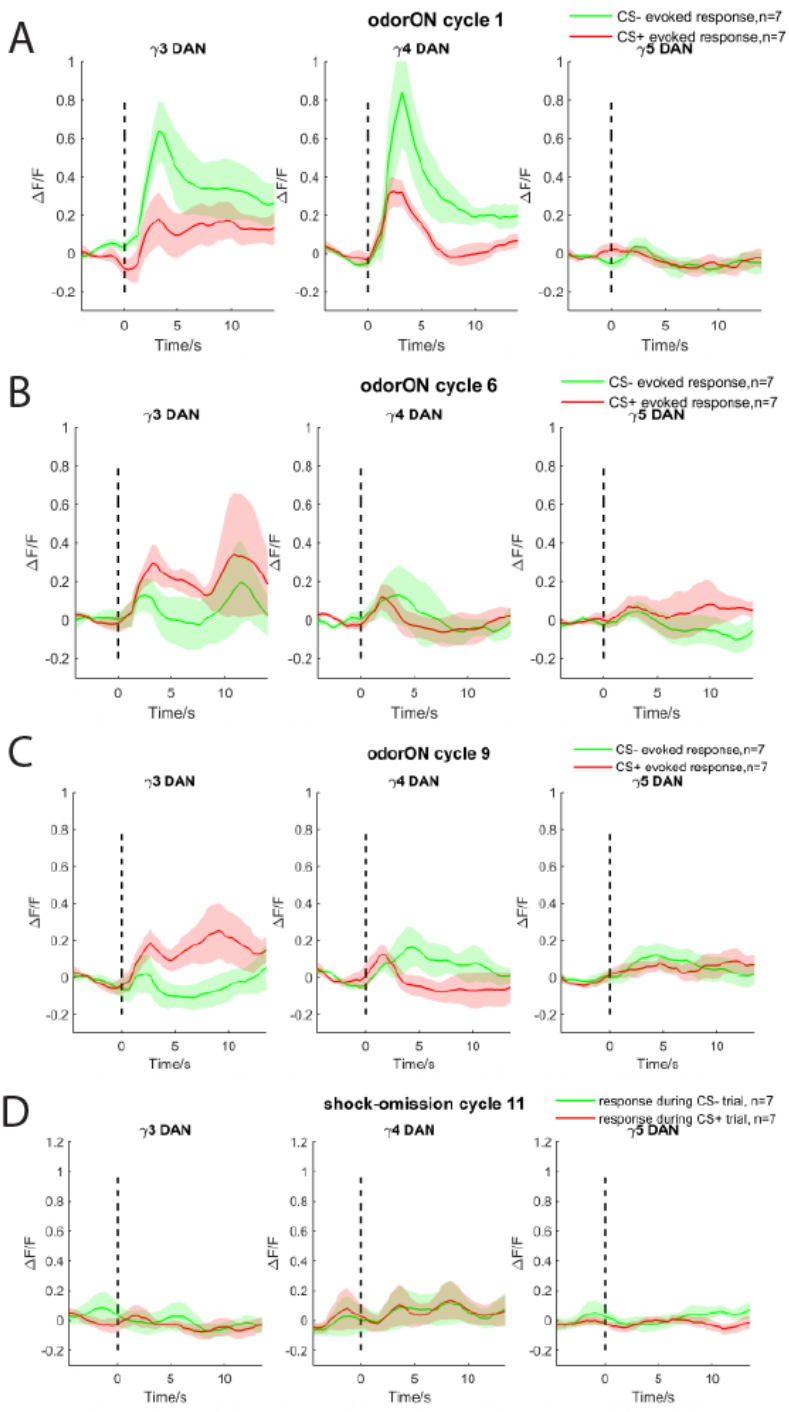


**Figure 11 Reward DANs don't respond to ES omission in delayed-shock paradigm**

(A-C) Activities of $\gamma 3, \gamma 4$ and $\gamma 5$ DANs in backward conditioning. Green trace denotes DANs activity during the first odor presentation and green trace denotes DANs activity during the second odor. Data are mean [solid line] $\pm$ MSE [shaded area] curves. Dashed line denotes odor onset. (A): Activities of DANs in the first cycle. (B): Activities of DANs in the 6th cycle. (C): Activities of DANs in the 9th cycle. (D): Activities of DANs in the test cycle.

# Chapter Five

# Discussion

In this study we took advantage of *Drosophila* mushroom body to gain a comprehensive understanding of how dopamine neurons (DANs) work in concert with other neurons, such as mushroom body output neurons (MBONs), when fruit flies go through aversive olfactory conditioning. Starting with a screen to identify neurons that modify its response to odors during conditioning, we discovered that most of PAM-DANs are plastic during aversive olfactory conditioning. On one hand, reward DANs suppresses its response to CS+ combined with electric shocks while maintaining or enhancing its response to CS-. On the other hand, punishment DANs not only fire strongly in response to punitive stimuli during the process of conditioning but also increase its response to CS+ relative to CS- after conditioning. In addition to plastic DANs, we also uncovered a novel group of neurons that feed the signal from MBONs back onto DANs, which we name as Recurrent Loop Neurons (RLNs). This new group of neurons is also required for aversive olfactory memory. Here we reveal that there exists a delicate tripartite feedback circuit encompassing MBONs, RLNs and DANs. In this feedback circuit, attraction MBONs or RLNs activate reward DANs while repulsion MBONs or RLNs activate punishment DANs, which creates a self-reinforcing system. It empowers a fly with the ability to modify its valence perception of odors based on past experience. As a major behavioral consequence of this feedback circuit, CS- was found to play a critical role in aversive olfactory memory. It turns out that a full memory score is essentially bipartite, consisting of half scores contributed by repulsion to CS+ and attraction to CS- respectively. It provides us an opportunity to gain a deeper understanding of olfactory memory in fruit flies.

**A comprehensive investigation of DANs, MBONs and RLNs activity during aversive olfactory conditioning**

Dopamine neurons in MB are activated by electric shocks or sugar ingestion to drive learned olfactory associations [84], whereas KC propagate odor identity information from olfactory sensory pathway. Pairing of these two types of stimulation is the critical step for olfactory association [73, 85], which naturally leads to the assumption that these two pathways operate independently in fruit fly brain. Our data, however, suggest that there exists a sophisticated interconnectivity network that bridges together these two pathways that appear independent and contributes to learned olfactory associations. Here we not only show that DANs can be activated by odors but also reveal that DANs' odor response can be modified by olfactory learning. Punishment DANs and reward DANs lie in different but adjacent compartments to encode punishment and reward predicting odors respectively. Punishment $\gamma 3$ DANs are directly activated by electric shocks but also encode stronger response to CS+ after conditioning, whereas reward DANs such as $\gamma 4$ are slightly inhibited by electric shocks with a small rebound response and encode stronger response to CS-. Moreover, different reward DANs are endowed with different learning dynamics. $\gamma 4$ DANs' initial response to CS+ is substantially higher than CS- whereas other reward DANs, such as $\beta' 2$ DANs respond similarly to CS+ and CS- in the first training cycle. During conditioning, it is the boosting of response to CS- that drives the differential response of $\gamma 4$ DANs whereas for $\beta' 2$ DANs, it is mainly the suppression of response to CS+. CS+ even triggers inhibition of $\beta 2$ DANs and $\alpha 1$ DANs. The fact that reward DANs encode CS- in different ways could be due to different functions exerted by different DANs and their corresponding MBONs.

Recent research suggests that compartmentalized DANs independently tune the synaptic transmission of its own postsynaptic MBON repertoire [71, 82]. By examining MBON activity during conditioning, we further confirmed this compartmentalization hypothesis. Odor

response of MBON is inhibited by dopamine release of its own DAN and dopamine release in neighboring zones won't interfere with its synaptic transmission. Moreover, attraction MBONs' dendrites overlap with punishment DANs' axons and repulsion MBONs' dendrites overlap with reward DANs' axons. As a consequence, after conditioning, avoidance MBONs including $\gamma 4$ and $\beta' 2$ MBONs stay relatively unchanged in response to CS+ while attraction MBONs including $\gamma 2$ and $\gamma 3$ MBONs are inhibited in response to CS+. In response to CS-, it is the opposite. Although distributed in separate zones, MBONs of different valence are orchestrated in the same way to fulfill the same behavioral outcome.

In addition to DANs and MBONs, we discovered a third group of neurons (RLNs) positioned between MBONs and DANs in the tripartite feedback circuit. Two groups of RLNs of opposite valence encode CS+ and CS- in opposite directions. At the first cycle of conditioning, attraction neuron RLN1 respond similarly to both CS+ and CS-. During conditioning, RLN1 response to CS+ is gradually inhibited. RLN2 is directly excited by electric shocks and it only displays a slight response to odors in mock-train controls. After multiple training cycles, RLN2 fires strongly and persistently in response to CS+ alone in the absence of electric shocks. It appears that RLN2 encodes the punitive valence of electric shock, which is then transferred to CS+.

**Multi-layer interconnectivity network provides feedback onto DANs**

In order to differentially respond to CS+/CS-, DANs should receive specific information of odor identity. Odor identity is encoded in sparse activity of~2000 KCs in mushroom body and thus the negative valence of CS+ and the positive valence of CS- are encoded in KCs activity in MB lobes. However, olfactory pathway shrinks onto ~34 MBONs downstream of ~2000 KCs. Presumably, 34 MBONs are too small a group of neurons to encode odor identity, which

means that odor identity will be lost after the shrinkage and MBONs alone won't be able to tell apart different odorants, such as CS+ and CS-. Therefore, there must exist well-arranged set of connections from KCs to DANs that relay the valence to DANs to allow DANs to encode odor valence of CS+ and CS-. It is very likely that this pathway includes MBONs and RLNs. For instance, during conditioning, in order for reward DANs to respond to CS- rather than CS+, reward DANs must be activated by attraction MBONs or inhibited by avoidance MBONs, since attraction MBONs stay unchanged while avoidance MBONs are inhibited during CS- presentation. The net response to CS- mediated by this pathway would thereby be activation. Otherwise, random connectivity with either attraction or repulsion MBONs will only let DANs be able to respond to odors but not to encode odor valence. Indeed, our data reveal that reward $\gamma 4$ DANs can be inhibited by avoidance $\beta'2$ MBONs and activated by attraction $\gamma 2\alpha'1$ MBONs. Reward $\beta'2$ DANs can be activated by $\gamma 2\alpha'1$ MBONs and inhibited by $\beta'2$ MBONs. Moreover, DANs are regulated oppositely by RLNs of opposite valence, adding another layer of regulation complexity to the feedback circuit. Reward $\beta'2$ DANs are activated by attraction neuron RLN1 and are inhibited by repulsion neuron RLN2, whereas punishment $\gamma 3$ DANs are slightly inhibited by RLN1 and slightly activated by RLN2.

Detailed anatomical analysis shows that MBONs, DANs and RLNs all extend branches into the regions surrounding MB lobes, including SMP and CRE. Those regions were referred as convergence zone. Analysis by GFP Reconstitution Synaptic Partner (GRASP) also indicates that MBONs directly connect with both DANs and RLNs and RLNs also connect with DANs directly in the convergence zone. Notably, repulsion neuron RLN2 connects extensively with punishment $\gamma 3$ DANs and attraction neuron RLN1 connects extensively with reward $\beta'2$ DANs, further corroborating valence-relay model. A recent study also shows that DANs can be

activated by MBONs [72]. Nevertheless, functional connectivity suggested in that piece of study cannot explain DANs' ability to differentially respond to CS+ and CS-.

**Novel mode of DAN activation by CS- and cessation of odor stimulation**

CS- tends to be ignored in research investigating function of dopamine neurons [27, 28, 86]. Our data for the first time shed light on the importance of CS- and shows that CS- can be conditioned as rewarding by activating reward DANs, representing its positive rewarding valence from absence of punishment. Researchers have speculated that relief from pain could be learned through timing-dependent mechanism, such as STDP, or dopamine release caused by punishment cessation [87]. Here obviously it is the activation by CS- that drives release of dopamine indicating relief from punitive stimuli. Therefore, a circuit level mechanism underlies pain relief learning instead of a molecular or synaptic mechanism. A study on reward prediction error show that rewarding dopamine release shifted to CS- as well [86], leading to a model of two-component response [88].

In addition, our data showed for the first time that dopamine neurons also respond to the cessation of odor stimulation, which we refer to as odor-OFF response. For instance, reward DANs respond strongly to cessation of odors. Particularly, $\gamma 4$ DANs response to cession of CS+ conditioned with punishment is significantly higher than to CS-, suggesting biological relevance of odor-OFF response. In addition, we show that attraction neuron RLN1 and attraction MBONs, including $\gamma 2$ and $\gamma 3$ MBONs, also respond to cessation of odor stimulation paired with punitive stimuli. Moreover, we also show that blank pure air can be conditioned as rewarding as well in aversive learning, due to dopamine odor-OFF response. Research on mammalian brain fails to report any similar case. It could be due to the fact that in fruit flies,

CS is presented for 60s, a much longer duration than a typical few seconds in mammalian research [28, 88]. After exposure to an environment for a longer period of time, any sensation change afterwards could trigger a larger dopamine activity. It is also likely that *Drosophila* possesses a different set of mechanisms of how dopamine neurons are controlled by feedback circuits.

**Olfactory memory is binary composed of repulsion to CS+ and attraction to CS-**

Aversive olfactory memory, especially electric shock paradigms, has been studied in detail over the past decades. Although animals experience both CS+ and CS-, repulsion to CS+ has been regarded as the only readout of memory, while CS- was ignored as a neutral blank reference odor. Our data, however, shows that CS- activates reward DANs, suggesting that CS- is conditioned as attractive, being integral part of aversive olfactory memory. Indeed, standard full performance score consists of two half scores: repulsion memory to CS+ and attraction memory to CS-. Repulsion score to CS+ is considerably lower than standard full score and attraction score to CS- contributes to full score at different proportions for different memory phases. For 1-cycle short-term memory (10min), attraction score contributes 0.15 to the full score of 0.75 while the rest 0.6 is made of repulsion score. For 5-cycle mid-term memory (3h), attraction and repulsion scores take up roughly equal proportion (0.3) of full score of 0.6. Notably, even protein-synthesis-dependent long-term memory (24h) is made of equal proportion of repulsion and attraction. Furthermore, repulsion memory decays relatively fast whereas attraction memory decays relatively slow, reminiscent of appetitive memory in sugar conditioning [45, 46]. Although flies need to be in hunger or thirst state for

appetitive conditioning to occur, artificial activation of PAM reward DANs by dTrpA1 have been shown to induce appetitive memory in satiated flies [8, 45].

Furthermore, MBONs of different valence are in charge of different memory types. On one hand, repulsion MBONs receiving dopamine input from punishment DANs, such as $\gamma 1$ MBON, are mostly responsible for repulsion memory to CS+. On the other hand, attraction MBONs receiving dopamine input from reward DANs, such as $\gamma 4$ MBON, not only mediate attraction memory to CS- but also repulsion memory to CS+, mostly likely due to inhibition of reward DANs during CS+ presentation [45]. In summary, when flies are making choices between CS+ and CS- after aversive olfactory conditioning, they not only feel repulsive to CS+ but also regard CS- as a benevolent smell.

**Bidirectional interaction between CS and US pathways**

Dopamine neurons in *Drosophila* receive input from both US and CS and thereby serves as the pivot of the interaction between US and CS. It has been established that dopamine release activated by US, as reinforcement signal, changes synaptic transmission from mushroom body to MBON, thus modifying CS pathway. Here we show that odor response changes activity of DANs in a self-reinforcing way, tweaking DANs' response to US. Moreover, we also show that electric shocks can directly potentiate odor-evoked response of DANs, bypassing modulating synaptic transmission from mushroom body. Such bidirectional interaction endows fruit flies with higher flexibility in learning.

**Relevance to dopamine system in mammals**

In mammalian dopamine system, such as mouse VTA, subset of dopamine neurons are also able to encode both reward and punishment predicting stimuli [12, 28]. Moreover, VTA dopamine neurons are also regulated by a large group of non-dopaminergic neurons, including glutamate and GABA neurons both from within VTA and a wide range of other brain regions, such as lateral habenula and prefrontal cortex. For instance, VTA GABA neurons increase their firing rate during exposure to reward-predicting cues and inhibition of VTA GABA neurons modulates activity of neighboring dopamine neurons and thus modulates prediction errors encoded by VTA DA neurons [29, 77]. Here we demonstrate that, in *Drosophila* brain, mushroom body non-dopaminergic neurons, including MBONs and RLNs, also regulate dopamine neurons in a way that is critical for dopamine neuron normal function. Blocking RLNs or MBONs output during conditioning also interferes with dopamine activity. A further thorough investigation of *Drosophila* dopamine neural network, could potentially provide insight into the fundamental rules of how regulation of dopamine neurons, especially feedback regulation, contributes to memory formation.

# Materials and Methods

## Summary of main methods

### Fly stocks

A detailed list of fly genotypes can be found blow. Flies were obtained from Bloomington Stock Center or Janelia Stock Center. GAL4 lines used for calcium imaging screening were selected by visual inspection from FlyLight project.

### Functional Calcium Imaging

All functional imaging experiments were performed on a Zeiss two-photon laser-scanning microscope (LSM780 NLO). Images were taken on a single focal plane with a frequency of 2.5Hz. GCaMP6s was expressed in all relevant neurons. Fly head with head cuticle removed and brain exposed was submerged in Schneider medium supplemented with 2mM $Ca^{2+}$ and 4mM $NaHCO_3$. Odor stimulation was achieved by a well-designed odor delivery system to ensure constant flow rate when switching valves. A continuous stream (2000ml/min) of air was directed at fly antenna through all time during training under microscope, even during cycle intervals. At a trigger, 10% of air stream was diverted through a vial containing odorants diluted in paraffin oil. 0.3% OCT and 0.15% MCH were used in all training experiments.

### Optogenetic activation of MBONs and RLNs

Larvae were grown on standard food. After eclosion, flies were kept on standard food supplemented with 1mM all-trans-retinal for 8-10 days. To monitor neuron responses, GCaMP6s was expressed by lexA lines. R58E02-lexA and lexAop>GCaMP6s were used to drive expression in horiztonal lobe DANs. CsChrimson was expressed in MBONs or RLNs by UAS>CsChrimson::tdTomato and corresponding split GAL4 or GAL4 lines. CsChrimson was activated through microscope built-in laser line (633nm) at the intensity of approximately 10-20$\mu$w/mm$^2$. We found that red light of high intensity causes DANs firing even in animals without CsChrimson expression. Intensity was lowered to a level that minimizes DANs' response to red light.

**Tethered individual fly conditioning**

A mounting chamber was designed to allow for clearer imaging of brain regions close to antenna, including MBs, SPM and CRE while keeping antenna intact (Fgiure S1). Fly was mounted on aluminum foil and the foil was glued to the chamber by grease oil. Fly legs were attached to paraffin wax with tips exposed in order to allow for copper wire attachment. Copper wires were held against fly legs without any glue. Agarose gel dissolved in saline was used to cover both copper wires and fly legs to make them conductive. Kwik silicone glue (World Precision Instruments) was then applied onto agarose gel to prevent it from drying out. Stimulator (S48 Stimulator, Grass Technology) was used to apply electric current through the fly.

**Classical aversive olfactory conditioning**

Fly training apparatus was built with the help of Harvard CSB machine shop. Experiments were performed as previously described in Tully et al. [89] 60V voltage was used to provide electrical stimulation to the flies. A custom-made T-maze was used to measure performance index. Performance index was calculated as $(n_1–n_2)$ / $(n_1+n_2)$; $n_1$ and $n_2$ denote number of flies that chose odor 1 and odor 2 respectively. 0.3% OCT and 0.15% MCH were used in all training experiments.

## Detailed description of methods

**Fly Strains**

Flies were grown on conventional cornmeal-agar-molasses medium at 25 °C and approximately 70 % humidity, under 12hr light/12hr dark cycle. Flies used for *shi$^{ts1}$* silencing behavior experiments were grown at 21 °C.

**Strains and sources:**

*R58E02-Gal4, R86D02-Gal4, R33G12-Gal4, R33E06-Gal4, R74B04-Gal4, R52G04-Gal4, R14C08-Gal4, R58E02-lexA, R86D02-lexA, R33E06-lexA, R41G06-lexA, R53D01-lexA, R52G04-lexA, R53H03-lexA* (Jenett et al 2012, http://flweb.janelia.org/cgi-bin/flew.cgi ). *MB077b, MB011b,*

*MB083c, MB112c, MB057b, MB441b, MB316B, MB056b.* (Aso et al 2014; http://splitgal4.janelia.org/cgi-bin/splitgal4.cgi ) $\gamma$4-splitGal4 (Shuai et al, 2016; a gift from Yichun Shuai) *UAS-GCaMP6s, lexAop-GCaMP6s, UAS-shi$^{ts1}$* (Aso et al, 2014), *UAS-kir2.1::GFP, UAS-CsChrimson::tdTomato, UAS-myr::GFP, UAS-dTrpA1, UAS-syt::GFP, UAS-Denmark, UAS-spGFP1-10, lexAop-spGFP11.*

***Detailed fly genotypes used by figures (with neuronal expression description).***

Figure 1C-E , 7 and S2, S3, S4:

R58E02-Gal4; UAS-GCaMP6s

Figure 2H, 2I:

R86D02-Gal4/R33E06-Gal4, UAS-GCaMP6s

Figure 3A, 3B, 3C:

R58E02-Gal4; UAS-GCaMP6s

Figure 3G:

Left: MB441b; R86D02-lexA; UAS-spGFP1-10, lexAop-spGFP1-11.

Right: UAS-CsChrimson::tdTomato/R58E02-lexA, lexAop-GCaMP6s; R86D02.

Figure 3H:

Left: MB316b; R86D02-lexA; UAS-spGFP1-10, lexAop-spGFP1-11.

Right: UAS-CsChrimson::tdTomato/R58E02-lexA, lexAop-GCaMP6s; R86D02.

Figure 3I:

Left: MB056b; R86D02-lexA; UAS-spGFP1-10, lexAop-spGFP1-11.

Right: UAS-CsChrimson::tdTomato/R58E02-lexA, lexAop-GCaMP6s; R86D02.

Figure 3J:

Left: MB441b; R33E06-lexA; UAS-spGFP1-10, lexAop-spGFP1-11.

Right: UAS-CsChrimson::tdTomato/R58E02-lexA, lexAop-GCaMP6s; R33E06.

Figure 3K:

Left: MB316b; R33E06-lexA; UAS-spGFP1-10, lexAop-spGFP1-11.

Right: UAS-CsChrimson::tdTomato/R58E02-lexA, lexAop-GCaMP6s; R33E06.

Figure 3L:

Left: MB056b; R33E06-lexA; UAS-spGFP1-10, lexAop-spGFP1-11.

Right: UAS-CsChrimson::tdTomato/R58E02-lexA, lexAop-GCaMP6s; R33E06.

Figure 4A: R74B04-Gal4, UAS-GCaMP6s.

Figure 4B: *R52G04-Gal4*, UAS-GCaMP6s.

Figure 4C: R74B04-Gal4, UAS-GCaMP6s.

Figure 4D: *R14C08-Gal4*, UAS-GCaMP6s.

Figure 4E: MB011b; R86D02-lexA; UAS-spGFP1-10, lexAop-spGFP1-11.

Figure 4F: MB077b; R86D02-lexA; UAS-spGFP1-10, lexAop-spGFP1-11.

Figure 4G: MB011b; R33E06-lexA; UAS-spGFP1-10, lexAop-spGFP1-11.

Figure 4H: MB077b; R33E06-lexA; UAS-spGFP1-10, lexAop-spGFP1-11.

Figure S4A: MB441b; R41G06-lexA; UAS-spGFP1-10, lexAop-spGFP1-11.

Figure S4B: $\gamma$4-splitGal4; R41G06-lexA; UAS-spGFP1-10, lexAop-spGFP1-11.

Figure S4C: MB441b; R53D01-lexA; UAS-spGFP1-10, lexAop-spGFP1-11.

Figure S4D: $\gamma$4-splitGal4; R53D01-lexA; UAS-spGFP1-10, lexAop-spGFP1-11.

Figure S4E: $\gamma$4-splitGal4; R58E02-lexA; UAS-spGFP1-10, lexAop-spGFP1-11.

Figure 5A, 5B, 5C, 5D:

MB112c, UAS-Kir2.1; MB077b, UAS-Kir2.1; $\gamma$4-splitGal4, UAS-Kir2.1; MB011b, UAS-Kir2.1

Figure 5E, 5F, 5G, 5H:

R58E02-Gal4, UAS-shi$^{ts1}$; R86D02-Gal4, UAS-shi$^{ts1}$; R33G12-Gal4, UAS-shi$^{ts1}$.

**Imaging**

All functional imaging experiments were performed on Zeiss LSM 780 NLO Multi-Photon Microscope at Harvard Center for Brain Imaging. Emitted fluorescence was detected with 4-channel non-descanned detector or 34 channel spectral detector. Images were acquired with a 20X, 0.9 numerical aperture objective at 512 pixels x 512 pixels or 256 pixels x 256 pixels resolution. For training-under-microscope imaging, images were acquired at a rate of 2.5 Hz. For optogenetics imaging, images were acquired at a rate of 5Hz.

**Functional Imaging**

For all in vivo imaging experiments, brains were dissected in 0.9x Schneider Insect Medium (Sigma) supplemented with 2mM $Ca^{2+}$ and 4mM $NaHCO_3$. A special chamber was designed for

robust imaging of mushroom body, SMP and CRE regions with high resolution and high clarity. Flies were prepared as below. 5-10 days old flies were anaesthetized on ice and glued to a hole cut out on a small piece of aluminum foil. Bio-compatible adhesive Kwik-Sil Adhesive (World Precision Instrument) was used as glue. The piece of aluminum foil with one fly tethered was then attached onto imaging chamber. The chamber was then filled with Schneider medium and the head capsule was opened by carefully cutting the cuticle covering the dorsal portion of the head. Obstructing trachea was removed with forceps. Care was taken to keep antenna and antennal nerves intact.

**Odor Stimulation**

Odor stimulation was achieved by directing a continuous stream (2000ml/min) of clean air through a 1/8 inch inner diameter Teflon tubing directed at the fly's antenna (carrier stream). 10% of the total air stream was diverted through a glass vial containing 5mL paraffin oil (odor stream). A third compensating air stream (200ml/min) was directed out of the system. At a trigger, a custom-built solenoid valve controller system redirected the third compensating air stream to a vial containing odorants diluted in 5mL paraffin oil (Sigma) and simultaneously switched the compensating air stream with the second air stream. This was designed to reduce air stream disturbance during valve switches. Final odorant dilutions were usually around 1:1000, depending on the identity of odorants. Odorants used were 3-octanol (CAS #589- 98-0) and methancyclohexanol (CAS #589-91-3).

**Tethered Fly Olfactory Conditioning**

Fly was mounted on aluminum foil as described in Functional Imaging. We chose to shock the fly through the legs since we believe that in standard training experiments, flies were shocked through legs instead of abdomen. Fly legs were first attached to paraffin wax with its tips exposed to allow for wire attachment. Copper wires were held against fly legs without any glue. Agarose gel dissolved in saline was used to cover both copper wires and fly legs to make the connection conductive. Kwik silicone glue (World Precision Instruments) was then applied onto agarose gel to prevent it from drying out and to immobilize the connection between legs and wires. Stimulator (S48 Stimulator, Grass Technology) was used to apply electric current through the fly. Total electric currents were measured in aversive olfactory

conditioning when an ensemble of ~100 flies were trained on copper grids in training tubes. Usually, a total electric current of around 200$\mu$A passed through the grids for 100 flies, e.g. 2$\mu$A per fly. Total resistance for 100 flies is usually ~500 KΩ, e.g. 50MΩ per fly. Current during imaging was measured by digital multimeter (Fluke 116 TRUE RMS multimeter). We adjusted voltage slightly in each tethered fly conditioning experiment to keep electrical current constant at ~1$\mu$A. Usually only ~10V voltage was enough to trigger a current of ~1$\mu$A. We delivered 500ms of ~1$\mu$A stimulation in each electric shock pulse.

**Classical Aversive Olfactory Conditioning**

Training apparatus was designed and made at Harvard Machine Shop. Training protocols were described in detail in literature. Briefly, during each training cycle, CS+ was first presented to the animals for 60 seconds while 10 pulses of electric shocks were delivered every 5 seconds. Each electric shock pulse lasted for 1 second. After an interval of 60 seconds, CS- was the presented for 60 seconds. For spaced training paradigm, animals were trained with 5 cycles of conditioning with an interval of 15min. Flies were then tested in a custom made T-maze for memory score.

**Image processing and Data Analysis**

Most image processing was done in FIJI/ImageJ (NIH). Further analysis was done using custom Matlab codes as described below. When necessary, to correct for motion during in vivo imaging, time series images were aligned using the TurboReg FIJI plugin.

***Calcium Intensity Plots***

For imaging of DANs and MBONs, ROIs were manually drawn based on clear anatomical segregation of the innervation patterns in different compartments. For imaging of RLNs, ROIs were manually drawn covering the entire axonal branches in the field of view, while avoiding inclusion of branches from irrelevant neurons. For DANs, we can clearly observe fluorescence punctae in each compartment. For MBONs and RLNs, we can clearly observe neuronal branches. In order to extract those punctae and branches while excluding background noise, a difference of Gaussian (DoG) filter for blob detection was applied to each frame to extract punctae and branch features. Two Gaussian kernels were used for DoG filter and the standard

deviation ($\sigma$) for each kernel was 1.8 and 2.4 pixels respectively. An image mask was calculated from DoG treated raw image. Then image mask was applied to each raw image to obtain punctae or branch blobs. Fluorescence intensity was finally calculated by averaging the fluorescence over the entire image. For calcium traces, ΔF/F was calculated by calculating the different between the pre-stimulus values, an average of 20 frames (~ 7 seconds) ending >1 frame before stimulus onset, and the post-stimulus values (for each frame) divided by pre-stimulus value. For $\Delta F/F_0$ in plot over training cycle, calculation was done by averaging $\Delta F/F_0$ values over the first 8 seconds after stimulus onset. Note that in the case of DAN imaging, DAN exhibit relatively strong fluctuations in their basal activity, making it more difficult to obtain an accurate estimate of basal activity. However, we suppose that 7 seconds before stimulus onset is long enough for an estimate of basal activity and thus we use the average of the fluorescence values as basal activity.

***Cross-correlation Analysis*** (Figure S2):

Pearson product-moment correlation coefficients between pairs of DANs were calculated for a 60 second recording in each animal in Matlab. The resulting coefficients were averaged and used to generate the cross-correlogram shown in Figure S2. A dashed line of significance was provided for each plot by Matlab functions.

**Statistical Analysis**

Statistical analysis was performed using custom scripts in Matlab. Paired T-test was used for all paired comparison of DAN, RLN and MBON response to CS+ and CS- (Figure 1, 2 and 4). Unpaired T-test was used for control/*Shi*$^{ts1}$ data (Figure 6) and DAN and RLN response comparison due to optogenetic activation by CsChrimson (Figure 3 and Figure 4). One-way ANOVA test was used for all aversive olfactory conditioning experiments, including inhibition experiments using Kir2.1 and *Shi*$^{ts1}$ (Figure 8).

**Optogenetic Activation by CsChrimson**

Flies expressing CsChrimson, a red-shifted channelrhodopsin variant, in MBONs or RLNs, were placed on food containing 400$\mu$M all-trans retinal, for 8-10 days prior to imaging. 633nm red light illumination was achieved by focused laser scanning in Zeiss LSM 780 NLO

Multi-Photon Microscope. A photo-bleaching option is available in Zeiss system and thus was used to provide red light stimulation when neuron activity was recorded by 2-photon laser scanning. External light source, such as mounted LED, was found to be so strong as to trigger response even in control animals without CsChrimson expression. Laser scanning allows us to focus light onto a tiny spot on fly brain (roughly estimate ~400 $\mu$m x 400 $\mu$m) to minimize light intensity, thus reducing natural light activated DANs' response to a negligible level. In addition, fly eyes were covered by aluminum foil during mounting to reduce direct light stimulation. 100ms light stimulation was used in each experiment.

**Adult Brain Immunostaining**

5-10 days old adult brains were dissected in 1X PBS pH7.4 and then immediately transferred to cold 1% supplemented PFA solution and fixed overnight at 4 ℃. Following overnight incubation, samples were washed in PBST (0.3% Triton/1X PBS pH 7.4) 3 times. Brains were then blocked in 3% Normal Goat Serum for 3 hours at 4 ℃. Primary antibody was incubated overnight at 4 ℃. Brains were then washed extensively in PBST 3 times at RT, 30min per wash. Secondary antibody was incubated at 4 ℃ from 1 day to 3 days. Brains were then again washed extensively in PBST 3 times at RT, 30min per wash. Samples were mounted in custom-made 70% glycerol. Images were acquired on a Zeiss LSM 880 using a 60X objective. Primary antibodies used include: rabbit anti-GFP (1:1000; Invitrogen; A11122), mouse anti-nc82 (1:33.3; Developmental Studies Hybridoma Bank, Univ. Iowa), mouse anti-*Drosophila* ChAT (ChAT4B1; 1: 100; Developmental Studies Hybridoma Bank, Univ. Iowa), rabbit anti-DvGluT (1:5000; a gift from Dr. A DiAntonio), rabbit anti-*Drosophila* GAD1 (1:1000; a gift from Dr. FR Jackson). Secondary antibodies used include: Cy3 goat anti-mouse (1:100; Jackson Labs), Cy5 donkey anti-rabbit (1:100; Jackson Labs).

# References


1. Missale, C., et al., *Dopamine receptors: from structure to function.* Physiol Rev, 1998. **78**(1): p. 189-225.

2. Hearn, M.G., et al., *A Drosophila dopamine 2-like receptor: Molecular characterization and identification of multiple alternatively spliced variants.* Proc Natl Acad Sci U S A, 2002. **99**(22): p. 14554-9.

3. Srivastava, D.P., et al., *Rapid, nongenomic responses to ecdysteroids and catecholamines mediated by a novel Drosophila G-protein-coupled receptor.* J Neurosci, 2005. **25**(26): p. 6145-55.

4. Hnasko, T.S., et al., *Vesicular glutamate transport promotes dopamine storage and glutamate corelease in vivo.* Neuron, 2010. **65**(5): p. 643-56.

5. Tritsch, N.X., J.B. Ding, and B.L. Sabatini, *Dopaminergic neurons inhibit striatal output through non-canonical release of GABA.* Nature, 2012. **490**(7419): p. 262-6.

6. Wise, R.A., *Dopamine, learning and motivation.* Nat Rev Neurosci, 2004. **5**(6): p. 483-94.

7. Wise, R.A. and H.V. Schwartz, *Pimozide attenuates acquisition of lever-pressing for food in rats.* Pharmacol Biochem Behav, 1981. **15**(4): p. 655-6.

8. Burke, C.J., et al., *Layered reward signalling through octopamine and dopamine in Drosophila.* Nature, 2012. **492**(7429): p. 433-+.

9. Masek, P., et al., *A dopamine-modulated neural circuit regulating aversive taste memory in Drosophila.* Curr Biol, 2015. **25**(11): p. 1535-41.

10. Huston, J.P., et al., *What's conditioned in conditioned place preference?* Trends Pharmacol Sci, 2013. **34**(3): p. 162-6.

11. Bromberg-Martin, E.S., M. Matsumoto, and O. Hikosaka, *Dopamine in motivational control: rewarding, aversive, and alerting.* Neuron, 2010. **68**(5): p. 815-34.

12. Matsumoto, M. and O. Hikosaka, *Two types of dopamine neuron distinctly convey positive and negative motivational signals.* Nature, 2009. **459**(7248): p. 837-41.

13. Abramson, C.I., C.W. Dinges, and H. Wells, *Operant Conditioning in Honey Bees (Apis mellifera L.): The Cap Pushing Response.* PLoS One, 2016. **11**(9): p. e0162347.

14. Pignatelli, M. and A. Bonci, *Role of Dopamine Neurons in Reward and Aversion: A Synaptic Plasticity Perspective.* Neuron, 2015. **86**(5): p. 1145-57.

15. Schultz, W., *Potential vulnerabilities of neuronal reward, risk, and decision mechanisms to addictive drugs.* Neuron, 2011. **69**(4): p. 603-17.

16. Bocklisch, C., et al., *Cocaine disinhibits dopamine neurons by potentiation of GABA transmission in the ventral tegmental area.* Science, 2013. **341**(6153): p. 1521-5.

17. Floresco, S.B., *The nucleus accumbens: an interface between cognition, emotion, and action.* Annu Rev Psychol, 2015. **66**: p. 25-52.

18. Lobo, M.K., et al., *Cell type-specific loss of BDNF signaling mimics optogenetic control of cocaine reward.* Science, 2010. **330**(6002): p. 385-90.

19. Calabresi, P., et al., *Direct and indirect pathways of basal ganglia: a critical reappraisal.* Nat Neurosci, 2014. **17**(8): p. 1022-30.

20. Lisman, J.E. and A.A. Grace, *The hippocampal-VTA loop: controlling the entry of information into long-term memory.* Neuron, 2005. **46**(5): p. 703-13.

21. Ripolles, P., et al., *Intrinsic monitoring of learning success facilitates memory encoding via the activation of the SN/VTA-Hippocampal loop.* Elife, 2016. **5**.

22. Takeuchi, T., et al., *Locus coeruleus and dopaminergic consolidation of everyday memory.* Nature, 2016. **537**(7620): p. 357-362.

23. Popescu, A.T., M.R. Zhou, and M.M. Poo, *Phasic dopamine release in the medial prefrontal cortex enhances stimulus discrimination.* Proc Natl Acad Sci U S A, 2016. **113**(22): p. E3169-76.

24. Kwon, O.B., et al., *Dopamine Regulation of Amygdala Inhibitory Circuits for Expression of Learned Fear.* Neuron, 2015. **88**(2): p. 378-89.

25. Stamatakis, A.M. and G.D. Stuber, *Activation of lateral habenula inputs to the ventral midbrain promotes behavioral avoidance.* Nat Neurosci, 2012. **15**(8): p. 1105-7.

26. Nieh, E.H., et al., *Inhibitory Input from the Lateral Hypothalamus to the Ventral Tegmental Area Disinhibits Dopamine Neurons and Promotes Behavioral Activation.* Neuron, 2016. **90**(6): p. 1286-98.

27. Schultz, W., P. Dayan, and P.R. Montague, *A neural substrate of prediction and reward.* Science, 1997. **275**(5306): p. 1593-9.

28. Cohen, J.Y., et al., *Neuron-type-specific signals for reward and punishment in the ventral tegmental area.* Nature, 2012. **482**(7383): p. 85-8.

29. Eshel, N., et al., *Arithmetic and local circuitry underlying dopamine prediction errors.* Nature, 2015. **525**(7568): p. 243-6.

30. Tian, J., et al., *Distributed and Mixed Information in Monosynaptic Inputs to Dopamine Neurons.* Neuron, 2016. **91**(6): p. 1374-89.

31. Shiraiwa, T., *Multimodal chemosensory integration through the maxillary palp in Drosophila.* PLoS One, 2008. **3**(5): p. e2191.

32. Kurtovic, A., A. Widmer, and B.J. Dickson, *A single class of olfactory neurons mediates behavioural responses to a Drosophila sex pheromone.* Nature, 2007. **446**(7135): p. 542-6.

33. Su, C.Y., K. Menuz, and J.R. Carlson, *Olfactory perception: receptors, cells, and circuits.* Cell, 2009. **139**(1): p. 45-59.

34. Wilson, R.I., G.C. Turner, and G. Laurent, *Transformation of olfactory representations in the Drosophila antennal lobe.* Science, 2004. **303**(5656): p. 366-70.

35. Bhandawat, V., et al., *Sensory processing in the Drosophila antennal lobe increases reliability and separability of ensemble odor representations.* Nat Neurosci, 2007. **10**(11): p. 1474-82.

36. Olsen, S.R. and R.I. Wilson, *Lateral presynaptic inhibition mediates gain control in an olfactory circuit.* Nature, 2008. **452**(7190): p. 956-60.

37. Turner, G.C., M. Bazhenov, and G. Laurent, *Olfactory representations by Drosophila mushroom body neurons.* J Neurophysiol, 2008. **99**(2): p. 734-46.

38. Caron, S.J., et al., *Random convergence of olfactory inputs in the Drosophila mushroom body.* Nature, 2013. **497**(7447): p. 113-7.

39. Tang, S., et al., *Visual pattern recognition in Drosophila is invariant for retinal position.* Science, 2004. **305**(5686): p. 1020-2.

40. Liu, G., et al., *Distinct memory traces for two visual features in the Drosophila brain.* Nature, 2006. **439**(7076): p. 551-6.

41. Vogt, K., et al., *Shared mushroom body circuits underlie visual and olfactory memories in Drosophila.* Elife, 2014. **3**: p. e02395.

42. Ofstad, T.A., C.S. Zuker, and M.B. Reiser, *Visual place learning in Drosophila melanogaster.* Nature, 2011. **474**(7350): p. 204-7.

43. D'Hooge, R. and P.P. De Deyn, *Applications of the Morris water maze in the study of learning and memory.* Brain Res Brain Res Rev, 2001. **36**(1): p. 60-90.

44. Galili, D.S., et al., *Converging circuits mediate temperature and shock aversive olfactory conditioning in Drosophila.* Curr Biol, 2014. **24**(15): p. 1712-22.

45. Liu, C., et al., *A subset of dopamine neurons signals reward for odour memory in Drosophila.* Nature, 2012. **488**(7412): p. 512-+.

46. Lin, S., et al., *Neural correlates of water reward in thirsty Drosophila.* Nature Neuroscience, 2014. **17**(11): p. 1536-42.

47. Keleman, K., et al., *Dopamine neurons modulate pheromone responses in Drosophila courtship learning.* Nature, 2012. **489**(7414): p. 145-9.

48. Tully, T. and W.G. Quinn, *Classical conditioning and retention in normal and mutant Drosophila melanogaster.* J Comp Physiol A, 1985. **157**(2): p. 263-77.

49. Waddell, S., et al., *The amnesiac gene product is expressed in two neurons in the Drosophila brain that are critical for memory.* Cell, 2000. **103**(5): p. 805-13.

50. Isabel, G., A. Pascual, and T. Preat, *Exclusive consolidated memory phases in Drosophila.* Science, 2004. **304**(5673): p. 1024-7.

51. Tully, T., et al., *Genetic dissection of consolidated memory in Drosophila.* Cell, 1994. **79**(1): p. 35-47.

52. Livingstone, M.S., P.P. Sziber, and W.G. Quinn, *Loss of calcium/calmodulin responsiveness in adenylate cyclase of rutabaga, a Drosophila learning mutant.* Cell, 1984. **37**(1): p. 205-15.

53. Keene, A.C. and S. Waddell, *Drosophila olfactory memory: single genes to complex neural circuits.* Nat Rev Neurosci, 2007. **8**(5): p. 341-54.

54. van der Bliek, A.M. and E.M. Meyerowitz, *Dynamin-like protein encoded by the Drosophila shibire gene associated with vesicular traffic.* Nature, 1991. **351**(6325): p. 411-4.

55. Yu, D., D.B. Akalal, and R.L. Davis, *Drosophila alpha/beta mushroom body neurons form a branch-specific, long-term cellular memory trace after spaced olfactory conditioning.* Neuron, 2006. **52**(5): p. 845-55.

56. Krashes, M.J., et al., *Sequential use of mushroom body neuron subsets during drosophila odor memory processing.* Neuron, 2007. **53**(1): p. 103-15.

57. Chen, C.C., et al., *Visualizing long-term memory formation in two neurons of the Drosophila brain.* Science, 2012. **335**(6069): p. 678-85.

58. Riemensperger, T., et al., *Behavioral consequences of dopamine deficiency in the Drosophila central nervous system.* Proc Natl Acad Sci U S A, 2011. **108**(2): p. 834-9.

59. Mao, Z. and R.L. Davis, *Eight different types of dopaminergic neurons innervate the Drosophila mushroom body neuropil: anatomical and physiological heterogeneity.* Front Neural Circuits, 2009. **3**: p. 5.

60. Aso, Y., et al., *Specific dopaminergic neurons for the formation of labile aversive memory.* Curr Biol, 2010. **20**(16): p. 1445-51.

61. Liu, Q., et al., *Two dopaminergic neurons signal to the dorsal fan-shaped body to promote wakefulness in Drosophila.* Curr Biol, 2012. **22**(22): p. 2114-23.

62. Azanchi, R., K.R. Kaun, and U. Heberlein, *Competing dopamine neurons drive oviposition choice for ethanol in Drosophila.* Proc Natl Acad Sci U S A, 2013. **110**(52): p. 21153-8.

63. Vogt, K., et al., *Shared mushroom body circuits underlie visual and olfactory memories in Drosophila.* Elife, 2014. **3**.

64. McGuire, S.E., P.T. Le, and R.L. Davis, *The role of Drosophila mushroom body signaling in olfactory memory.* Science, 2001. **293**(5533): p. 1330-3.

65. Aso, Y., et al., *Mushroom body output neurons encode valence and guide memory-based action selection in Drosophila.* Elife, 2014. **3**: p. e04580.

66. Aso, Y., et al., *The neuronal architecture of the mushroom body provides a logic for associative learning.* Elife, 2014. **3**: p. e04577.

67. Sejourne, J., et al., *Mushroom body efferent neurons responsible for aversive olfactory memory retrieval in Drosophila.* Nature Neuroscience, 2011. **14**(7): p. 903-10.

68. Placais, P.Y., et al., *Slow oscillations in two pairs of dopaminergic neurons gate long-term memory formation in Drosophila.* Nature Neuroscience, 2012. **15**(4): p. 592-599.

69. Aso, Y., et al., *Mushroom body output neurons encode valence and guide memory-based action selection in Drosophila.* Elife, 2014. **4**: p. e04580.

70. Berry, J.A., et al., *Sleep Facilitates Memory by Blocking Dopamine Neuron-Mediated Forgetting.* Cell, 2015. **161**(7): p. 1656-67.

71. Hige, T., et al., *Heterosynaptic Plasticity Underlies Aversive Olfactory Learning in Drosophila.* Neuron, 2015. **88**(5): p. 985-98.

72. Cohn, R., I. Morantte, and V. Ruta, *Coordinated and Compartmentalized Neuromodulation Shapes Sensory Processing in Drosophila.* Cell, 2015. **163**(7): p. 1742-55.

73. Claridge-Chang, A., et al., *Writing memories with light-addressable reinforcement circuitry.* Cell, 2009. **139**(2): p. 405-15.

74. Masek, P., et al., *A dopamine-modulated neural circuit regulating aversive taste memory in Drosophila.* Current Biology, 2015. **25**(11): p. 1535-41.

75. Waddell, S., *Neural Plasticity: Dopamine Tunes the Mushroom Body Output Network.* Current Biology, 2016. **26**(3): p. R109-12.

76. Riemensperger, T., et al., *Punishment prediction by dopaminergic neurons in Drosophila.* Current Biology, 2005. **15**(21): p. 1953-60.

77. Morales, M. and E.B. Margolis, *Ventral tegmental area: cellular heterogeneity, connectivity and behaviour.* Nat Rev Neurosci, 2017. **18**(2): p. 73-85.

78. Hong, W. and L. Luo, *Genetic control of wiring specificity in the fly olfactory system.* Genetics, 2014. **196**(1): p. 17-29.

79. Vosshall, L.B., *Into the mind of a fly.* Nature, 2007. **450**(7167): p. 193-7.

80. Nern, A., B.D. Pfeiffer, and G.M. Rubin, *Optimized tools for multicolor stochastic labeling reveal diverse stereotyped cell arrangements in the fly visual system.* Proc Natl Acad Sci U S A, 2015. **112**(22): p. E2967-76.

81. Feinberg, E.H., et al., *GFP Reconstitution Across Synaptic Partners (GRASP) defines cell contacts and synapses in living nervous systems.* Neuron, 2008. **57**(3): p. 353-63.

82. Owald, D., et al., *Activity of defined mushroom body output neurons underlies learned olfactory behavior in Drosophila.* Neuron, 2015. **86**(2): p. 417-27.

83. Niewalda, T., et al., *Synapsin determines memory strength after punishment- and relief-learning.* The Journal of neuroscience : the official journal of the Society for Neuroscience, 2015. **35**(19): p. 7487-502.

84. Perisse, E., et al., *Shocking revelations and saccharin sweetness in the study of Drosophila olfactory memory.* Current Biology, 2013. **23**(17): p. R752-63.

85. Aso, Y., et al., *Three dopamine pathways induce aversive odor memories with different stability.* PLoS Genet, 2012. **8**(7): p. e1002768.

86. Day, J.J., et al., *Associative learning mediates dynamic shifts in dopamine signaling in the nucleus accumbens.* Nature Neuroscience, 2007. **10**(8): p. 1020-8.

87. Gerber, B., et al., *Pain-relief learning in flies, rats, and man: basic research and applied perspectives.* Learn Mem, 2014. **21**(4): p. 232-52.

88. Schultz, W., *Dopamine reward prediction-error signalling: a two-component response.* Nat Rev Neurosci, 2016. **17**(3): p. 183-95.

89. Tully, T., et al., *Genetic Dissection of Consolidated Memory in Drosophila.* Cell, 1994. **79**(1): p. 35-47.

# Appendix

# Supplementary Figures

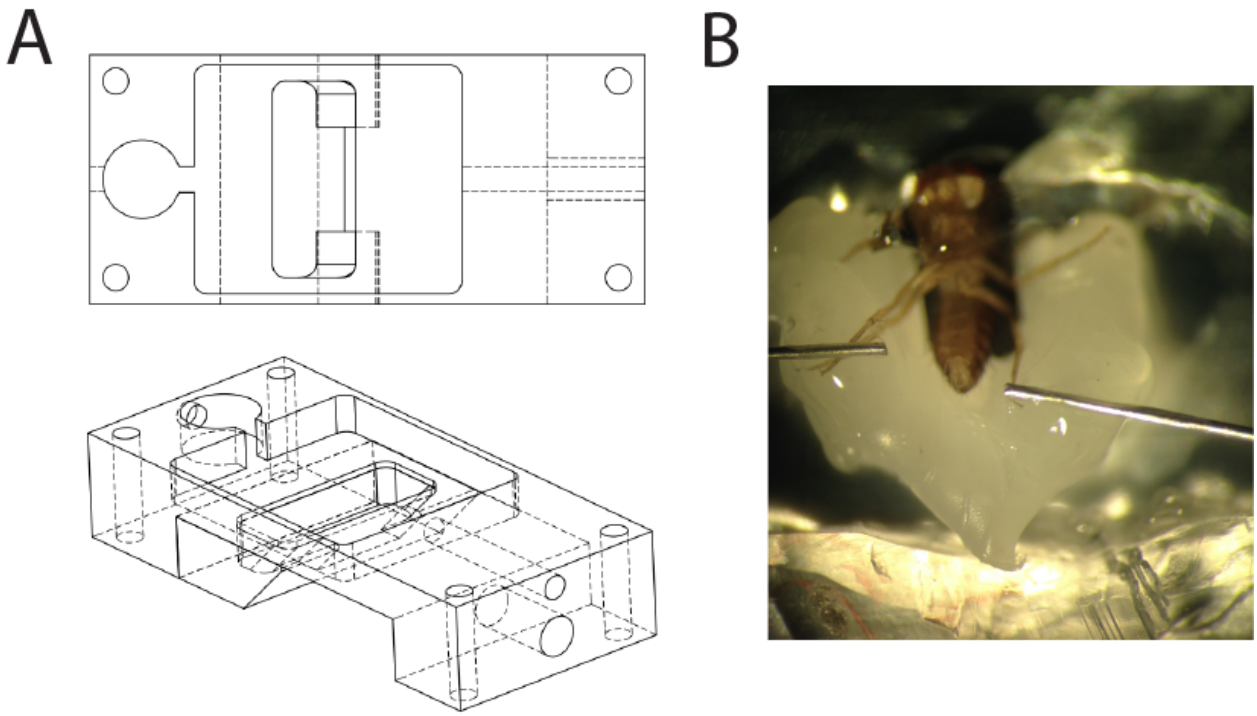


**Figure S1 Preparation of tethered fly for training under the microscope**
(A) Diagram of mounting chamber for functional imaging. Slope was designed to let the hole opened on fly head capsule face upwards. This allow for imaging of regions surrounding mushroom body with a better image quality. (B) Picture of an example fly with its legs immobilized on wax and attached to copper wires.

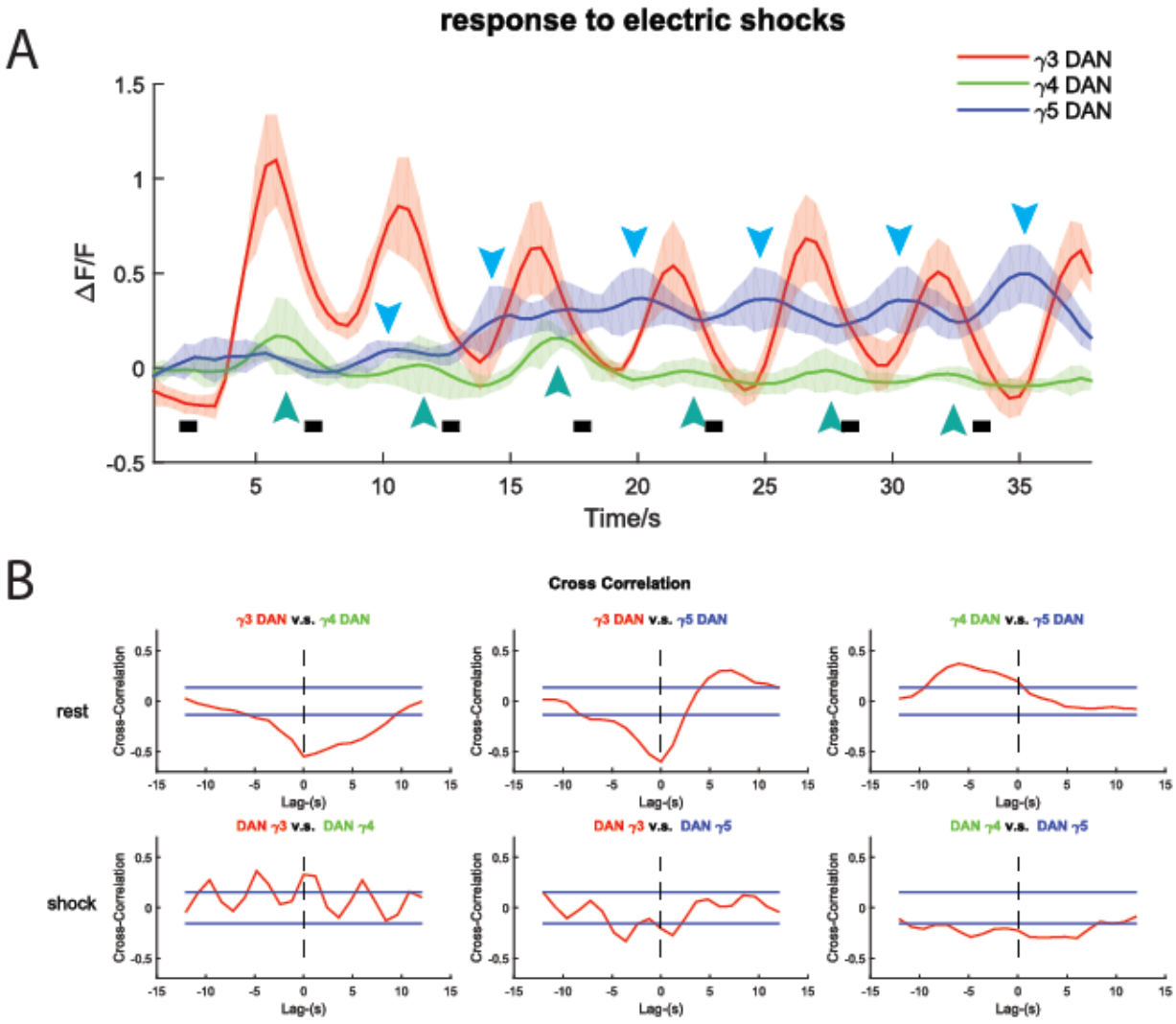


**Figure S2 Activity of DANs in response to electric shocks**

(A) $\gamma 3, \gamma 4$ and $\gamma 5$ DANs response to electric shocks alone in the absence of odors. Calcium traces of $\gamma 3, \gamma 4$ and $\gamma 5$ DANs are presented in red, green and blue respectively (n=5). Green and blue arrowheads denote local peaks of $\gamma 4$ and $\gamma 5$ DANs calcium traces. Black bars denote presentation of electric shocks (500ms each). (B) Cross-correlogram of pairs of DANs. Top panel: cross correlation of DANs during rest state; bottom panel: cross correlation of DANs in response to electric shocks. Blue line in each plot denotes significance level. Values above blue significance line indicates strong correlation beyond random.

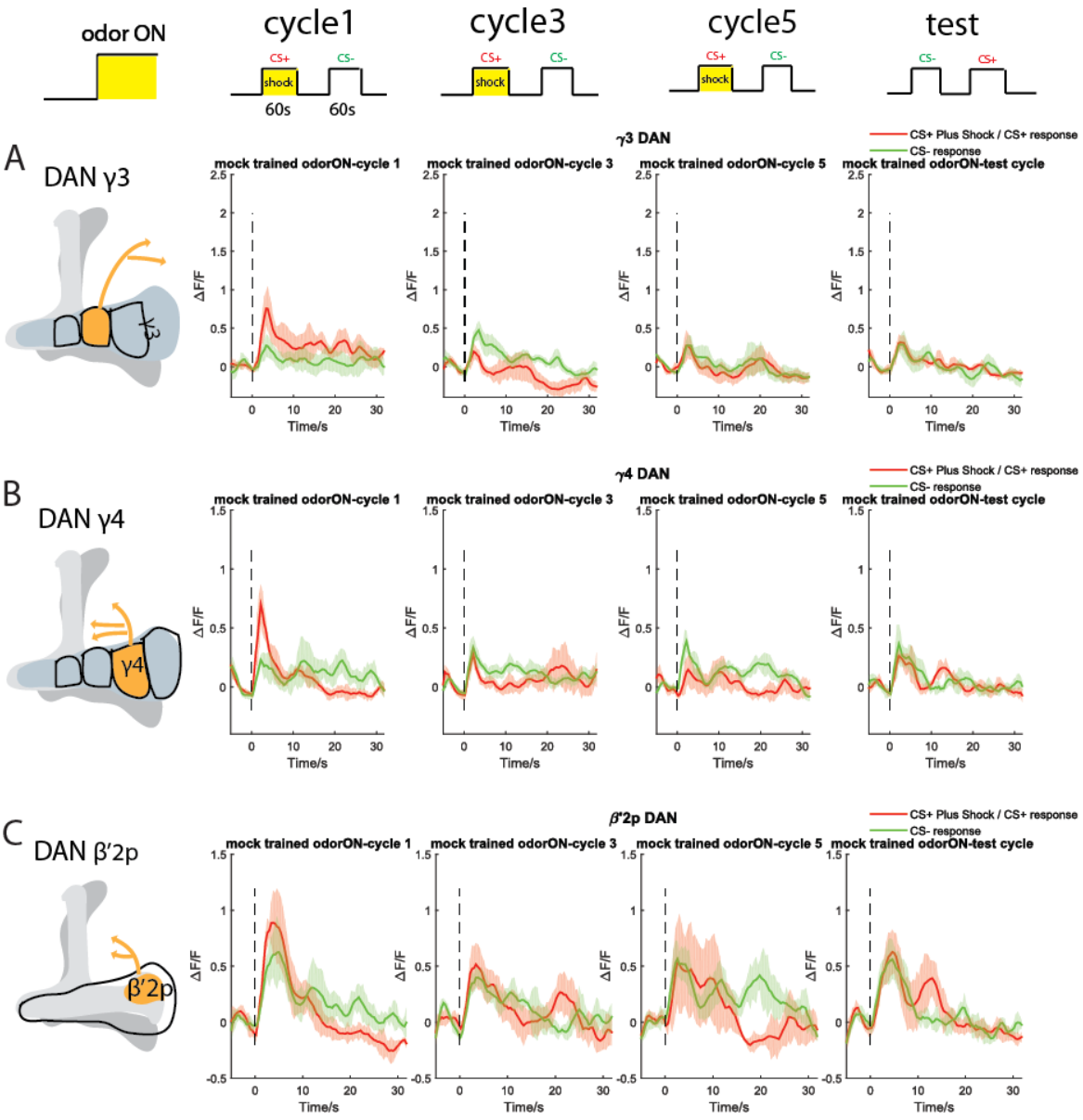


**Figure S3a Activity of DANs Odor-On response in mock trained controls**

(A-C) Calcium activity of $\gamma 3$ (n=7), $\gamma 4$ (n=7) and $\beta'2$ (n=6) DANs were imaged during 5-cycle mock trained controls. The first 3 columns display DANs calcium traces in cycle 1,3,5 (training cycles) and the last column displays DANs calcium trace in test cycle. Dashed line denotes odor onset. Red trace denotes DANs activity during CS+ presentation (CS+ plus shock in training cycles) and green trace denotes DANs activity during CS- presentation. Data are mean [solid line] $\pm$ MSE [shaded area] curves.

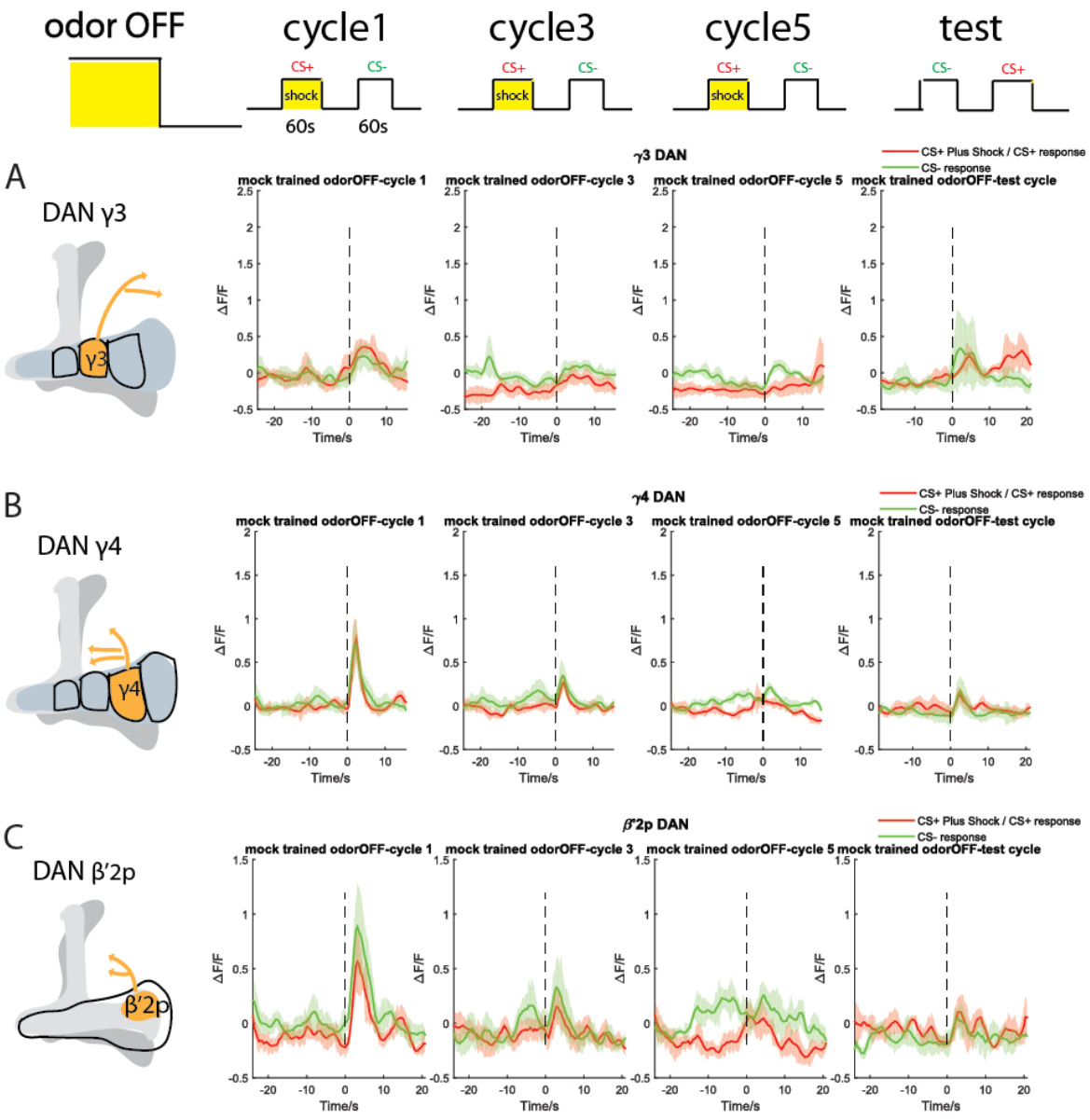


**Figure S3b Activity of DANs Odor-Off response in mock trained controls**

(A-C) Calcium activity of $\gamma 3$ (n=7), $\gamma 4$ (n=7) and $\beta'2$ (n=6) DANs were imaged during 5-cycle mock trained controls. The first 3 columns display DANs calcium traces in cycle 1,3,5 (training cycles) and the last column displays DANs calcium trace in test cycle. Dashed line denotes odor cessation. Red trace denotes DANs activity during CS+ presentation (CS+ plus shock in training cycles) and green trace denotes DANs activity during CS- presentation. Data are mean [solid line] $\pm$ MSE [shaded area] curves.

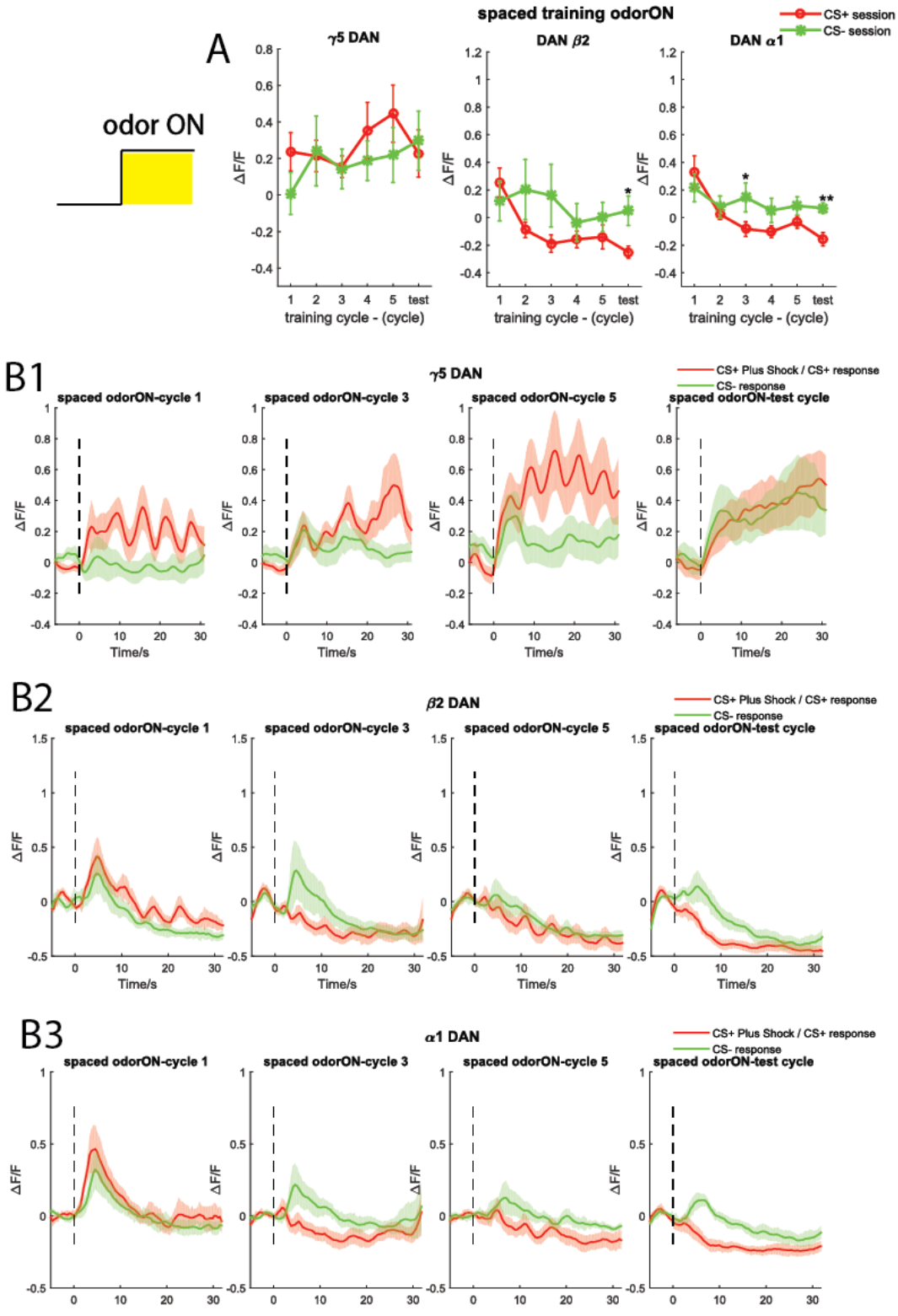


**Figure S4a Activity of other DANs Odor-On response in aversive olfactory conditioning**

Figure S4a (Continued). (A) Plot of DANs GCaMP6s fluorescence over training cycles. Calcium activity was calculated by averaging the fluorescence over the first 8 seconds after odor onset. (B-D) Calcium activity of $\gamma 5$ (n=11), $\beta 2$ (n=9) and $\alpha 1$ (n=9) DANs were imaged during 5-cycle conditioning.

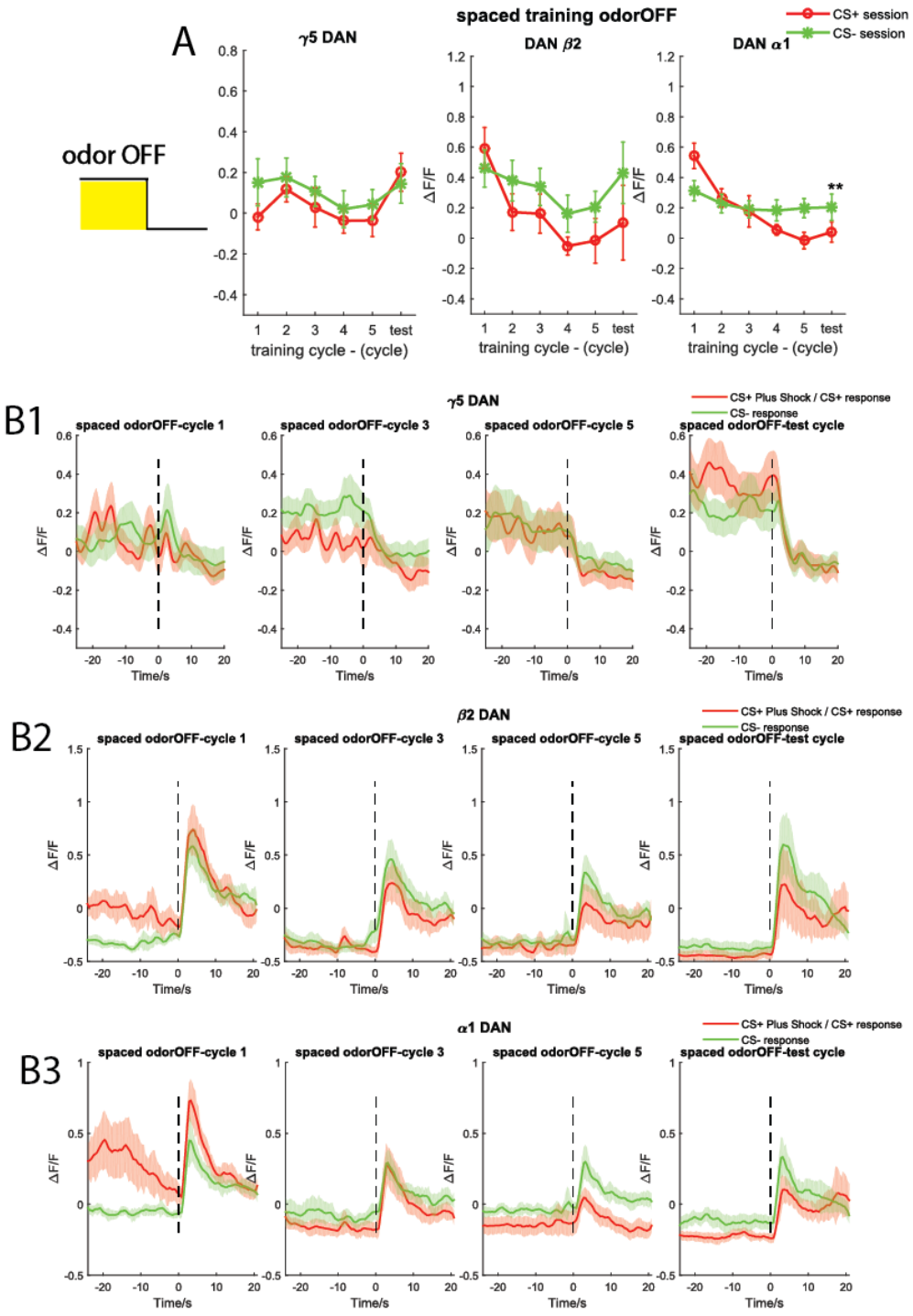


**Figure S4b Activity of other DANs Odor-OFF response in aversive olfactory conditioning**
(A) Plot of DANs GCaMP6s fluorescence over training cycles. Calcium activity was calculated by averaging the fluorescence over the first 8 seconds after odor onset. (B-D) Calcium activity of $\gamma 5$ (n=11), $\beta 2$ (n=9) and $\alpha 1$ (n=9) DANs were imaged during 5-cycle conditioning.

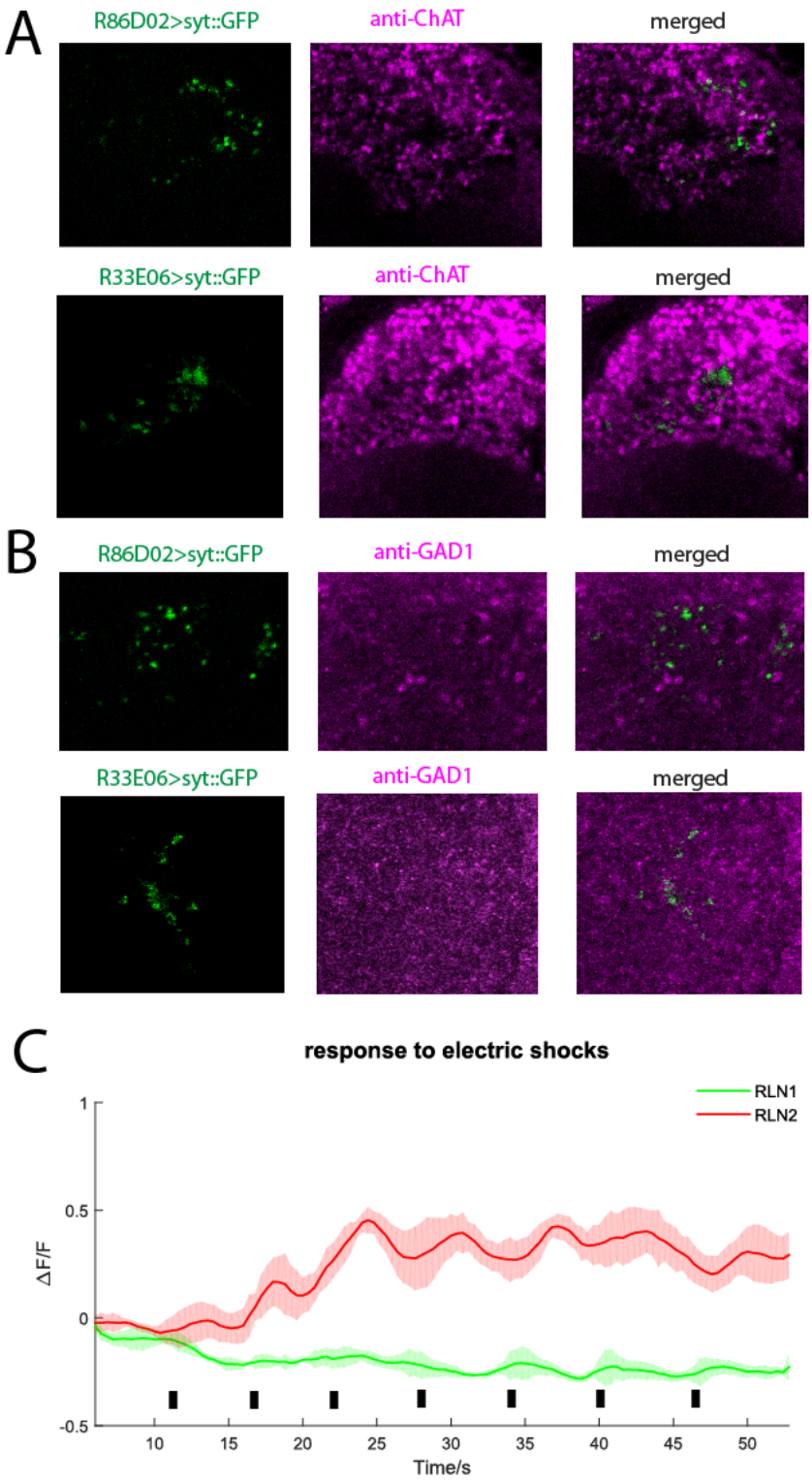


**Figure S5 More properties of RLN neurons**

(A) Neither RLN1 or RLN2 are cholinergic. (B) Neither RLN1 or RLN2 are GABAergic. (C) RLNs' response to electric shocks alone in the absence of odors. Calcium traces of RLN1 and RLN2 are presented in green and red respectively (n=5). Black bars denote presentation of electric shocks (500ms per pulse).

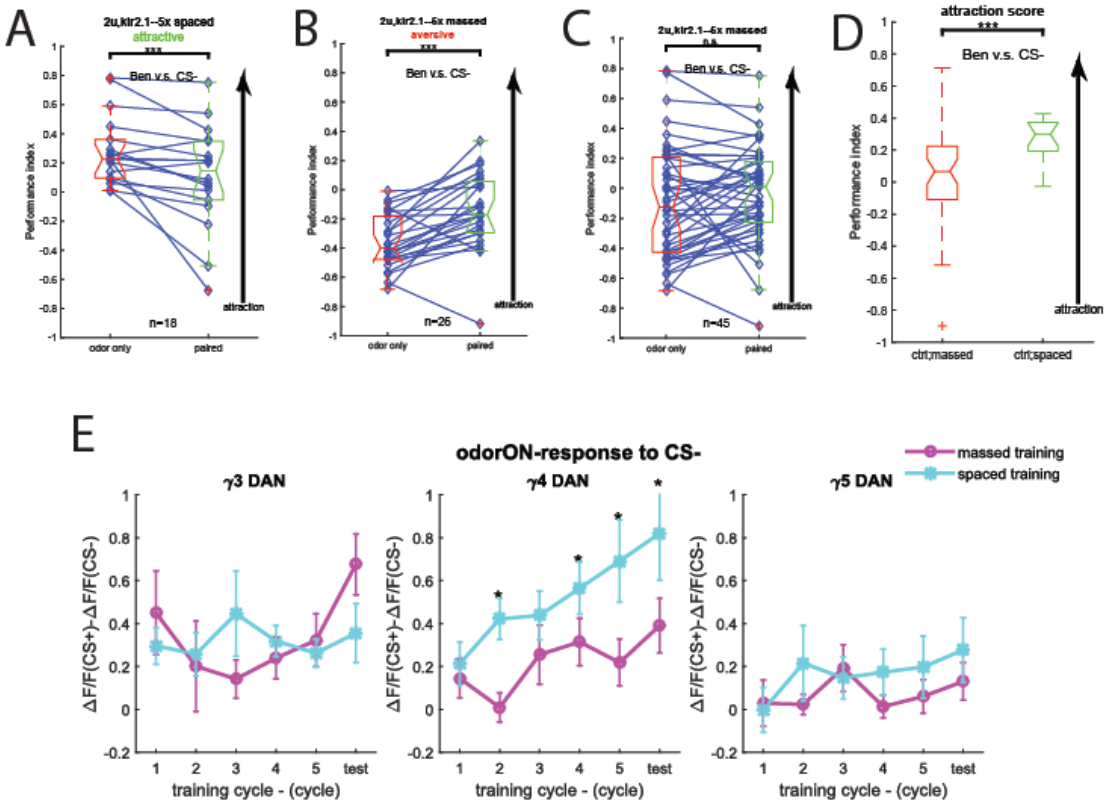


**Figure S6 Attraction memory induced by massed training is weaker than spaced training**

(A-C) Attraction memory to CS- depends on initial odor preference. In each panel is performance index (PI) for trained and mock-trained flies. Three asterisks denotes p<0.001. (Paired t-test) PI scores were averaged over MCH and OCT. (A): CS- preference was reduced if flies initially preferred CS- to Ben. (n=18) (B): CS- aversion was reduced if flies initially preferred Ben to CS-. (n=26) (C): PI scores of trained animals are no different from mock-trained ones if data from (A) and (B) are lumped together (D): Attraction memory PI scores from massed trained animals are significantly lower than spaced trained ones. (Two-sample T-test) (E): Plot of DANs response to CS- over training cycles. Calcium activity was calculated by averaging the fluorescence over the first 8 seconds after odor onset. Cyan curved lines denote DAN activity response to CS- during spaced training and purple curved line during massed training. Data are mean ± MSE. One asterisk denotes p<0.05. (Two-sample T-test)